

# **Carbonate Radical in Natural Waters**

by

**Jiping Huang**

**A thesis submitted in conformity with the requirements  
for the degree of Doctor of Philosophy  
Department of Chemistry  
University of Toronto**

© Copyright by Jiping Huang 2000



**National Library  
of Canada**

**Acquisitions and  
Bibliographic Services**

**395 Wellington Street  
Ottawa ON K1A 0N4  
Canada**

**Bibliothèque nationale  
du Canada**

**Acquisitions et  
services bibliographiques**

**395, rue Wellington  
Ottawa ON K1A 0N4  
Canada**

*Your file Votre référence*

*Our file Notre référence*

**The author has granted a non-exclusive licence allowing the National Library of Canada to reproduce, loan, distribute or sell copies of this thesis in microform, paper or electronic formats.**

**The author retains ownership of the copyright in this thesis. Neither the thesis nor substantial extracts from it may be printed or otherwise reproduced without the author's permission.**

**L'auteur a accordé une licence non exclusive permettant à la Bibliothèque nationale du Canada de reproduire, prêter, distribuer ou vendre des copies de cette thèse sous la forme de microfiche/film, de reproduction sur papier ou sur format électronique.**

**L'auteur conserve la propriété du droit d'auteur qui protège cette thèse. Ni la thèse ni des extraits substantiels de celle-ci ne doivent être imprimés ou autrement reproduits sans son autorisation.**

**0-612-50045-4**

**Canada**

# **Carbonate Radical in Natural Waters**

**Ph. D. Thesis, 2000**

**Jiping Huang**

**Department of Chemistry, University of Toronto**

## **ABSTRACT**

Sunlight plays an important role in natural cleansing of field waters through direct photolysis and indirect photolysis by different transients. The carbonate radical ( $\bullet\text{CO}_3^-$ ) is a secondary radical that results from the scavenging of hydroxyl radical ( $\bullet\text{OH}$ ) by carbonate/bicarbonate and is itself strongly electrophilic. *N, N*-dimethylaniline (DMA) was found to be a selective probe for measuring the steady state concentration of this radical in a variety of natural waters. The pH, nitrate, total carbonate/bicarbonate, and DOC in selected field waters were quantitatively analyzed. Steady-state carbonate radical concentrations  $[\bullet\text{CO}_3^-]_{\text{ss}}$  in natural waters were investigated in a photoreactor and in summer sunlight. The measured  $[\bullet\text{CO}_3^-]_{\text{ss}}$  strongly depended on light intensity; the range of  $[\bullet\text{CO}_3^-]_{\text{ss}}$  found in natural waters was  $5 \times 10^{-15}$  to  $10^{-13}$  M. A linear relationship of  $[\bullet\text{CO}_3^-]_{\text{ss}}$  to the major components in natural waters was derived. A novel method was used to produce the  $\bullet\text{CO}_3^-$  with KOONO as solid  $\bullet\text{OH}$  source. Using a competition kinetic method, the second-order constants of nine pesticides were measured ranging from  $2.0 \times 10^7 \text{ M}^{-1}\text{s}^{-1}$  for fenthion to  $2.0 \times 10^5 \text{ M}^{-1}\text{s}^{-1}$  for methyl parathion. Thioanisole, dibenzothiophene, and fenthion were selected as probes to determine the reaction pathway with  $\bullet\text{CO}_3^-$ . Using HPLC, GC, GC-MS and LC-MS for structural confirmation, the major photodegradation products were the corresponding sulfoxides, followed by further oxidation to the sulfones. The

photoreactivities of these probes in different reaction matrices were investigated. Since fenthion provided an excellent structural template in order to observe the influence of photo-oxidation on hydrolysis rates, the hydrolysis kinetics of fenthion and five metabolites were studied at different pHs and temperatures. Fenthion and its metabolites were relatively stable in neutral media, and their stability decreased as pH increased. The photo-oxidation of fenthion with  $\bullet\text{CO}_3^-$  results in intermediates that are rapidly degraded through hydrolytic cleavage. Carbonate radical is a selective oxidant existing in natural waters with relatively high steady-state concentration that could contribute to limiting the persistence of electron-rich compounds.

## **ACKNOWLEDGEMENTS**

I would like to express my sincere thanks to my supervisor, Professor Scott A. Mabury for his inspiration, enthusiastic encouragement and friendship during my time as a graduate student in his research group. He gave me both research freedom and excellent guidance to my projects. For all these reasons and many beyond, I am deeply indebted to him.

I would like to thank Dan Mathers, the supervisor of ANALEST, for assistance of setting up the instruments and method development utilized significantly in my research. In particular, I would like to express my appreciation to Prof. Imre Csizmadia for his invaluable suggestion about some physical organic questions in my research work. I would also like to thank Prof. Michael Thompson, Prof. Ulrich Krull, Prof. Imre Csizmadia, and Dr. Rick Bourbonniere for serving as committee members.

I would like to acknowledge Dr. Charles Shiu Wong for his valuable comments on my thesis. I am also very grateful to other members of Professor Mabury's group, including David Ellis, Adam Marsella, Ruth Wilson and Patrick Lee. During my graduate study, they have given me much help in many ways.

I would like to express my deepest gratitude to my parents, Mr. Jiatang Huang and Mrs. Zhaowu Meng, for their unconditional love and support to me. They provided an excellent environment for my early education and deserve a lot of the credit for my current success. I would also like to thank my older brother, Dr. Jianping Huang, for his long-term encouragement and inspiration in my scientific career. I would also thank my parents-in-

law, Mr. Wenxiu Du and Mrs. Shumin Xiao, for carefully looking after my baby son and family for one year and support to my graduate study.

Finally I would like to thank my dear wife, Xiaohong Du for her deep love, endless inspiration, patient waiting, travelling around the world with me, and my lively son, Eric Huang.

**To my parents, my wife and my son**

## Table of Contents

Abstract	ii
Acknowledgement	iv
List of Tables	xi
List of Figures	xii
Glossary of Symbols and Acronyms	xiv

### Chapter one: Introduction to Carbonate Radical

1.0	Preamble	2
1.1	Properties of carbonate radical	2
1.2	Experimental generation of carbonate radicals	4
1.3	Reaction with organic compounds	6
1.4	Reaction with inorganic compounds	11
1.5	Carbonate radicals in biological systems	12
1.6	Carbonate radicals in environment	14
	1.6.1 Photooxidants in natural waters	14
	1.6.2 Sources of hydroxyl radical as $\bullet\text{CO}_3^-$ precursor	15
	1.6.3 Steady-state concentration of carbonate radical in natural waters	19
	1.6.4 Carbonate radical in environmental applications	21
1.7	Scope of dissertation research	23
1.8	References	24

### Chapter Two: Steady State Concentration of Carbonate Radical in Natural Waters

2.1	Introduction	37
2.2	Materials and Methods	40
	2.2.1 Chemicals	40
	2.2.2 Field water analysis	41

2.2.3	Photolysis	41
2.2.4	Analysis	42
2.2.5	Reaction pathways	43
2.3	Results and Discussion	43
2.3.1	Field water analysis	43
2.3.2	DMA reaction with $\bullet\text{CO}_3^-$	46
2.3.3	Control experiments	47
2.3.4	Photolysis in photoreactor	49
2.3.5	Steady state concentration of carbonate radical	51
2.3.6	Photolysis under sunlight	55
2.3.7	Factors to determine $[\bullet\text{CO}_3^-]_{ss}$	56
2.4	Conclusions	63
2.5	References	64

### **Chapter Three: A New Method for Measuring Carbonate Radical Reactivity towards Pesticides**

3.1	Introduction	68
3.2	Materials and Methods	72
3.2.1	Chemicals	72
3.2.2	Analytical methodologies	73
3.2.3	Competition kinetics	74
3.2.4	Stopped-flow kinetic experiment	76
3.3	Results and Discussion	76
3.3.1	Formation of the carbonate radical	76
3.3.2	Nitrogen dioxide radicals in our system	78
3.3.3	Competition kinetic method	79
3.3.4	Pesticide reactivity toward carbonate radicals	83
3.4	Conclusions	88
3.5	References	89

## **Chapter Four: The role of Carbonate Radical in Limiting the Persistence of Sulfur-Containing Chemicals in Sunlit Natural Waters**

4.1	Introduction	93
4.2	Materials and Methods	96
4.2.1	Chemicals	96
4.2.2	Photolysis	97
4.2.3	Field water analysis	97
4.2.4	Analysis	98
4.3	Results and Discussion	99
4.3.1	Reaction Pathways	99
4.3.2	Reaction Mechanism	101
4.3.3	Persistence in different matrix	103
4.3.4	Photodegradation products	109
4.4	Conclusions	110
4.5	References	110

## **Chapter Five: Hydrolysis Kinetics of Fenthion and its Metabolites**

5.1	Introduction	115
5.2	Materials and Methods	118
5.2.1	Chemicals	118
5.2.2	Synthesis of compounds	118
5.2.3	Experimental procedures	122
5.2.4	Analysis by HPLC	123
3.3	Results and Discussion	124
5.3.1	Effect of pH on hydrolysis	124
5.3.2	Effect of temperature on hydrolysis	128
5.3.3	Stability of the hydrolysis products	132
5.3.4	Hydrolysis mechanisms	136

5.4	Conclusions	139
5.5	References	139

## **Chapter Six: Conclusions and Future Work**

6.1	Conclusions	144
6.2	Future work	147
6.3	References	150

## **List of Tables**

<b>Table 2.1</b>	<b>Analysis results of natural field waters and the fraction of hydroxyl radical scavenged by carbonate/bicarbonate ion in field waters.</b>	<b>45</b>
<b>Table 2.2</b>	<b>Rate constants and steady-state concentrations of carbonate radical in field water under the photoreactor with minimum irradiance level at 250 W/m<sup>2</sup>.</b>	<b>53</b>
<b>Table 2.3</b>	<b>Kinetic analysis of the reaction pathways for hydroxyl radicals in the selected field samples.</b>	<b>58</b>
<b>Table 3.1</b>	<b>HPLC conditions for competitor analysis.</b>	<b>73</b>
<b>Table 3.2</b>	<b>Rate constants and Hammett constants for substituted anilines.</b>	<b>81</b>
<b>Table 3.3</b>	<b>Measured rate constants for pesticides towards carbonate radical.</b>	<b>85</b>
<b>Table 4.1</b>	<b>Synthetic field waters and photolysis solutions.</b>	<b>104</b>
<b>Table 4.2</b>	<b>Photoreaction rate constants and half-lives of selected compounds at different matrices.</b>	<b>105</b>
<b>Table 5.1</b>	<b>HPLC Analysis Conditions.</b>	<b>124</b>
<b>Table 5.2</b>	<b>Hydrolysis rate constants k and half-life t<sub>1/2</sub> at different temperatures.</b>	<b>127</b>
<b>Table 5.3</b>	<b>Activation energy E<sub>a</sub>, frequency factor A and activation entropy ΔS<sup>‡</sup>.</b>	<b>131</b>
<b>Table 5.4</b>	<b>Percentage of reactant converted into the relative products.</b>	<b>134</b>

## List of Figures

Figure 1.1	The source of hydroxyl radical and production of carbonate radical in natural waters.	20
Figure 2.1	DMA reaction pathways with $\bullet\text{CO}_3^-$ .	47
Figure 2.2	Photoreaction kinetics of DMA in deionized water, dark control, decarbonation of the Thames River, carbonate radical matrix, and some selected field waters.	50
Figure 2.3	Steady state concentration of carbonate radical in selected natural waters under a photoreactor with high light intensity ( $765 \text{ W/m}^2$ ) and low light intensity ( $250 \text{ W/m}^2$ ).	54
Figure 2.4	Steady state concentration of carbonate radical in selected natural waters under different sunlight conditions.	56
Figure 2.5	The relationship of indirect photolysis rate constants ( $k_I$ ) to the nitrate concentration (A); the relationship of indirect photolysis rate constants ( $k_I$ ) to the DOC concentration (B)	61
Figure 2.6	Using the derived formula in twenty natural waters to obtain the linear regression curve of $[\bullet\text{CO}_3^-]_{ss}$ towards $f_{\bullet\text{OH}}(\text{CO}_3^{2-} + \text{HCO}_3^-) \times \{[\text{NO}_3^-] + 12 + 1.3 [\text{DOC}]\}$ .	62
Figure 3.1	Chemical structures of pesticides used in this investigation.	72
Figure 3.2	Hammett plot of substituted aniline reactivity towards carbonate radicals.	82
Figure 3.3	Typical results indicating pesticide reactivity towards carbonate radicals.	84
Figure 4.1	Chemical structures of selected sulfur-containing compounds	94
Figure 4.2	Thioanisole photoreaction with carbonate radical for 1 h; the sample was concentrated through SPE and separated by HPLC (60% acetonitrile and 40% water as mobile phase; flow rate =	100

1.0 ml/min) (A); Methyl phenyl sulfoxide photoreaction with carbonate radical for 1.2 h; the sample was concentrated through SPE and separated through HPLC (40% acetonitrile and 60% water as mobile phase; flow rate = 1.0 ml/min) (B).

Figure 4.3	Primary reaction pathways towards carbonate radical.	102
Figure 4.4	Photoreaction kinetics of thioanisole under different reaction matrices.	106
Figure 5.1	Fenthion (I), its five metabolites (II-VI) and three hydrolysis products H-I to H-III.	117
Figure 5.2	Hydrolysis rate of I-III at 50 °C (a) and IV-VI at 50 °C (b); N=2.	126
Figure 5.3	Effect of temperature on the rate constants at pH 7 (a) and pH 9 (b).	129
Figure 5.4	At 50 °C, the percentage of fenthion and its metabolites converted into H-I to H-III at the first time point.	135
Figure 5.5	Stability of three hydrolysis products at 50 °C.	136
Figure 5.6	Proposed primary hydrolysis pathway for I to VI at pH 7 and pH 9.	138

## **Glossary of Symbols and Acronyms**

$\nu$	frequency
$\lambda$	wavelength
$\varepsilon$	molar absorptivity
$\phi$	quantum yield
$\rho$	reaction constant
$\sigma$	substituent constant
A	frequency factor
AOT	advanced oxidation techniques
AOP	advanced oxidation processes
$[\bullet\text{CO}_3]_{\text{ss}}$	Steady-state concentrations of carbonate radicals
$[\bullet\text{OH}]_{\text{ss}}$	Steady-state concentrations of hydroxyl radicals
DOC	dissolved organic carbon
CDOM	colored dissolved organic materials
E <sub>a</sub>	activation energy
E <sub>red</sub>	electron reduction potential
EPR	electron paramagnetic resonance
ESR	electron spin resonance
FPD	flame photometric detector
GC	gas chromatography
HPLC	high performance liquid chromatography
I	ionic strength
k	rate constant
k <sub>C</sub>	rate constant to competitor
k <sub>D</sub>	direct photolysis rate constant
k <sub>I</sub>	indirect photolysis rate constant
k <sub>P</sub>	rate constant to probe
MS	mass spectrometry
NMR	nuclear magnetic resonance

<b>PDA</b>	<b>photodiode array</b>
<b><math>\Delta S^\ddagger</math></b>	<b>activation entropy</b>
<b>SFW</b>	<b>synthetic field water</b>
<b>S<sub>N</sub>2</b>	<b>bimolecular nucleophilic substitution reaction</b>
<b>SPE</b>	<b>solid phase extraction</b>
<b>SPME</b>	<b>solid phase microextraction</b>
<b>SRFA</b>	<b>Suwannee River fulvic acid</b>
<b>t<sub>1/2</sub></b>	<b>half-life</b>
<b>TLC</b>	<b>thin layer chromatography</b>
<b>UV</b>	<b>ultraviolet</b>

## **Chapter One**

### **Introduction to Carbonate Radical**

## **1.0 Preamble**

The carbonate radical ( $\bullet\text{CO}_3^-$ ) is a secondary radical formed from the scavenging of the hydroxyl radical by carbonate/bicarbonate ion in natural waters. It is strongly electrophilic towards electron-rich compounds such as anilines, phenols, and sulfur-containing compounds (Neta and Huie, 1988). The steady-state concentrations of carbonate radicals are expected to be significantly higher than those of hydroxyl radicals in natural waters since carbonate radicals are more selective oxidants than hydroxyl radicals (Larson and Zepp, 1988). It is hypothesized that carbonate radical is important in limiting the persistence of chemical pollutants, especially electron-rich compounds in natural waters. Therefore, it is necessary to review the properties of carbonate radical, its experimental generation, reaction with organic and inorganic compounds, and chemistry in biological systems. The importance of carbonate radical in natural waters in regards to its sources, steady-state concentrations, and reactivities towards aquatic pollutants will also be discussed

### **1.1 Properties of carbonate radicals**

Both flash photolysis and pulse radiolysis have been used to investigate the short-lived carbonate radical. Weeks and Rabani (1966) first observed the absorption spectra of the carbonate radical using pulse radiolysis giving the maximum absorption coefficient of  $1860 \pm 160 \text{ dm}^3 \text{ mol}^{-1} \text{ cm}^{-1}$  at 600 nm. It was therefore possible to monitor the formation and reactions of this radical in the 500-700 nm range. Behar *et al.* (1970) found that the spectra of the radical were identical at pH 8 and 13. Chen *et al.* (1973)

suggested that the  $\bullet\text{CO}_3^-$  could be protonated to form  $\bullet\text{HCO}_3$  through the following equilibrium (I) with an observed  $\text{pK}_a$  of  $9.6 \pm 0.3$  (Chen *et al.*, 1973).



The corresponding dependence on pH, however, was negligible at low ionic strength, from which the two forms of the radical were suggested to have similar intrinsic reactivities (Chen and Hoffman, 1974, 1975; Larson and Zepp, 1988). Zuo *et al.* (1999) reinvestigated the acid-base equilibrium of carbonate radical at even higher ionic strength (0.5 M) and found the  $\text{pK}_a$  to be  $9.5 \pm 0.2$ . This result was in good agreement with that reported by Chen *et al.* (1973a). Eriksen *et al.* (1985) have investigated the possible protonation of the carbonate radical by pulse radiolysis, and obtained a tentative estimate of  $\text{pK}_a = 7.9$ . Bisby *et al.* (1998) have used time-resolved resonance Raman spectroscopy to demonstrate that the radical is unprotonated at pH 7.5.

Walsh (1953) has discussed the structure of 23 electron systems such as  $\bullet\text{CO}_3^-$  and the isoelectronic  $\bullet\text{NO}_3$  radical, and concluded that their structures should be planar. Recently, the structure of  $\bullet\text{CO}_3^-$  was determined using time-resolved resonance Raman spectroscopy (Bisby *et al.*, 1998; Tavender *et al.*, 1999). The spectrum was found to be invariant with pH and contained a strongly polarized and intense band at  $1062 \text{ cm}^{-1}$ . This result was consistent with the radical having  $\text{C}_{2v}$  symmetry, indicating some distortion from the predicted  $\text{D}_{3h}$  structure. Evidence for distortion from  $\text{D}_{3h}$  to  $\text{C}_{2v}$  symmetry was also found in the EPR spectra obtained for the  $\bullet\text{CO}_3^-$  (Chantry *et al.*, 1962). These results suggest that the structures of carbonate radical have planar  $\text{C}_{2v}$  symmetry.

Free radicals should be detectable by the electron paramagnetic resonance techniques (EPR). However, most free radicals are so highly reactive in biological and

environmental systems that they seldom reach a concentration high enough to be detected by EPR at room temperature (Kochany and Lipczynska-Kochany, 1992). Behar and Fessenden (1972a) investigated the EPR spectrum of inorganic radicals in irradiated aqueous solution and found no ESR lines for the carbonate radical. Using the anion of nitromethane as a spin trap reagent,  $\bullet\text{CO}_3^-$  could be identified through spin adducts (Behar and Fessenden, 1972b). In the presence of DMPO, the DMPO- $\bullet\text{CO}_3^-$  adduct was also detected in irradiated suspensions of bacteria (Wolcott *et al.*, 1994). More recently, the carbonate radical was directly detected by the use of rapid mixing continuous flow electron paramagnetic resonance (EPR) (Bonin *et al.*, 1999).

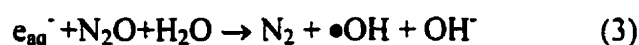
Carbonate radicals typically exist in aqueous solution; however, the gaseous  $\bullet\text{CO}_3^-$  ions have been detected in mass spectrometry and an  $\text{O}^-$  transfer reaction has also been observed (Franklin and Hardland, 1974). In addition, defects in lithium vanadate ( $\text{Li}_3\text{VO}_4$ ) exposed to X rays were studied by ESR (Murata and Miki, 1993). Two types of trapped-hole centers were produced at 77 K irradiation. One of which was presumed to be the carbonate radical, which is thermally stable even at room temperature.

## 1.2 Experimental generation of carbonate radicals

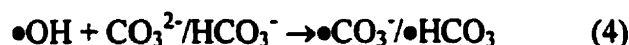
The carbonate radical has experimentally been generated by three methods: (I) pulse radiolysis, (II) flash photolysis and (III) photodecomposition of carbonatoammine complexes of cobalt.

Carbonate radicals can be generated by pulse radiolysis of aqueous solutions of carbonate or bicarbonate saturated with  $\text{N}_2\text{O}$  (Weeks and Rabani, 1966). An electron pulse from a linear accelerator is used, and  $\bullet\text{OH}$ ,  $e_{aq}^-$ ,  $\text{H}$  are formed as illustrated in

equation (2). Hart and Boag (1962) reported that the absorption of  $e_{aq}^-$  is about 5 times higher than  $\bullet CO_3^-$  at 600 nm. Thus,  $e_{aq}^-$  must be eliminated in the system in order to investigate the reactivity of carbonate radical. Most of these experiments are carried out in saturated  $N_2O$ , which react rapidly with  $e_{aq}^-$  to form  $\bullet OH$  and  $OH^-$  as illustrated in equation (3).



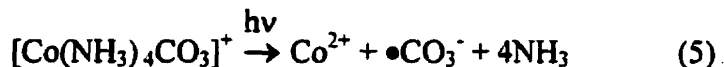
The hydroxyl radical is then scavenged by carbonate/bicarbonate ion to form carbonate radicals (equation 4).



Carbonate radical can be produced through flash photolysis methods. Using short wavelength flash photolysis through either direct photoionisation of carbonate (Hayon and McGarvey, 1967), or photolysis of  $H_2O_2$  in solutions containing  $HCO_3^-/CO_3^{2-}$  (Behar *et al.*, 1970) or persulphate containing  $Na_2CO_3$  (Clifton and Huie, 1993). The photo-induced  $\bullet OH$  and  $\bullet SO_4^-$  are more powerful oxidizing reagents than  $\bullet CO_3^-$  since the one electron reduction potential of  $\bullet OH$  ( $E_{red}=2.4$  V) (Elango *et al.*, 1988) and  $\bullet SO_4^-$  ( $E_{red}=2.43$  V) (Huie *et al.*, 1991a) are higher than that of  $\bullet CO_3^-$ . The  $\bullet CO_3^-$  is formed through the subsequent free radical reaction of  $\bullet OH$  and  $\bullet SO_4^-$  with carbonate ions. Carbonate ions are maintained in large excess at high pH (Chawla and Fessenden, 1975); hence, this procedure is not suitable in acid or neutral media.

Carbonate radical can also be produced through flash photolysis of certain carbonatoamine complexes such as  $[Co(NH_3)_4CO_3]^+$  as shown by equation (5) (Chen et

al, 1973; Cope *et al.*, 1973). Irradiation of these solutions with 254 nm sources (low pressure Hg lamp) can also produce the carbonate radicals.



During irradiation, ligand to metal charge transfer band excitation takes place. The singlet CT state crosses inter-system to triplet CT state which eventually dissociates to yield  $\text{Co}^{2+}$  and  $\bullet\text{CO}_3^-$ . This method is well suited for investigations in the pH range 4-11 and consequently is uniquely appropriate for investigations under acid/neutral conditions.

### 1.3 Reaction with organic compounds

Although  $\bullet\text{CO}_3^-$  reacts more slowly than  $\bullet\text{OH}$  with most organic substrates (Neta and Huie, 1988), it is nonetheless a powerful oxidant with a one electron reduction potential of 1.59 V vs the NHE at pH 12 (Huie *et al.*, 1991). The carbonate radical acts predominantly as an electron acceptor; it oxidizes many organic and inorganic compounds. Rate constants for the reaction of carbonate radicals with various reactants have been compiled by Neta and Huie (1988). Carbonate radicals show a wide range of reactivity with aromatic compounds with their rate constants depending upon the nature of the substituents and the aromatic system (Chen and Hoffman, 1973). The rate constants for reaction with a series of substituted benzene derivatives ranged from  $3 \times 10^3 \text{ M}^{-1} \text{ s}^{-1}$  for benzene to  $1.8 \times 10^9 \text{ M}^{-1} \text{ s}^{-1}$  for dimethylaniline (Chen *et al.*, 1975). These results correlate well with the Hammett equation using  $\sigma_{\text{para}}^+$  values for electrophilic substitution yielding  $\rho = -3.6$ . In comparison, a reaction constant of  $\rho = -0.41$  was measured for the reaction of  $\bullet\text{OH}$  with benzene derivatives although the range of rate

constants measured varied over less than a factor of 4 (Anhar *et al.*, 1966). The high reactivity of  $\bullet\text{OH}$  ( $k \sim 10^9 \text{ M}^{-1}\text{s}^{-1}$ ) results in a low selectivity ( $\rho = -0.41$ ) and the lower reactivity of  $\bullet\text{CO}_3^-$  should result in a high degree of selectivity ( $\rho = -3.6$ ). More recently, the rate constant of  $\bullet\text{CO}_3^-$  with eight aromatic compounds in aqueous solution were determined using a laser photolysis laser long-path absorption (LP-LPLA) apparatus which was designed for direct time-resolved studies of radical reactions (Umschlag and Herrmann, 1999). The measured rate constants ranged from  $3.0 \pm 0.6 \times 10^7 \text{ M}^{-1}\text{s}^{-1}$  for hydroquinone dimethyl ether to less than  $1.3 \times 10^2 \text{ M}^{-1}\text{s}^{-1}$  for benzonitrile, while the rate constants of corresponding reactions to hydroxyl radical were in the  $10^9 \text{ M}^{-1}\text{s}^{-1}$  magnitude. Therefore,  $\bullet\text{CO}_3^-$  can be viewed as a selective electrophilic reagent.

Elango *et al.* (1985a) reviewed the reaction of carbonate radical with aromatic, aliphatic and cyclic amines. Three kinds of amines displayed the different reactivities and mechanisms towards carbonate radicals. Rate constants for the reaction of carbonate radical with aniline and some para-substituted anilines were determined by the flash photolysis technique (Elango *et al.*, 1984). Using  $\sigma_{\text{para}}^+$  values of these para-substituent of aniline, the rate constants at pH 8.5 correlated very well with the Hammett equation yielding  $\rho = -1$ . Larson and Zepp (1988) also investigated the reactivity of carbonate radicals with aniline derivatives at pH 8.3 and pH 11.6. Using the  $\sigma$  substituent constant, the rate constant for the reaction of ring-substituted anilines correlated well with Hammett equation yielding  $\rho = -1.09$ . Moreover, the rate constants of aromatic amine derivatives reacting with  $\bullet\text{CO}_3^-$  showed an equally good correlation with half-wave potentials determined in alkaline solution (Meites and Zuman, 1977). So, it is probable that the rate-determined step for the reaction is the removal of an electron by  $\bullet\text{CO}_3^-$ , that

electron most likely being one of those associated with the basic nitrogen atom, to produce the anilino radical cation and  $\text{CO}_3^{2-}$  (Elango *et al.*, 1984; Larson and Zepp, 1988). During flash photolysis, a transient absorption attributable to anilino radical was observed (Elango *et al.*, 1984).

The rate constant of the reaction of phenol to  $\bullet\text{CO}_3^-$  depends on pH (Chen *et al.*, 1975b). The increase in rate constant between pH 9 and 11 is due to the ionization of phenolic OH group. A  $\rho$  value of -1 was obtained for the reaction of the carbonate radical with *p*-substituted phenol using  $\sigma_{\text{para}}^+$  values of para-substituents (Moore *et al.*, 1977). The greater negative value of  $\rho$  confirms the selectivity of carbonate radical, which is well established in its reaction with amino acids and enzymes through pulse radiolysis at pH 11.2 (Adams *et al.*, 1972a,b). Chen and Hoffman (1973) had also measured the rate constants of carbonate radical reaction with 36 compounds of biological interest including amino acids, sulfur-containing compounds, and enzymes. The rate constant of investigated compounds were low ( $k < 10^5 \text{ M}^{-1}\text{s}^{-1}$ ) for the non-sulfur-containing aliphatic compounds but higher ( $k = 10^6\text{-}10^7 \text{ M}^{-1}\text{s}^{-1}$ ) for the sulfur compounds. The highest rates ( $k > 10^8 \text{ M}^{-1}\text{s}^{-1}$ ) were for indole and its derivatives. The reactivity of the enzyme generally reflected the reactivity of constituent aromatic amino acids. The rate constants for tryptophan and its derivatives with  $\bullet\text{CO}_3^-$  have been measured as a function of pH (Chen and Hoffman, 1974). Amino-containing compounds show variation of rate constants according to the pKa of the  $\text{NH}_3^+$  group with the rate constant being greater by almost a factor of 2 for  $\text{NH}_3^+$  than for  $\text{NH}_2$ . A small but significant enhancement of the rate was noted for amino compounds lacking the carboxylate group.

Elango *et al.* (1985b) have also investigated the reaction of carbonate radicals with a variety of aliphatic amines, including open chain amines and cyclic amine with bridgehead nitrogen atoms. The rate constant ranged from  $1.7 \times 10^4 \text{ M}^1\text{s}^{-1}$  for hexamethylenetetramine to  $1.7 \times 10^7 \text{ M}^1\text{s}^{-1}$  for 1, 4-diazabicyclo[2,2,2]octane. Carbonate radicals can react with the aliphatic amines either through electron transfer for tertiary amines or hydrogen abstraction mechanism for primary amines (Elango *et al.*, 1985b). Kuzmin (1972) measured the rate constants of  $\bullet\text{CO}_3^-$  reaction with the lower alcohols, acetone, benzophenone, parabenoquinone and acetophenone and suggested a hydrogen abstraction mechanism for reaction with these compounds. The range of rate constant constants was from  $5.0 \times 10^3 \text{ M}^1\text{s}^{-1}$  for methanol to  $2.0 \times 10^7 \text{ M}^1\text{s}^{-1}$  for parabenoquinone. Clifton and Huie (1993) have measured the rate constants for hydrogen abstraction reactions of the carbonate radical with several saturated alcohols and one cyclic ether. At room temperature, the rate constant ranged from  $10^3 \text{ M}^1\text{s}^{-1}$  to  $10^5 \text{ M}^1\text{s}^{-1}$ . The activation energies and Arrhenius pre-exponential factors were also determined. Since the reactions of similar compounds investigated for sulfate radicals had a clear relationship between the activation energy and the C-H bond strength (Clifton and Huie, 1989), these reactions were suggested to be pure hydrogen abstraction. However, the reactions investigated for carbonate radicals did not display a clear relationship between the activation energy and the C-H bond strength. It was suggested that the reactions with carbonate radicals were not pure hydrogen abstraction and probably involved an additional interaction of the carbonate radical with the -OH or -O-linkage.

Huie *et al.* (1991) have measured the rate constants of  $\bullet\text{CO}_3^-$  with a number of organic and inorganic reactants as a function of temperature; the activation energies ranged from  $-11.4$  to  $18.8$  kJ/mol and the pre-exponential factors ranged from  $\log A = 6.4$  to  $10.7$ . For many of the organic reactants, the activation energies were very low, such as for methionine ( $-9.2 \pm 1.5$  kJ/mol) and tryptophan ( $-0.9 \pm 0.2$  kJ/mol), and independent of driving force, suggesting that the oxidation occurred via an inner sphere mechanism. Umschlag and Herrmann (1999) have also studied the temperature effect on three aromatic compounds. In addition, the influence of temperature on the kinetics of carbonate radical reactions in near critical and supercritical water were also reported (Ferry *et al.*, 1999). The rate constants for four aniline derivatives with  $\bullet\text{CO}_3^-$  all displayed negative temperature dependence, consistent with the formation of an intermediate association complex (Huie *et al.*, 1991).

The rate constant for carbonate radical oxidation of the basic form of maleic hydrazine (MH<sup>-</sup>) to the corresponding diazasemiquinone radical through pulse radiolysis was  $7.7 \pm 0.8 \times 10^8 \text{ M}^1\text{s}^{-1}$  (Eriksen *et al.*, 1983). The reaction of carbonate radical with methyl orange at pH 11.0 and 25 °C had a second-order rate constant of  $2.1 \pm 0.3 \times 10^8 \text{ M}^1\text{s}^{-1}$ , which was two orders of magnitude lower than that of the reaction of hydroxyl radicals ( $2.0 \times 10^{10} \text{ M}^1\text{s}^{-1}$ ) (Padmaja and Madison, 1999).

Carbonate radical was also employed as the oxidant for the polymerisation of pyrrole (Bhattacharya *et al.*, 1998). As a strong electron oxidant, the carbonate radical can oxidize pyrrole monomer by abstraction of an electron to form a radical cation; this radical cation then undergoes several transformations to form the bipyrrrole and terpyrrrole.

#### 1.4 Reaction with inorganic compounds

Reaction of the carbonate radical with itself and other radicals such as  $\bullet\text{NO}_2$ ,  $\bullet\text{NO}_2^-$ ,  $\bullet\text{SO}_3^-$ ,  $\bullet\text{SO}_3^{2-}$  and  $\bullet\text{CH}_3$  via transfer of an  $\text{O}^-$  ion has been reported (Lilie *et al.*, 1978); both the conductivity and optical absorption changes of irradiated solutions were recorded. It was concluded that  $\text{CO}_2$  and  $\text{CO}_4^{2-}$  were products of the bimolecular reaction between two  $\bullet\text{CO}_3^-$  radicals by the detection of conductivity changes. Electron transfer reactions of the carbonate radical anion with azide, bromide, and hypochlorite ions have been studied by pulse radiolysis (Huie *et al.*, 1991). The inorganic anions ( $\text{SO}_3^{2-}$ ,  $\text{ClO}_2^-$ ,  $\text{NO}_2^-$ ,  $\text{I}^-$ , and  $\text{SCN}^-$ ) have rate constants at room temperature ranging from  $4 \times 10^5$  to  $1 \times 10^8 \text{ M}^{-1}\text{s}^{-1}$  (Gogolev *et al.*, 1989]. Cyano complex of Fe(II), Mo(IV) were reported to react with  $\bullet\text{CO}_3^-$  with rate constant of  $5 \times 10^8$  and  $6.5 \times 10^7 \text{ M}^{-1}\text{s}^{-1}$ , respectively. Temperature dependence of the rate constants for  $\bullet\text{CO}_3^-$  with three cyano complexes of metal (Fe(II), Mo(IV), and W(IV)) and some inorganic anions ( $\text{SO}_3^{2-}$ ,  $\text{ClO}_2^-$ ,  $\text{NO}_2^-$ ,  $\text{I}^-$ , and  $\text{SCN}^-$ ) was also investigated (Huie *et al.*, 1991). The activation energies for such metal complexes and inorganic anions generally decrease with increasing driving force for the reaction, as expected for an outer sphere electron transfer.

Carbonate radicals can oxidize transition metal complexes. The carbonate radical reacts with a moderate reactivity ( $k = 1.8 \times 10^7 \text{ M}^{-1}\text{s}^{-1}$ ) with Ni(II)-glycine complex predominantly by hydrogen abstraction from the ligand (Elango *et al.*, 1988). One electron oxidation of Ni(II)-iminodiacetate by carbonate radical was reported (Mandal *et al.*, 1995). Using flash photolysis, reactions of carbonate radical with Ni (II), Co (II) and Cu (II) complexes of iminodiaacetic (IDA) and ethylenediaminetetraacetic acid (EDTA)

have been studied through time-resolved spectroscopy (Mandal *et al.*, 1991; 1992; 1999), with rate constants on the order of  $10^6$ - $10^7 M^{-1}s^{-1}$ . In these reactions, the carbonate radicals oxidized the metal center to its higher oxidation state through electron transfer.

### **1.5 Carbonate radicals in biological systems**

As a powerful oxidant, the carbonate radical is capable of the one-electron oxidation of several amino acids and proteins (Adams *et al.*, 1972a,b; Chen and Hoffman, 1973). Recently, it has been proposed that under certain circumstances carbonate radicals may be intermediates in free radical-mediated damage in biological systems (Bisby *et al.*, 1998) and its involvement in biological oxidation seems ubiquitous (Wolcott *et al.*, 1994). Bicarbonate ion is abundant in biological systems. The concentration of bicarbonate is approximately 25 mM in phagosomes. Therefore, there is ample bicarbonate available in biological systems to form carbonate radical from the scavenging of hydrogen peroxide-derived  $\bullet OH$  and these might be a significant contributor to radical-mediated damage (Lymar and Hurst, 1996). The low reactivity and longer lifetime of the carbonate radical relative to hydroxyl would allow it to diffuse further and to react more selectively with critical cellular targets (Lymar and Hurst, 1996). Peroxynitrite ( $OONO^\bullet$ ), a potent oxidant formed from a diffusion-controlled reaction between superoxide ( $\bullet O_2^-$ ) and nitrogen oxide ( $\bullet NO$ ), can cause oxidative damage to biological tissues (Lymar and Hurst, 1995b). Peroxynitrite has been reported to react with  $CO_2$  to generate an intermediate ( $ONO_2CO_2^-$ ), with a rate constant of  $3 \times 10^4 M^{-1}s^{-1}$  at 25 °C (Lymar and Hurst, 1995) and  $5.8 \times 10^4 M^{-1}s^{-1}$  at 37 °C (Denicola *et al.*, 1996). The cellular concentrations of  $CO_2$  *in vivo* are relatively high (1.3 mM) (Meli,

1999) due to high levels of bicarbonate in intracellular (12 mM) and interstitial fluids (30 mM) (Goldstein and Czapski, 1998). This suggests that the reaction of peroxynitrite with CO<sub>2</sub> is the predominant pathway for peroxynitrite disappearance in biological systems (Goldstein and Czapski, 1998; Meli, 1999). The formed intermediate has been proposed to consist of a caged radical pair ( $\bullet\text{CO}_3^- / \bullet\text{NO}_2$ ) which then decomposes into  $\bullet\text{CO}_3^-$  (Denicola *et al.*, 1996; Goldstein and Czapski 1998; Lyman and Hurst, 1998) as suggested by the chemiluminescence detected in this reaction (Radi *et al.*, 1993; Denicola *et al.*, 1996). Goldstein and Czapski (1998) used competition kinetic methods to measure the rate constants in peroxynitrite with excess carbon dioxide. These rate constants were similar to those determined directly for reactions of these substrates with  $\bullet\text{CO}_3^-$ . More recently, the carbonate radical was directly detected by rapid mixing continuous flow EPR. Carbonate radicals were formed in flow mixtures of peroxynitrite with bicarbonate-carbon dioxide over the physiological pH range of 6-9 (Bonin *et al.*, 1999; Meli *et al.*, 1999).

Hodgson and Fridovich (1976) reported that the addition of carbonate anion to an aerobic xanthine/xanthine oxidase system produced luminescence. This effect was attributed to a dimerization of  $\bullet\text{CO}_3^-$  (Lemercier *et al.*, 1997). Goss *et al.* (1999) examined the effect of bicarbonate on the peroxidase activity of copper-zinc superoxide dismutase (SOD1), using nitrite anion as a peroxidase probe. In contrast to a previous report (Sankarapandi and Zweier, 1999), bicarbonate is not an absolute requirement for eliciting the peroxidase activity of SOD1. However, bicarbonate enhanced the peroxidase activity of SOD1 via carbonate radicals.

## **1.6 Carbonate radical in the environment**

Estimations obtained from preliminary computational modeling study suggest carbonate radical concentrations are low in atmospheric aerosols and raindrops; hence, its presence in the atmosphere is considered unimportant (Graedel, 1981). However, the carbonate radical reaches for higher concentrations in surface waters and therefore may contribute to be important in limiting the persistence of some aquatic pollutants.

### **1.6.1 Photooxidants in natural waters**

Agrochemicals and other organic pollutants are introduced into aquatic environments either via direct application or through indirect pathways such as runoff, partitioning into condensed phases in the troposphere, and atmospheric deposition into freshwater and marine systems. Sunlight-induced direct and indirect photolysis are an important sink for chemical pollutants in such environments (Zepp, 1991). The rate constants for direct photolysis in sunlight of a specific chemical are a function of the absorption spectrum of the chemical, the quantum yield of the process, and the light intensity (Zepp and Cline, 1977). Direct photolysis, however, accounts for only a part of these sunlight-induced reactions. Indirect or sensitized photolysis has been shown to be an important degradation mechanism for some organic compounds that do not undergo rapid direct photolysis and are resistant to hydrolysis (Mabury and Crosby, 1996). Indirect photolysis is thought to involve various photooxidants in natural water (Zepp, 1991). The photooxidants include hydroxyl radical (Draper and Crosby, 1984), alkylperoxy radical (Mill *et al.*, 1980), singlet oxygen (Haag and Hoigne, 1986), triplet state (Zepp *et al.*, 1985), carbonate radical (Larson and Zepp, 1988), dibromide ion radical

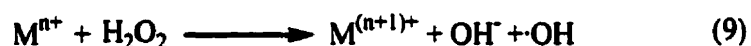
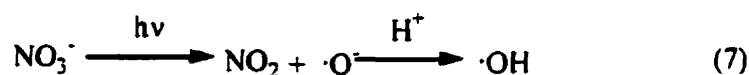
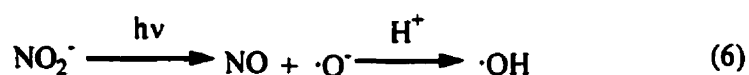
(Zafiriou *et al.*, 1984), solvated electrons (Zepp *et al.*, 1987a) and superoxide (Petasne and Zika, 1987). Hydrogen peroxide, a widely distributed oxidant in natural waters that is produced via the intermediacy of superoxide radicals (Cooper and Zika, 1983), may be involved in the oxidation of these compounds by the Fenton reaction (Zepp *et al.*, 1992) or by peroxidase-catalyzed oxidation (Cooper and Zepp, 1990). Each oxidant contributes to this systematic cleansing by reaction with and ultimately degradation of aquatic pollutants. Armbrust (1999) recently reviewed the photochemical processes influencing pesticide degradation in rice paddies. Degradation by the hydroxyl radical, the carbonate radical and by singlet oxygen has been shown to be important for selective classes of pesticide chemistry.

#### **1.6.2 Sources of hydroxyl radical as $\bullet\text{CO}_3^-$ precursor**

The hydroxyl radical is the most reactive oxidant known in the environment, with diffusion-limited second-order reaction rate constants for most organic pollutants of  $10^9$  to  $10^{10} \text{ M}^{-1}\text{S}^{-1}$  (Buxton and Greenstock, 1988). As the precursor of carbonate radical, the source of hydroxyl radical in natural waters is important in determining the steady state concentration of carbonate radical.

A variety of reaction pathways are available for the generation of hydroxyl radical in natural waters (Mabury and Crosby, 1994). The major sources appear to be the photolysis of nitrate (Hagg and Hoigne, 1985, Zepp *et al.*, 1987b), nitrite (Zafiriou, 1974), hydrogen peroxide (Draper and Crosby, 1981), and dissolved organic carbon (DOC) (Mill *et al.*, 1980). Production of hydroxyl by nonphotochemical pathways proceed via Fenton-type reactions between reduced metals (Fe, Cu, Mn) and hydrogen

peroxide (Barne & Sugden, 1986, Zepp et al, 1992). Equations (6-9) describe the photolysis of nitrite, nitrate, hydrogen peroxide and Fenton-type reactions respectively, to generate  $\bullet\text{OH}$ . The relative importance of any one of these pathways depends on the concentration, quantum yield, and absorption coefficient of the reactive solute. Haag and Hoigne (1985) have suggested that nitrate could well be the dominant precursor of photolytic production of hydroxyl radical in lake water.



Most natural waters contain substantial concentrations of nitrate and nitrite ions, which undergo direct photolysis to form hydroxyl radicals. Quantum yields ( $\phi$ ) for hydroxyl production from nitrate have been reported in the range of  $9.2\text{-}17 \times 10^{-3}$  at wavelengths greater than 290 nm (Zepp, 1987b). Nitrite quantum yields are wavelength dependent, decreasing as wavelength increases; typical values range from  $\phi = 0.015\text{-}0.08$  between 298 and 371 nm (Zafiriou, 1987). Generation of hydroxyl radicals from nitrate shows a nonlinear increase as nitrate concentration increases (Russi *et al.*, 1982; Hagg and Hoigne, 1985; Zepp *et al.*, 1987b). This may result from either a quenching of the excited state of nitrate (Hagg and Hoigne, 1985) or by scavenging of hydroxyl radical by nitrite (Zepp *et al.*, 1987b).

In sunlit surface waters, aquatic humic substances act as sensitizers or precursors for the production of different kinds of photooxidants including hydroxyl radicals (Mill *et al.*, 1980), hydrogen peroxide (Cooper and Zika, 1983; Draper and Crosby, 1981), singlet oxygen (Haag and Hoigne, 1986), organoperoxy radicals (Mill *et al.*, 1980; Faust and Hoigne, 1987), triplet states (Zepp *et al.*, 1985), solvated electrons (Zepp, 1987a) and superoxide (Petasne and Zika, 1987). Humic substances undergo reactions directly by various mechanisms, including energy transfer from the triplet state, and abstraction of electrons or hydrogen atoms (Zepp, 1985). Alternatively, the excited state can produce other reactive intermediates. Hydroxyl, singlet oxygen, solvated electrons, and hydrogen peroxide were identified as products of the photolysis of dissolved organic carbon (DOC) using electron spin resonance (ESR) spectroscopy (Takahashi *et al.*, 1988). These authors concluded that the formation of hydroxyl took place directly through homolytic cleavage of the humic acid, while photolysis of hydrogen peroxide represented a minor pathway. Most likely, the primary sources of most of these reactive species are photochemical reactions involving humic substances.

Mopper and Zhou (1990) reported that the total  $\bullet\text{OH}$  production rate in seawaters was significantly larger than expected from the sum of these processes including photolysis of nitrite, nitrate and photo-Fenton reactions. They concluded that there was a "missing source" of hydroxyl radical production and that this source was most likely due to the direct photolysis of (colored) dissolved organic matter (CDOM). Vaughan and Blough (1998) also reported that photolysis of Suwannee River fulvic acid (SRFA) solutions produced the hydroxyl radical under anaerobic conditions in proportion to the CDOM concentration. Since the excited triplet state of benzoquinone and certain

substituted benzoquinones is capable of abstracting a hydrogen atom from water to generate hydroxyl radical (Alegria *et al.*, 1997). It is suggested that the excited quinone groups existing within humic substances was capable of abstracting a hydrogen atom from water to generate hydroxyl radical (Vaughan and Blough, 1998).

Agricultural waters have concentrations of hydrogen peroxide as high as 6.8  $\mu\text{M}$ , while highly eutrophic waters have levels up to 32  $\mu\text{M}$  (Mabury and Crosby, 1994). Hydrogen peroxide was hypothesized to be formed via the solvated electron-superoxide radical pathway (Cooper and Zika, 1983). Solvated electrons are scavenged by dissolved oxygen ( $2 \times 10^{10} \text{ M}^{-1} \text{ s}^{-1}$ ) (Takahashi *et al.*, 1988), forming the superoxide radical anion which rapidly dismutates to form hydrogen peroxide. The generation of hydrogen peroxide in water correlated well with total organic carbon content and the amount of light absorbed by the sample; quantum yield was observed to decrease with increasing wavelength (Cooper and Zika, 1983).

Hydrogen peroxide produces hydroxyl cleanly upon irradiation by homolysis of the peroxide bond (Buxton and Greenstock, 1988). Quantum yields were low due to the weak absorption in the actinic portion of the sunlight spectrum (Hagg and Hoigne, 1985; Draper and Crosby, 1981). Production of hydroxyl radical by non-photochemical pathways proceed via Fenton-type as shown in Equation 9. In certain seawater microenvironments, where concentration of Fe (II) and Cu (I) could reach a level of  $10^{-12}$  and  $10^{-10} \text{ M}$ , respectively, the reduction of  $\text{H}_2\text{O}_2$  would yield a significant amount of hydroxyl radicals (Moffett and Zika, 1987).

The high reactivity of hydroxyl radical leads to its rapid scavenging by numerous constituents normally found in natural water. Typically, DOC, bicarbonate, and carbonate

account for nearly all the scavenging of OH in most waters (Haag and Hoigne, 1985). The rate constant of DOC scavenging hydroxyl radical is  $2.5 \times 10^4 \text{ (mg of C/L)}^{-1}\text{s}^{-1}$  (Zepp *et al.*, 1987b; Larson and Zepp, 1988). Brezonik and Fulkerson-Brekken (1998) also reported the rate constant for  $\bullet\text{OH}$  scavenging by DOC from five field waters in the narrow range of  $2.3 \pm 0.77 \times 10^4 \text{ (mg of C/L)}^{-1}\text{s}^{-1}$ . Carbonate/bicarbonate ion, a major component in natural waters, can react with hydroxyl radicals to form carbonate radicals, with second order rate constants of  $4.2 \times 10^8 \text{ M}^{-1}\text{s}^{-1}$  and  $1.5 \times 10^7 \text{ M}^{-1}\text{s}^{-1}$ , respectively (Chen and Hoffman, 1973). Sources of hydroxyl radical and production of carbonate radical in natural waters are shown in Figure 1.1.

### **1.6.3 Steady-state concentration of carbonate radical in natural waters**

Carbonates and bicarbonates are major inorganic components of natural waters and they are extremely important for photosynthesis/respiration as well as for the regulation of pH in the aquatic environment (Stumm and Morgan, 1981). Steady-state concentrations of radicals can be obtained through the photoproduction rate and lifetime of the transients (Zepp, 1991). The production rate of carbonate radicals is determined by the production rate of hydroxyl radicals, and its subsequent scavenging through carbonate and bicarbonate ions in natural waters (Larson and Zepp, 1988). In fresh waters, the reaction of carbonate radical with DOC is a major fate of such radicals, so the concentration of DOC influences the lifetime of the carbonate radical (Larson and Zepp, 1988). As a result, the computed steady-state concentration of the carbonate radical in Lake Greifensee surface waters in summer sunlight was reported to be approximately  $3 \times 10^{-14} \text{ M}$  (Larson and Zepp, 1988). In comparison, steady-state hydroxyl concentration in field waters is much lower, in the

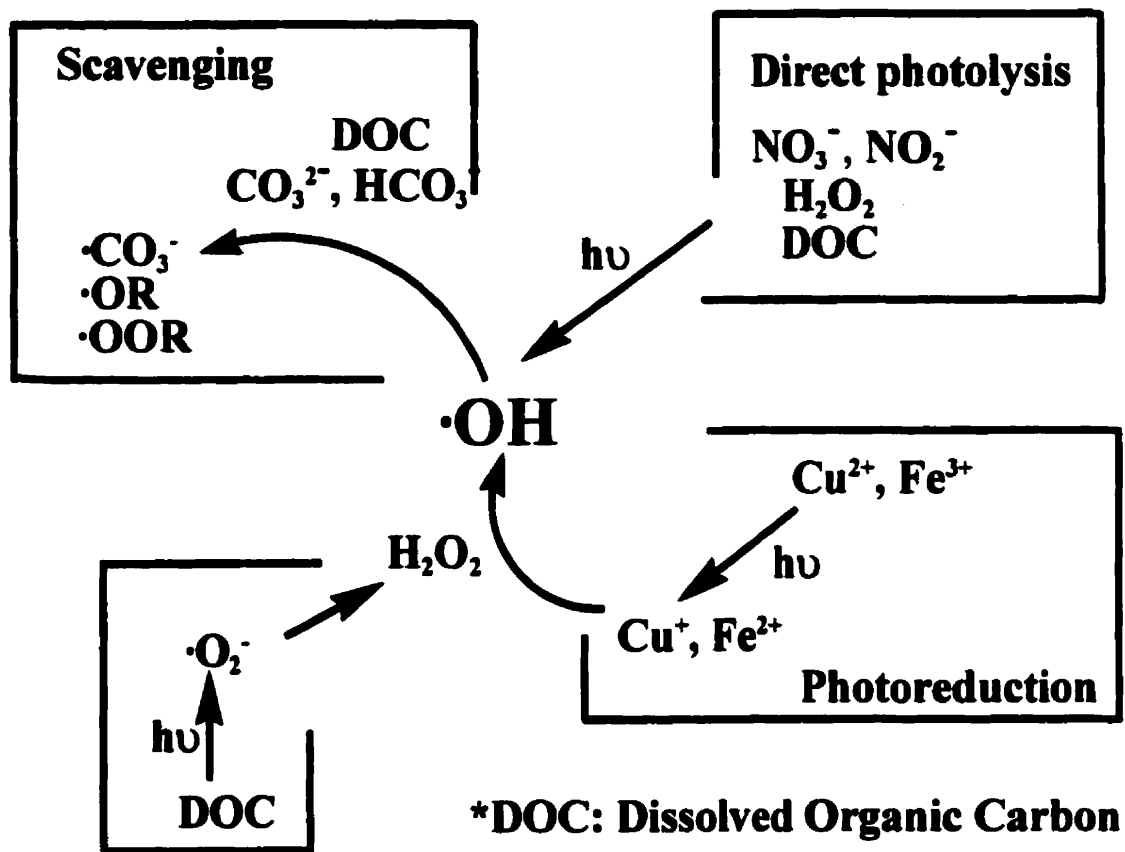


**Figure 1.1.** Sources of hydroxyl radical and production of carbonate radical in natural waters.

range of  $5 \times 10^{-16}$  to  $1.5 \times 10^{-18}$  M in natural fresh waters (Mill *et al.*, 1980; Russi *et al.*, 1982) and  $1.1$  to  $12 \times 10^{-18}$  M in coastal and open ocean surface waters (Mopper and Zhou, 1990). The effect of carbonate and bicarbonate on steady-state concentrations of hydroxyl radical in natural waters through nitrate-induced photolysis was reported recently (Brezonik and Flukerson-Brekken, 1998). The steady-state concentrations of hydroxyl radical decreased with increasing carbonate/bicarbonate concentration in natural waters. The relatively high steady-state concentrations of carbonate radical in natural waters make this radical important in limiting the persistence of some electron-rich aquatic pollutants.

#### **1.6.4 Carbonate radical in environmental applications**

Larson and Zepp (1988) reported that carbonate radicals reacted very rapidly with the human carcinogens benzidine and 1-naphthylamine with the second-order rate constant above  $10^9 \text{ M}^{-1}\text{s}^{-1}$ , at intermediate rates with the urea herbicide monuron, and at low rates with the triazine herbicide atrazine and the carbamate herbicide protham. Kochany (1992) investigated the photodegradation of the herbicide bromoxynil in the presence of carbonate and bicarbonate. However, a quenching effect by carbonate and a much smaller effect by bicarbonate was observed. It was suggested that hydrated electrons were the primary transients degrading the bromoxynil. More distinct quenching of photolysis by carbonate can be explained by the higher reactivity of carbonate radical toward hydrated electrons ( $k = 3.6 \times 10^6 \text{ M}^{-1}\text{s}^{-1}$ ) compared to

bicarbonate radical ( $k < 10^6 \text{ M}^{-1} \text{ s}^{-1}$ ) as well as higher absorption of the former (Eriksen *et al.*, 1985).

Advanced oxidation techniques (AOT) usually use  $\bullet\text{OH}$  radical to oxidize aquatic pollutants. Hong *et al.* (1996) reported a new AOT modeling of illuminated and dark advanced oxidation processes. Kinetic data of carbonate radical reaction with aromatic pollutants was used in this simple model system to investigate the implications of carbonate radical kinetics in water treatment processes (Umschlag and Herrmann, 1999). The degradation of aromatic pollutants in  $\bullet\text{OH}$ -based water treatment may proceed via the carbonate radical in carbonate-containing waters.

Carbonate radicals lead to bromate and chlorate formation during drinking water treatment. These two compounds are contaminants being considered for regulation in drinking water. As proven carcinogens, bromate and chlorate are disinfection by-products (DBP) of the ozonation of bromide and chlorine-containing waters. During ozonation, carbonate radicals formed from hydroxyl radical scavenging, oxidize the intermediate hypobromite to bromite, which is then further oxidized by ozone to bromate (Gunten *et al.*, 1994; 1995). Carbonate radicals formed in alkaline waters act as secondary oxidants of bromine leading to the enhanced bromate formation (Ozegin *et al.*, 1998). During ozonation of chlorine-containing waters, the presence of alkalinity also enhanced chlorate formation due to the secondary reactions between carbonate radicals and chlorine species (Siddiqui *et al.*, 1996).

## **1.7 Scope of Dissertation Research**

The objectives of this dissertation research are to determine the steady state concentration of carbonate radical in natural waters, measure the second-order rate constant of carbonate radical towards chemical pollutants, investigate the reaction pathways and reactivities of carbonate radical to sulfur-containing compounds, and determine the influence of photooxidation on the hydrolysis rates of photo-induced products.

Chapter 2 discusses a new method to measure the steady-state concentration of carbonate radical in a variety of natural waters using *N, N*-dimethylaniline as a specific probe. The measured steady-state concentration strongly depended on light intensity and ranged from  $5 \times 10^{-15}$  to  $10^{-13}$  *M*. A linear relationship was also obtained between steady state concentration of carbonate radicals and major components in natural waters, especially nitrate and DOC concentrations. Chapter 3 reports a competition kinetic method to measure the second-order rate constants of carbonate radical toward pesticides. Of nine pesticides investigated, fenthion was the most reactive, followed by phorate, with rate constants for both species above  $10^7$   $M^{-1}s^{-1}$ . Fluometuron and atrazine were of intermediate reactivity, and methyl parathion was slowest with rate constant of  $2.0 \times 10^5$   $M^{-1}s^{-1}$ . Chapter 4 discusses the reaction pathways and reactivities of carbonate radical towards sulfur-containing compounds. Thioanisole, fenthion and dibenzothiophene were selected as model sulfur-containing compounds. The reaction pathways were through the corresponding sulfoxides, followed by the sulphone products. Each probe was further investigated in a sunlight simulator under varying conditions, and carbonate radical was found to contribute toward the photo-degradation of these

compounds. Chapter 5 discusses the influence of photooxidation on the hydrolysis rates of photo-induced products of fenthion. The hydrolysis kinetics of fenthion and its five metabolites were investigated at different pHs and temperatures. In comparison with fenthion, all metabolites had more rapid hydrolysis rates, especially under basic conditions. Chapter 6 summarizes the final conclusions and suggests areas for future investigation.

### **1.8 References**

Adams, G.E., Aldrich, J.E., Bisby, R.H., Cundall, R.B, Redpath, J.L., Willson, R.L., 1972. Selective free radical reactions with proteins and enzymes: reactions of inorganic radical with amino acids. *Radiation Research* 49, 278-289.

Adams, G.E., Bisby, R.H., Cundall, R.B, Redpath, J.L., Willson, R.L., 1972. Selective free radical reactions with proteins and enzymes: the inactivation of ribonuclease. *Radiation Research* 49, 290-299.

Alegria, A., Ferrer, A., Sepulveda, E., 1997. Photochemistry of water-soluble quinones. Production of a water-derived spin adduct. *Photochem. Photobiol.* 66, 436-442.

Anbar, M., Meyerstein, D., Neta, P., 1966. The reactivity of aromatic compounds toward hydroxyl radicals. *J. Phys. Chem.* 70, 2660-2662.

Armbrust, K.L., 1999. Photochemical processes influencing pesticide degradation in rice paddies. *J. Pestic. Sci.* 24, 69-73.

Behar, D., Czapski, G., Duchovny, I., 1970. Carbonate radical in flash photolysis and pulse radiolysis of aqueous carbonate solutions. *J. Phys. Chem.* 74, 2206-2210.

Behar, D., Fessenden, R.W., 1972a. Electron spin resonance studies of inorganic radicals in irradiated aqueous solutions. I. Direct observation. *J. Phys. Chem.* 76, 1706-1710.

Behar, D., Fessenden, R.W., 1972b. Electron spin resonance studies of inorganic radicals in irradiated aqueous solutions. II. Radical trapping with nitromethane. *J. Phys. Chem.* 76, 1710-1721.

Beitz, T., Bechmann, W., Mitzner, 1998. Investigations of reactions of selected azaarenes with radicals in water. 1. Hydroxyl and sulfate radicals. *J. Phys. Chem. A* 102, 6760-6765.

Bhattacharya, A., De, A., Mandal, P.C., 1998. Carbonate radical induced polymerisation of pyrrole: a steady state and flash photolysis study. *J. Radional. Nucl. Chem.* 230, 91-95.

Bisby, R.H., Johnson, S.A., Parker, A.W., Tavender, S.M., 1998. Time-resolved resonance Raman spectroscopy of the carbonate radical. *J. Chem. Soc., Faraday Trans.* 94, 2069-2072.

Bonini, M.G., Radi, R., Ferrer-Sueta, G., 1999. Direct EPR detection of the carbonate radical anion produced from peroxyxynitrite and carbon dioxide. *J. Biol. Chem.* 274, 10802-10806.

Brezonik, P.L., Fulkerson-Brekken, J., 1998. Nitrate-induced photolysis in natural waters. Controls on concentrations of hydroxyl radical photo-intermediates by natural scavenging agents. *Environ. Sci. Technol.* 32, 3004-3010.

Buxton, G.V., Greenstock, C.L., 1988. Critical review of rate constants for reaction of hydrated electrons, hydrogen atoms and hydroxyl radicals ( $\bullet\text{OH}/\bullet\text{O}^-$ ) in aqueous solution. *J. Phys. Chem. Ref. Data.* 17, 513-886.

Chantry, G.W., Horsfield, A., Morton, J.R., Whiffen, D.H., 1962. The structure, electron resonance and optical spectra of trapped  $\text{CO}_3^-$  and  $\text{NO}_3^-$ . *Mol. Phys.* 5, 589-599.

Chawla, O.P., Fessenden, 1975. Electron spin resonance and pulse radiolysis studies of some reactions of  $\text{SO}_4^{\bullet-}$ . *J. Phys. Chem.* 79, 2693-2700.

Chen, S.N., Cope, V.W., Hoffman, M.Z., 1973. Behavior of  $\text{CO}_3^-$  radicals generated in the flash photolysis of carbonatoamine complexes of cobalt (III) in aqueous solution. *J Phys Chem* 77, 1111-1116.

Chen, S.N., Hoffman, M.Z., 1973. Rate constants for the reaction of the carbonate radical with compounds of biochemical interest in neutral aqueous solution. *Radiation Research* 56,40-47.

Chen, S.N., Hoffman, M.Z., 1974. Reactivity of the carbonate radical in aqueous solution. Tryptophan and its derivatives. *J. Phys. Chem.* 78, 2099-2102.

Chen, S.N., Hoffman, M.Z., 1975. Effect of pH on the reactivity of the carbonate radical in aqueous solution. *Radiation Research* 62:18-27.

Chen, S.N., Hoffman, M.Z., Parsons, G.H., Jr., 1975. Reactivity of the carbonate radical toward aromatic compounds in aqueous solution. *J. Phys. Chem.* 79, 1911-1912.

Clifton, C.L., Huie, R.E., 1989. Rate constants for hydrogen abstraction reaction of the sulfate radical,  $\text{SO}_4^{\bullet-}$  alcohols. *Int. J. Chem. Kinet.* 21, 677-687.

Clifton, C.L., Huie, R.E., 1993. Rate constants for some hydrogen abstraction reactions of carbonate radical. *Int. J. Chem. Kinet.* 25, 199-203.

Cooper, W.J., Zika, R.G., 1983. Photochemical generation of hydrogen peroxide in surface and ground waters exposed to sunlight. *Science* 220, 711-712.

- Cooper, W.C., Zepp, R.G., 1990. Hydrogen peroxide decay in waters with suspended soils: evidence for biologically mediated processes. *Can. J. Fish. Aq. Sci.* 47, 883-893.
- Cope, V.W., Chen, S.N., Hoffman, M.Z., 1973. Intermediates in the photochemistry of carbonato-amine complexes of cobalt (III).  $\text{CO}_3^-$  radicals and the aquocarbonato complex. *J. Am. Chem. Soc.* 95, 3116-3121.
- Crable, G.F., Kearns, G.L., 1962. Effect of substituent groups on the ionization potentials of benzenes. *J. Phys. Chem.* 66, 436-439.
- Czapski, G., Lyman, S.V., Schwart, H.A., 1999. Acidity of the carbonate radical. *J. Phys. Chem. A* 103, 3447-3450.
- Denicola, A., Freeman, B.A., Trujillo, M., Radi, R., 1996. Peroxynitrite reaction with carbon dioxide/bicarbonate kinetics and influence on peroxynitrite-mediated oxidation. *Arch. Biochem. Biophys.* 333, 49-58.
- Draper, W.M., Crosby, D.G., 1984. Solar photooxidation of pesticides in dilute hydrogen peroxide. *J. Agric. Food Chem.* 32, 231-237.
- Elango, T.P., Ramkrishnan, V., Vancheesan, S., Kuriacose, J.C., 1984. Reaction of the carbonate radical with substituted anilines. *Proc. Indian Acad. Sci.* 93, 47-52.
- Elango, T.P., Ramkrishnan, V., Kuriacose, J.C., 1985a. Generation and reaction of inorganic radicals with special reference to carbonate radicals. *J. Indian Chem. Soc.* LXII:1033-1037.
- Elango, T.P., Ramkrishnan, V., Vancheesan, S., Kuriacose, J.C., 1985b. Reaction of the carbonate radical with aliphatic amines. *Tetrahedron* 41, 3837-3843.

- Elango, T.P., Vancheesan, S., Ramkrishnan, V., Kuriacose, J.C., 1988. Radiation chemical studies of nickle-glycine reaction with carbonate radical. *J. Radional. Nucl. Chem.* 125, 151-155.
- Eriksen, T.E., Lind, J., 1983. Radical-induced oxidation of pyridazine-3,6-diol (maleic hydrazide). *J. Chem. Soc. Faraday Trans.* 79, 1493-1501.
- Eriksen, T.E., Lind, J., Merenyi, G., 1985. On the acid-base equilibrium of the carbonate radical. *Radiat. Phys. Chem.* 26, 197-199.
- Faust, B.C., Hoigné, J., 1987. Sensitized photooxidation of phenols by fulvic acid and in natural waters. *Environ. Sci. Technol.* 21:957-964.
- Ferry, J.L., Fox, M.A., 1999. Temperature effects on the kinetics of carbonate radical reactions in near-critical and supercritical water. *J. Phys. Chem. A* 103, 3483-3441.
- Franklin, J. L., Harland, P. W., 1974. Gaseous negative ions. *A. Rev. Phys. Chem.* 25, 485-526.
- Gogolev, A.V., Fedoseev, A.M., Makarow, I.E., Pikaev, A.K., 1989. Pulse radiolysis study of the reactivity of inorganic free radicals with ferrocyanide and octacyanomolybdate ions in aqueous solutions. *High Energy Chem.* 23, 162-166.
- Goldstein, S., Czapski, G., 1998. Formation of peroxyxynitrite from the reaction of peroxyxynitrite with CO<sub>2</sub>: Evidence for carbonate radical production. *J. Am. Chem. Soc.* 120, 3458-3463.
- Goss, S.P.A., Singh, R.J., Kalyanaramant, B., 1999. Bicarbonate enhances the peroxidase activity of Cu, Zn-superoxide dismutase. *J. Biol. Chem.* 274, 28233-28239.

Graedel, T.E., Weschler, C.J., 1981. Chemistry within aqueous atmospheric aerosols and raindrops. *Rev. Geophys. Space Phys.* 19, 505-539.

Gunten, U.V., Hoigné, J., 1994. Bromate formation during ozonation of bromide-containing waters; interaction of ozone and hydroxyl radical reactions. *Environ. Sci. Technol.* 28, 1234-1242.

Gunten, U.V., Hoigné, J., Bruchet, A., 1995. Bromate formation during ozonation of bromide-containing waters. *Water Supply* 13, 45-50.

Hagg, W.R., Hoigné, J., 1985. Photo-sensitized oxidation in natural water via  $\bullet\text{OH}$  radicals. *Chemosphere* 14:1659-1671.

Hagg, W.R., Hoigné, J., 1986. Singlet oxygen in surface waters. 3. Photochemical formation and steady-state concentrations in various types of waters. *Environ. Sci. Technol.* 20, 341-348.

Hart, E.J., Boag, J.W., 1962. Absorption spectrum of the hydrated electron in water and in aqueous solutions. *J. Am. Chem. Soc.* 84, 4090-4095.

Hayon, E., McGarvey, J.J., 1967. Flash photolysis in the vacuum ultraviolet region of  $\text{SO}_4^{2-}$ ,  $\text{CO}_3^{2-}$ , and  $\text{OH}^-$  ions in aqueous solutions. *J. Phys. Chem.* 71, 1472-1477.

Hodgson, E.K., Fridovich, I., 1976. The mechanism of the activity-dependent luminescence of xanthine oxidase. *Arch Biochem. Biophys.* 172, 202-205.

Hoigné J, Bader H. 1979. Ozonation of water: "Oxidation-competition values" of different types of waters used in Switzerland. *Ozone Sci. Eng.* 1:357-372.

Hong, A., Zappi, M.E., Kuo, C.H., Hill, D., 1996. Modeling kinetics of illuminated and dark advanced oxidation processes. *J. Environ. Eng.* 122, 58-62.

Huie, R.E., Clifton, C.L., Neta, P., 1991a. Electron transfer reaction rates and equilibria of the carbonate and sulfate radical anions. *Radiat. Phys. Chem.* 38, 477-481.

Huie, R.E., Shoute, L.C.T., Neta, P., 1991b. Temperature dependence of the rate constants for reactions of the carbonate radical with organic and inorganic reductants. *Int. J. Chem. Kinet.* 23, 541-552.

Kochany, J., Lipczynska-Kochany, E., 1992. Application of the EPR spin-trapping technique for the investigation of the reaction of carbonate, bicarbonate, and phosphate anions with hydroxyl radicals generated by the photolysis of H<sub>2</sub>O<sub>2</sub>. *Chemosphere.* 25, 1769-1782.

Kochany, J., 1992. Effects of carbonates on the aquatic photodegradation rate of bromoxynil (3, 5-dibromo-4-hydroxybenzoxynitrile) herbicide. *Chemosphere* 24, 1119-1126.

Kuzmin, V.A., 1972. Reactions of the CO<sub>3</sub><sup>•-</sup> and SiO<sub>3</sub><sup>•-</sup> radical anions. *High Energy Chem.* 6, 338-339.

Larson, R.A., Zepp, R.G., 1988. Reactivity of the carbonate radical with aniline derivatives. *Environ. Toxicol. Chem.* 7, 265-274.

Lemercier, J.N., Padamaja, S., Cueto, R., Squadrito, G.L., Uppu, R.M., Pryor, W.A., 1997. Carbon dioxide modulation of hydroxylation and nitration of phenol by peroxyxynitrite. *Arch. Biochem. Biophys.* 345, 160-170.

Lilie, J., Hanrahan, R.J., Hengkein, A., 1978. O<sup>•-</sup> transfer reactions of the carbonate radical anion. *Radia. Phys. Chem.* 11, 225-227.

Lymar, S., Hurst, J.K., 1995. Rapid reaction between peroxonitrite ion and carbon dioxide; implication for biological activity. *J. Am. Chem. Soc.* 117, 8867-8868.

Lymar, S.V., Hurst, J.K., 1996. Peroxynitrite-mediated cellular damage or cellular protectant. *Chem. Res. Toxicol.* 8, 845-850.

Lymar, S., Hurst, J.K., 1998. CO<sub>2</sub>-catalyzed one-electron oxidation by peroxynitrite: properties of the reactive intermediate. *Inorg. Chem.* 37, 392-301.

Mabury, S.A., Crosby, D.G., 1994. The relationship of hydroxyl reactivity to pesticide persistence. Aquatic and surface photochemistry. CRC Press, Boca Raton, FL, USA, pp 149-161.

Mabury, S.A., Crosby, D.G., 1996. Pesticide reactivity toward hydroxyl and its relationship to field persistence. *J. Agric. Food Chem.* 44, 1920-1924.

Mandal, P.C., Bardhan, D.K., Sarkar, S., Bhattacharyya, S.N., 1991. Oxidation of Nickle (II) ethylenediaminetetraacetate by carbonate radical. *J. Chem. Soc. Dalton Trans.* 1457-1461.

Mandal, P.C., Bardhan, D.K., Bhattacharyya, S.N., 1992. Reactions of carbonate radical with cobalt(II) aminopolycarboxylates. *J. Radional. Nucl. Chem.* 166, 87-96.

Mandal, P.C., Bardhan, D.K., 1995. One-electron oxidation of Ni(II)-iminodiacetate by carbonate radical. *J. Radional. Nucl. Chem.* 191, 349-359.

Mandal, P.C., Bardhan, D.K., 1999. Oxidation of Cu(II)-aminopolycarboxylates by carbonate radical: A flash photolysis study. *J. Radional. Nucl. Chem.* 241, 553-560.

Meites, L., Zuman, P., 1977. CRC handbook series of organic electrochemistry. Vols. 1-3 CRC press, Cleveland, OH.

- Meli, R., Nauser, T., Koppenol, W.H., 1999. Direct observation of intermediates in the reaction of peroxyxynitrite with carbon dioxide. *Helv. Chim. Acta* 82, 722-725.
- Mill, T., Hendry, D.G., Richardson, H., 1980. Free-radical oxidants in natural waters. *Science* 207:886-887.
- Moffett, J.W., Zika, R.G., 1987. Reaction kinetics of hydrogen peroxide with copper and iron in seawater. *Environ. Sci. Technol.* 21, 804-810.
- Moore, J.S., Phillips, G.O., Sosnowski, A., 1977. Reaction of the carbonate radical anion with substituted phenols. *Int. J. Radiat. Biol.* 31, 603-605.
- Mopper, K., Zhou, X. 1990. Hydroxyl radical photoproduction in the sea and its potential impact on marine process. *Science* 250, 661-664.
- Murata, T., Miki, T., 1993. Trapped-hole centers in irradiated  $\text{Li}_3\text{VO}_4$ . *J. Appl. Phys.* 73, 1110-1113.
- Neta, P., Huie, R.E., 1988. Rate constants for reactions of inorganic radicals in aqueous solution. *J. Phys. Chem. Ref. Data* 17, 1028-1079.
- Ozekin, K., Westerhoff, P., amy, G.L., Siddiqui, M., 1998. Molecular ozone and radical pathways of bromate formation during ozonation. *J. Environ. Eng.* 456-462.
- Padmaja, S., Madison, S.A., 1999. Hydroxyl radical-induced oxidation od azo dyes: a pulse radiolysis study. *J. Phys. Org. Chem.* 12, 221-226.
- Petasne, R.G., Zika, R.G., 1987. Fate of superoxide in costal sea water. *Nature* 325, 516-518.

Radi, R., Cosgrove, T.P., Beckman, J.S., Freeman, B.A., 1993. Peroxynitrite-induced luminol chemiluminescence. *Biochem. J.* 290, 51-57.

Russi, H., Kotzias, D., Korte, F., 1982. Photoinduzierte hydroxylierungsreaktionen organischer chemikalien in natürlichen gewässern. *Chemosphere* 11:1041-1048.

Sankarapandi, S., Zweier, J.L., 1999. Bicarbonate is required for the peroxidase function of Cu, Zn-superoxide dismutase at physiological pH. *J. Biol. Chem.* 274, 1226-1232.

Siddiqui, M.S., 1996. Chlorine-ozone interactions: formation of chlorate. *Wat. Res.* 30, 2160-2170.

Stumm, W., Morgan, J.J., 1981. Aquatic chemistry. An introduction emphasizing chemical equilibrium in natural waters. J. Wiley and Sons, New York, pp.171-228.

Takahashi, N.M.I., Mikami, N., Matsuda, T., Miyamoto, J., 1988. Identification of reactive oxygen species generated by irradiation of aqueous humic acid solution. *J. Pestic. Sci.* 13, 429-435.

Tavender, S.M., Johnson, S.A., Balsom, D., Parker, A.W., Bisby, R.H., 1999. The carbonate,  $\text{CO}_3^{\bullet-}$  solution studied by resonance Raman spectroscopy. *Laser Chemistry* 19, 311-316.

Umschlag, T., Herrmann, H., 1999. The carbonate radical ( $\text{HCO}_3/\text{CO}_3^{\bullet-}$ ) as a reactive intermediate in water chemistry: kinetics and modelling. *Acta Hydrochim. Hydrobiol.* 27, 214-222.

Vaughan, P.P., Blough, N.V., 1998. Photochemical formation of hydroxyl radical by constituents of natural waters. *Environ. Sci. Technol.* 32, 2947-2953.

Walsh, A.D., 1953. The electronic orbitals, shapes, and spectra of polyatomic molecules. Art V. Tetratomic, non-hydride molecules, AB<sub>3</sub>. *J. Chem. Soc.* 2301-2306.

Weeks, J. L., Rabani, J., 1966. The pulse radiolysis of deaerated aqueous solutions. I. Transient optical spectrum and mechanism. II. pk for OH radicals. *J. Phys. Chem.* 70, 2100-2106.

Wolcott, R. G., Franks, B.S., Hannum, D.M., Hurst, J.K., 1994. Bactericidal potency of hydroxyl radical in physiological environments. *J. Biol. Chem.* 269, 9721-9728.

Zafiriou, O.C., Jousset-Dubien, J., Zepp, R.G., Zika, R.G., 1984. Photochemistry of natural waters. *Environ. Sci. Technol.* 18, 358A-371A.

Zafiriou, O.C., Bonneau, R., 1987. Wavelength-dependent quantum yield of OH radical formation from photolysis of nitrite ion in water. *Photochem. Photobiol.* 45,723-727.

Zafiriou, O.C., 1974. Sources and reactions of OH and daughter radicals in seawater. *J. Geophys. Res.* 79, 4491-4497.

Zepp, R.G., Schotzhauer, P.F., Sink, R.M., 1985. Photosensitized transformation involving electronic energy transfer in natural waters: role of humic substances. *Environ. Sci. Technol.* 19, 74-81.

Zepp, R.G., Braun, A.M., Hoigné, J., Leenheer, J.A., 1987a. Photoproduction of hydrated electrons from natural organic solutes in aquatic environments. *Environ. Sci. Technol.* 21, 485-490.

Zepp, R.G., Hoigné, J., Bader, H., 1987b. Nitrate-induced photooxidation of trace organic chemicals in waters. *Environ. Sci. Technol.* 21, 443-450.

Zepp, R.G., Faust, B.C., Hoigné, J., 1992. Hydroxyl radical formation in aqueous reactions (pH 3-8) of iron (II) with hydrogen peroxide: the photo-Fenton reaction. *Environ. Sci. Technol.* 26, 313-319.

Zepp, R.G., 1991. Photochemical fate of agrochemicals in natural waters. Pesticide Chemistry: advances in international research, development, and legislation. Proceedings of the Seventh International Congress of Pesticide Chemistry (IUPAC), Hamburg, Germany, August 5-10, 1990, PP. 329-345.

Zepp, R.G., Cline, D.M., 1977. Rates of direct photolysis in aquatic environment. *Environ. Sci. Technol.* 11, 359-366.

Zuo, Z., Cai, Z., Katsumura, Y., Chitose, N., Muroya, Y., 1999. Reinvestigation of the acid-base equilibrium of the (bi) carbonate radical and pH dependence of its reactivity with inorganic reactants. *Radia. Phys. Chem.* 55, 15-23.

## **Chapter Two**

### **Steady State Concentrations of Carbonate Radicals in Natural Waters**

## 2.1 INTRODUCTION

In natural waters, the persistence of chemical pollutants is limited by the ability of such waters to cleanse themselves of xenobiotics. Sunlight-induced direct and indirect photoreactions provide an important sink for these pollutants in the aquatic environment. Direct photolysis, however, accounts for only a part of these sunlight-induced reactions. Indirect photoreactions involve photochemically produced reactive chemical transients (Zepp, 1991). These transients include hydroxyl, alkylperoxy, and carbonate radicals, singlet oxygen, aqueous electrons, and triplet states (Mabury and Crosby, 1996). Each transient contributes towards this systematic self-cleansing by reacting with and ultimately degrading aquatic pollutants. Natural bodies of water exhibit pronounced variation in composition, as is made evident by their change in appearance. The nature and concentrations of these transients, and thus indirect photoreaction rates, strongly depend on the composition of the water, in particular, on the concentrations of dissolved organic carbon (DOC), nitrate, nitrite, and trace metals (Zepp, 1991).

Carbonate radical ( $\bullet\text{CO}_3^-$ ) is a selective oxidant which reacts rapidly with electron-rich aromatic anilines and phenols (Larson and Zepp, 1988). It may play an important role in oxidizing sulfur-containing compounds (rate constants  $\sim 10^6$  to  $10^7 \text{ M}^{-1}\text{s}^{-1}$ ) (Chen and Hoffman, 1973) and thus in limiting the persistence of such compounds in the environment. The carbonate radical is generated through the reaction of hydroxyl radical ( $\bullet\text{OH}$ ) with either carbonate or bicarbonate ions (Hoigné and Bader, 1977), however, little attention has been afforded the carbonate radical reaction in natural waters. In most natural waters, the hydroxyl radical is generated through sunlight interaction with nitrate (Zepp *et al.*, 1987a), nitrite (Zafiriou, 1974), DOC (Mill *et al.*, 1980), hydrogen peroxide (Draper and Crosby,

1981) and various dissolved metal species through a photo-Fenton reaction (Zepp *et al.*, 1992). Haag and Hoigné (1985) have suggested nitrate could well be the dominant precursor of photolytic production of  $\bullet\text{OH}$  in natural waters. DOC in sunlit surface waters plays a role in producing or consuming different types of transient species including hydroxyl radicals, hydrogen peroxide, singlet oxygen and peroxy radicals. The fate of the hydroxyl radical involves competitive interactions with DOC, carbonate ion, and bicarbonate ion, thereby influencing the subsequent rate of carbonate radical production. The formation of carbonate radicals through reaction with hydroxyl is particularly favorable in high-carbonate waters (more than  $1 \times 10^{-3} \text{ M}$ ) (Larson and Zepp, 1988).

Two general approaches have been used in examining the transient reactants involved in photochemical processes in natural waters: laser flash photolysis and continuous irradiation. Triplet states, singlet oxygen, and solvated electrons have been studied using laser flash photolysis to observe these transients directly (Zepp, 1987b; Zafiriou and Bonneau, 1987). However, the high intensities of laser pulses can sometimes produce transients in much higher quantum yields than those observed with natural light, which limit their range of application. In most cases, the identity and concentration of transients produced on irradiation of natural waters have been inferred indirectly through steady-state analysis of the kinetic results obtained in continuous irradiations with monochromatic light or with sunlight. This approach involves the addition of a readily detected "probe" substance to a system that reacts with the transient in a well-defined way. The steady-state concentration of each transient formed during solar irradiation was determined from the apparent first-order disappearance rate of added organic probe compounds. The probe compounds used had selective reactivities with the

individual transient species of interest. For example, butyl chloride has been used to scavenge photochemically produced hydroxyl radicals (Hagg and Hoigné, 1985), halocarbons to trap the solvated electron (Zepp *et al.*, 1987b), and trimethylphenol to trap organoperoxy radicals (Faust and Hoigné, 1987).

Steady-state concentrations of radicals can also be obtained through the photoproduction rate and lifetime of the transients. The photoproduction rate of hydroxyl radicals probably falls within the range of  $10^{-12}$  to  $10^{-10}$  M/s, depending on the concentrations of nitrate and DOC besides the intensity of sunlight (Zepp *et al.*, 1987a; Hagg and Hoigné, 1985). The transient lifetime can be approximately estimated on the basis of the kinetic parameters for the reaction of the transient, or determined experimentally.

Steady-state hydroxyl concentrations ( $[\bullet\text{OH}]_{ss}$ ) have been reported in the range of  $5 \times 10^{-16}$  to  $1.5 \times 10^{-18}$  M in natural fresh waters (Mill *et al.*, 1980; Russi *et al.*, 1982) and 1.1 to  $12 \times 10^{-18}$  M in coastal and open ocean surface waters (Mopper and Zhou, 1990). Carbonate radical steady-state concentrations are a function of the hydroxyl production rate and the ratio of scavenging between carbonate species and DOC, and are also related to the lifetimes of carbonate radicals in natural waters (Larson and Zepp, 1988). In fresh waters, the reaction of carbonate radicals with DOC is a major fate of such radicals. In natural waters, concentrations of carbonate radical are expected to be significantly higher than those of hydroxyl radicals, since carbonate radical is a more selective oxidant than hydroxyl radical. Larson and Zepp (1988) reported that the computed steady-state concentration of carbonate radical ( $[\bullet\text{CO}_3]_{ss}$ ) in Lake Greifensee surface waters in summer sunlight was approximately  $3 \times 10^{-14}$  M.

Carbonate radicals are not directly observable at predicted environmental concentrations. Thus a probe, selective for the carbonate radical, is required. *N, N*-dimethylaniline (DMA) was selected as a specific probe owing to its high selectivity toward carbonate radicals ( $1.8 \times 10^9 M^{-1} s^{-1}$ ) (Neta and Huie, 1988). Our objectives were first, to develop an analytical method for identifying the carbonate radical using a selective probe; second, to determine its concentration in various natural waters; and, third, to investigate the dynamics of its generation and quenching. In particular, we hoped to discover the basic relationship between the steady state concentration of the carbonate radical and the concentration of the carbonate/bicarbonate ion, the nitrate ion, DOC and pH value in natural field waters under actinic irradiation. This relationship could then be used to predict and compare the approximate steady state concentration of carbonate radical in selected field waters analyzed under different sunlight conditions. This investigation is part of a larger effort to determine the role this reactive oxidant species plays in limiting the persistence of some aquatic pollutants.

## **2.2 MATERIALS AND METHODS**

### **2.2.1 Chemicals**

*N, N*-dimethylaniline (DMA) and *N*-methylaniline (NMA) were obtained from Aldrich (Oakville, ON), as were sodium nitrate, sodium carbonate, sodium bicarbonate, and hydrogen peroxide (30%); the carbonyl derivatization reagent, 2,4-dinitrobenzenhydrazine (DNPH), was from Fluka (Buchs, Switzerland) and was recrystallized once from carbonyl-free acetonitrile. All solvents were of HPLC grade and were purchased from Caledon (Georgetown, ON). 18 M $\Omega$  deionized water was used in all water solutions. A concentrated humic acid (Aldrich) solution was exposed to direct sunlight for 2 weeks, and

then diluted with water to give a final absorbance of 0.43 in a 1 cm path length at 370 nm; [DOC] was determined using a DOC-analyzer (OI Corporation Model 1010 TOC analyzer) and stored in the cold room.

### **2.2.2 Field Water Analysis**

Twenty field waters were collected in brown bottles without headspace at different sites across Ontario and filtered through 0.45  $\mu\text{m}$  nylon membrane and kept in a cold room at 2 °C. DOC was determined as above, while nitrate, carbonate and bicarbonate were analyzed by ion chromatography using a Perkin Elmer series 200 IC pump, an Alltech 550 conductivity detector with ERIS 1000 HP autosuppressor, and an IonPac AS 14 4-mm and IonPac AG 14 4-mm column (Dionex). Nitrate concentrations were determined using an isocratic 3.5 mM  $\text{Na}_2\text{CO}_3$  and 1 mM  $\text{NaHCO}_3$  buffer at a flow rate of 1.2 ml/min, and total carbonate and bicarbonate concentrations were determined with a gradient of 50 mM borate and deionized water at a flow rate at 1.5 ml/min. The pHs were measured using a Sargent-Welch pH meter (Model 800).

### **2.2.3 Photolysis**

Typically, field waters were spiked to 1  $\mu\text{M}$  DMA and placed into capped 100 ml quartz tubes. Irradiation of the sample solutions were carried out in an sunlight simulator (Atlas Suntest CPS, Chicago, Illinois), which was set at either a minimum irradiance level of 250  $\text{W}/\text{m}^2$  or maximum irradiance level of 765  $\text{W}/\text{m}^2$ ; each field water was irradiated in duplicate tubes. Seven field waters were selected for sunlight experiments and were irradiated, in the same quartz tubes, twice under 4 hours of mid-day (11 am-3

pm) sunlight during July and August, 1999 in Toronto. A DMA solution was also irradiated in deionized water, and in a high carbonate radical matrix spiked to 100 ppm nitrate and 1000 ppm bicarbonate concentrations. Dark controls were run excluding light. Thames River and Big Otter Creek waters were decarbonated by adding dilute hydrochloric acid to pH 5 followed by bubbling the solution to remove carbon dioxide; the pH was then readjusted to ~8 with dilute NaOH and spiked with DMA for subsequent irradiation. Other control experiments involved addition of ascorbate, bicarbonate, and nitrate to observe changes in DMA degradation.

The major photodegradation product, NMA, was also irradiated in the selected field waters. In order to determine the relative contribution of nitrate and DOC towards steady-state concentration of carbonate radical, a DMA solution was irradiated in 1000 ppm bicarbonate ion with a variable nitrate concentration from 0.2 ppm to 25 ppm, and DOC from 2.5 ppm to 15 ppm.

#### **2.2.4 Analysis**

DMA/NMA in the irradiated samples were directly analyzed by reverse-phase HPLC (Waters 600S) with a 996 PDA (252 nm)) with a C18 column (250 mm x I.D. 4.6 mm). Isocratic conditions were carried out with acetonitrile:water in a 60:40 ratio at a flow rate of 1.0 ml/min; each sample was determined in duplicate.

#### **2.2.5 Reaction Pathways**

DMA reaction pathways with carbonate radical were investigated in the laboratory in a Rayonet photo-reactor (Hamden, Connecticut) with a 300 nm Lamp.

Carbonate radical was generated from the photolysis of 3 *mM* hydrogen peroxide in 0.1 *M* carbonate buffered pure water (Larson and Zepp, 1988). DMA photo-degradation products were determined through solid-phase extraction (C-18) and subsequent HPLC-UV determination. Structural confirmation was obtained through GC-MS (Trio 1000) analysis in comparison with authentic standards. The GC column was equipped with DB-1 (30 m x 0.53-mm) column and injector temperature of 250 °C; initial temperature was 50 °C for 1 min, followed by a 10 °C/min ramp to 280 °C, with a final 5 min at 280 °C.; He was used as carrier gas and spectra were obtained at 70 eV with a scan range of 50 to 500 m/z.

## **2.3 RESULTS AND DISCUSSION**

### **2.3.1 Field Water Analysis**

The field water samples were collected from different lakes, rivers and ponds across Ontario. Fresh water typically is much more dilute in terms of inorganic solutes than sea water. The primary anion components in freshwater include  $\text{HCO}_3^-$ ,  $\text{SO}_4^{2-}$ ,  $\text{Cl}^-$ ,  $\text{NO}_3^-$ , while the cation components include  $\text{Ca}^{2+}$ ,  $\text{Mg}^{2+}$ ,  $\text{Na}^+$ ,  $\text{K}^+$  and  $\text{Fe}^{3+}$ . The sum of the chemical equivalents of inorganic cations normally exceeds the sum of the anions. This is because of the occurrence of DOC, whose anions are mainly carboxyl groups (Larson and Weber, 1994). In fresh surface waters, a large part of  $\bullet\text{OH}$  is produced from the slow photolysis of nitrate. Dissolved organic material (DOC) in surface waters has a role both in producing and consuming different types of transient species, including the hydroxyl radical. The pH value of field water can determine the ratio of carbonate to bicarbonate ion, and can thereby influence the fraction of  $\bullet\text{OH}$  that reacts with the scavenger to

produce carbonate radicals (Larson and Zepp, 1988). In order to investigate the factors determining the steady-state concentration of carbonate radicals in field waters, it is necessary to analyze the pH, nitrate, bicarbonate/carbonate, and DOC; values for the field waters selected in this study are shown in **Table 2.1**. No nitrite was measured in any of the field waters.

Nitrate ranged from 0.20 ppm to 20.1 ppm and for illustrative purposes the waters were segregated into high (4.99 ppm to 20.1 ppm), middle (0.94 ppm to 2.85 ppm) and low concentrations (0.20 ppm to 0.60 ppm). The range of total carbonate/ bicarbonate ion were from 22.1 ppm in the South Branch River with a pH of 6.92 to 273 ppm in the HWY 8 Creek with a pH of 8.45. DOC values ranged from 1.63 mg/L to 5.91 mg/L in most of the field waters, while two had values above 10 mg/L.

**Table 2.1. Analysis results of natural field waters and the fraction of hydroxyl radical scavenged by carbonate/bicarbonate ion in field waters.**

Name	NO <sub>3</sub> <sup>-</sup> (ppm)	DOC (mg c/L)	pH	CO <sub>3</sub> <sup>2-</sup> /HCO <sub>3</sub> <sup>-</sup> (ppm)	f <sub>•OH</sub> <sup>a</sup> (CO <sub>3</sub> <sup>2-</sup> +HCO <sub>3</sub> <sup>-</sup> )
<b>High Nitrate Field waters</b> ( 4.99-20.1 ppm NO <sub>3</sub> <sup>-</sup> )					
Thames River	20.1	3.08	8.40	269	0.53
Big Otter Creek	13.4	2.47	8.18	226	0.52
Lynn River	9.84	1.89	8.15	237	0.59
Grand River	7.00	5.80	8.29	225	0.32
Big Creek	6.88	2.64	8.21	227	0.50
Biosphere Reserve Pond	4.99	3.04	8.25	209	0.45
<b>Middle Nitrate Field Waters</b> ( 0.94–2.85 ppm NO <sub>3</sub> <sup>-</sup> )					
Credit River	2.85	5.91	8.26	205	0.29
Lake Ontario (Toronto)	1.75	1.65	8.12	136	0.48
Lake Huron (Southampton)	1.51	2.43	7.95	121	0.34
St. Lawrence River	1.16	2.20	8.16	123	0.39
Lake Erie (Long Point)	1.16	4.32	8.41	171	0.34
Lake Erie (Port Dover)	1.06	1.63	8.32	137	0.51
Mazzinaw Lake	0.96	5.14	7.80	28.1	0.053
HWY 8 Creek	0.94	12.9	8.45	273	0.22
<b>Low Nitrate Field Waters</b> ( 0.20–0.62 ppm NO <sub>3</sub> <sup>-</sup> )					
South Branch River	0.62	4.87	6.92	22.1	0.033
Moira River	0.33	11.5	7.64	52.9	0.043
Lake Simcoe	0.32	4.55	8.45	172	0.35
Severn River	0.24	5.24	8.40	127	0.25
Georgian Bay (Lake Huron)	0.23	7.84	8.48	138	0.19
Gull Lake	0.20	4.53	7.48	29.8	0.058

<sup>a</sup> The calculation examples of f<sub>•OH</sub>(CO<sub>3</sub><sup>2-</sup>+HCO<sub>3</sub><sup>-</sup>) are shown in Table 2.3.

### 2.3.2 DMA Reaction Pathway with $\bullet\text{CO}_3^-$

The major photo-degradation product observed in the high carbonate radical matrix was *N*-methylaniline (NMA) indicating an *N*-dealkylation pathway. NMA was also observed as the primary product in irradiated field waters; only minor quantities were observed following direct photolysis in DI water. Laboratory studies indicated *N*-methylaniline was sequentially dealkylated by the carbonate radical to form aniline, followed by the rapid oxidation of aniline to nitrobenzene which was found to be relatively stable.

We hypothesized the dealkylated methyl group would form formaldehyde following cleavage. After adding the carbonyl derivatization reagent, 2, 4-dinitrophenylhydrazine (DNPH), into the irradiated DMA solution and incubating for 1 hour, no hydrozone was detected by HPLC analysis (Mopper and Stahovec, 1986). Alternatively, we then attempted to observe methanol in the irradiated solution. The irradiated DMA solution was adjusted to neutral pH with dilute HCl, and the solution then passed through an SPE cartridge to remove DMA and other organic compounds. Hydrogen peroxide was then added to the extracted solution and irradiated for 10 minutes in order to transform any methanol present to formaldehyde; a positive control indicated quantitative conversion of methanol to formaldehyde. DNPH was then added to the photolysis solution and the formaldehyde hydrozone was identified by HPLC-UV at 365 nm. These results appear to indicate methanol was produced from the dealkylated methyl group in the DMA reaction with carbonate radicals. The DMA reaction pathways with  $\bullet\text{CO}_3^-$  is shown in Fig. 2.1.

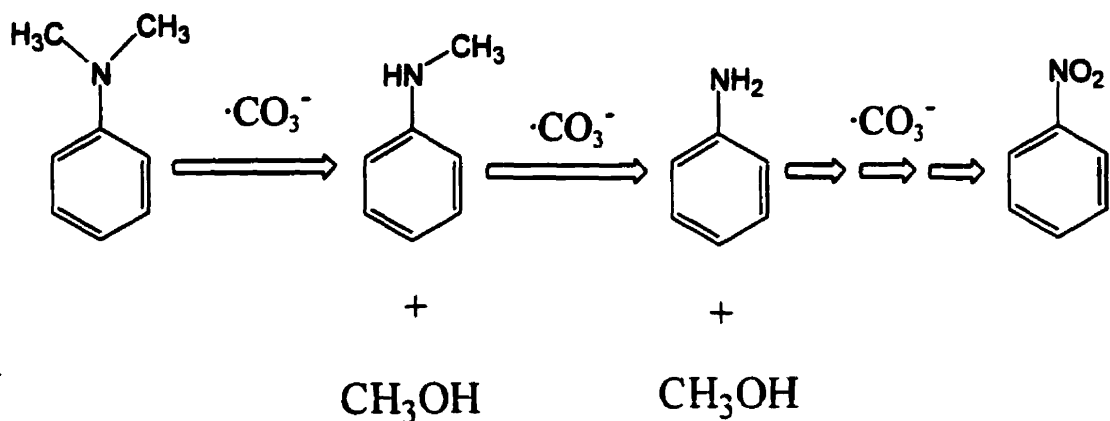


**Figure 2.1.** DMA reaction pathways with  $\bullet\text{CO}_3^-$ .

### 2.3.3 Control Experiments

In order to confirm DMA as a selective probe for measuring the steady-state concentration of carbonate radical it was necessary to carry out a number of control experiments. Specifically, we carried out the following experiments to observe the effect on DMA degradation: 1) DMA run in the dark to control for microbial losses; 2) removal of all dissolved carbonate species; 3) addition of a known radical scavenger, ascorbate, to a field water; 4) addition of both nitrate; and 5) bicarbonate. The selected natural field waters for the first three experiments were the Thames River and Big Otter Creek, which had the highest rate constants among all field samples. DMA was stable in these two waters in the dark for 9 hours at room temperature (Fig. 2.2). This result indicated that microbial degradation, hydrolysis, or other non-photolytic oxidation reactions were not responsible for the observed DMA. Secondly, decarbonation of the field water would remove the bicarbonate/carbonate hydroxyl scavenging pathway and thus preclude the production of carbonate radical. Both Thames River ( $0.0015 \text{ min}^{-1}$ ) and Big Otter Creek

( $0.0014 \text{ min}^{-1}$ ) showed essentially the same DMA photolysis rate following removal of carbon dioxide as direct photolysis ( $0.0015 \text{ min}^{-1}$ ). This indicates that other photo-induced transients such as hydroxyl, alkyloxyl and organoperoxy radicals and singlet oxygen did not contribute significantly to DMA degradation. For experiments 3 to 5 we used two lake waters from California, Clear Lake and Lake Berryessa. Addition of 1 mM ascorbate to Clear Lake water resulted in the DMA rate constant being reduced from  $0.0087 \text{ min}^{-1}$  to  $0.0016 \text{ min}^{-1}$  which was nearly the same as DI water ( $0.0015 \text{ min}^{-1}$ ). We would expect ascorbate, at this concentration, to trap all the carbonate radical and most other aqueous oxidants as well. The addition of bicarbonate to Clear Lake water would be expected to increase the overall scavenging of hydroxyl by bicarbonate and result in higher production of carbonate radical. Results indicated a linear increase in  $k_t$  (indirect photolysis rate) with added bicarbonate with a slope of  $5 \times 10^{-6} \text{ min}^{-1}/\text{ppm HCO}_3^-$  ( $r^2 = 0.945$ ). The final experiment of spiking additional nitrate into Lake Berryessa water would be expected to increase the overall production of hydroxyl and thus  $[\bullet\text{CO}_3]_{ss}$  given no change in the relative scavenging by bicarbonate/DOC. A linear increase in  $k_t$  with added nitrate was observed with a slope of  $2.6 \times 10^{-4} \text{ min}^{-1}/\text{ppm nitrate}$  ( $r^2 = 0.999$ ). We conclude from these experiments that carbonate radicals are the primary reagents produced in sunlit field waters responsible for the observed DMA degradation.

The major product of DMA photoreaction with carbonate radical was *N*-methylaniline (NMA) through *N*-dealkylation. Irradiation of NMA solution in the Thames River, Big Otter Creek, and in a high carbonate radical matrix was carried out respectively in a photoreactor under low light intensity ( $250 \text{ W/m}^2$ ). The rate constants of NMA were  $0.0022 \text{ (min}^{-1}\text{)}$  in the Thames River,  $0.0022 \text{ (min}^{-1}\text{)}$  in Big Otter Creek,

and  $0.0121(\text{min}^{-1})$  in the high carbonate radical matrix. The rate constant of NMA was lower than that of DMA in the same waters. This result was consistent with the result reported by Larson and Zepp (1988), of which the carbonate radical was generated in  $0.092\text{ M}$  sodium bicarbonate with  $3\text{ mM}$   $\text{H}_2\text{O}_2$ . NMA as the major degradation product had a relatively lower concentration and a slower reaction rate with carbonate radical than DMA, suggesting NMA did not compete with DMA for reaction with carbonate radicals.

#### **2.3.4 Photolysis in Photoreactor**

Irradiation of  $1\ \mu\text{M}$  DMA solution in DI water and in twenty field water samples, as well as in a carbonate radical matrix (100 ppm nitrate ion and 1000 ppm bicarbonate ion) was carried out in the photoreactor. At a minimum irradiance level ( $250\ \text{W}/\text{m}^2$ ), the direct photolysis rate of DMA in DI water was the slowest among all samples investigated. The first order rate constant of direct photolysis ( $k_D$ ) was  $0.0015\ \text{min}^{-1}$ , with a half-life of 462 min. In contrast, the most rapid photoreaction occurred in the carbonate radical matrix with the high concentrations of nitrate and bicarbonate ion with a rate constant of  $0.0312\ \text{min}^{-1}$  (half-life 22.2 min). Typical photolysis kinetics of DMA in selected field waters are shown in Fig. 2.2. The rate constants and half-lives of degradation of DMA in all the field waters are shown in Table 2; rate constants were reproducible with a relative error less than 3%. The high nitrate field waters showed more rapid degradation of DMA than either the middle or low nitrate field waters. The highest rate constant occurred in the Thames River water with a rate constant of  $0.0069\ \text{min}^{-1}$ , followed by the Big Otter Creek ( $0.0047\ \text{min}^{-1}$ ) and the Biosphere reserve pond

( $0.0037\text{min}^{-1}$ ). In field waters with mid-level nitrate concentrations, the rate constant ranged from  $0.0033\text{ min}^{-1}$  in Lake Ontario (Toronto) to  $0.0020\text{ min}^{-1}$  in Mazzinaw Lake; while low nitrate waters ranged from  $0.0033\text{ min}^{-1}$  in Moira River to  $0.0019\text{ min}^{-1}$  in Gull Lake.

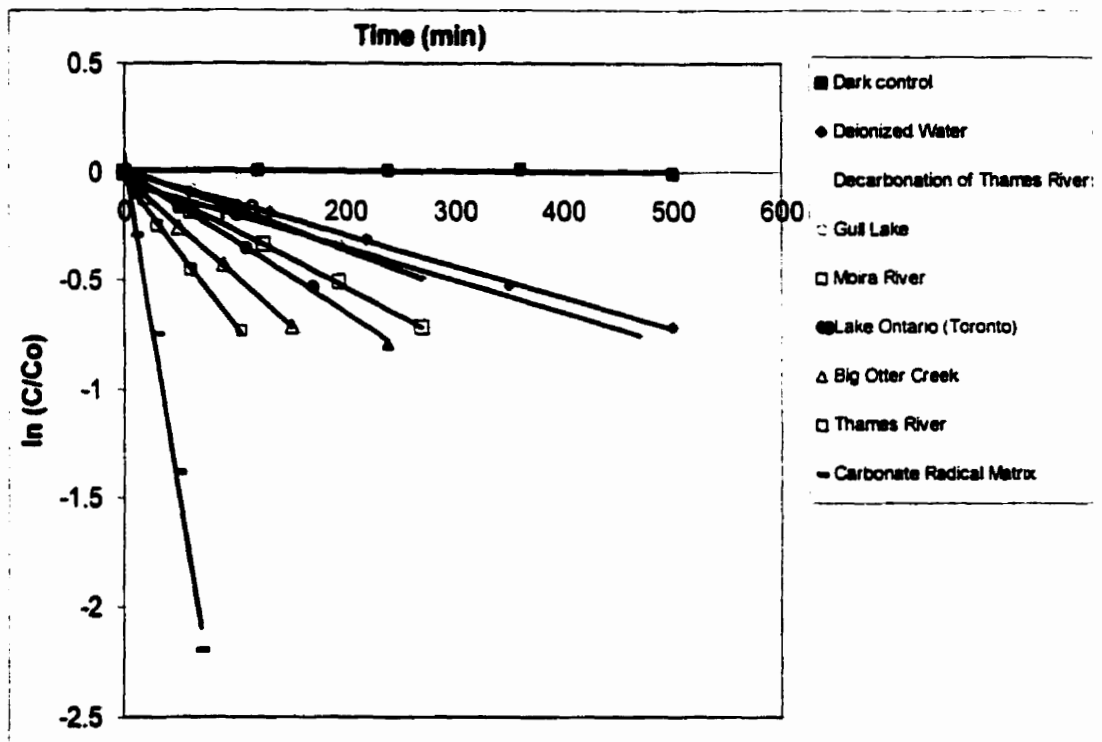


**Figure 2.2.** Photoreaction kinetics of DMA in deionized water, dark control, decarbonation of the Thames River, carbonate radical matrix, and some selected field waters.

In the carbonate radical matrix and natural field waters, the rapid degradation of DMA was due primarily to indirect photolysis involving carbonate radical. In field waters with a high nitrate concentration, most hydroxyl radicals were presumably formed through photolysis of nitrate, and then scavenged by bicarbonate if the concentration was

high enough (>200 ppm). In other field waters, with lower nitrate concentrations, hydroxyl radicals likely resulted from both nitrate and DOC photolysis. The slowest degradation of DMA occurred in Gull Lake, Mazzinaw Lake, and South Branch River, with rate constants less than  $0.0021 \text{ min}^{-1}$  due to the low concentration (less than 30 ppm) of bicarbonate ion.

At the maximum irradiance level ( $765 \text{ W/m}^2$ ), the direct photolysis rate constant in DI water increased to  $0.0042 \text{ min}^{-1}$ . All other rate constants in the selected field waters also increased due to enhanced photoconversion of nitrate/DOC to hydroxyl radical, thereby increasing the steady state concentration of carbonate radical.

### 2.3.5 Steady State Concentration of Carbonate Radicals

The photodegradation of DMA in natural field waters under a photoreactor shows the pseudo-first order reaction with rate constant  $k$ . It is assumed the rate constant  $k$  is the sum of the rate constants for direct photolysis in DI water ( $k_D$ ) and the rate constant of indirect photolysis ( $k_I$ ) involving the carbonate radical in equation 1.

$$k = k_D + k_I \quad (1)$$

All  $k_I$  in the field waters was obtained from the rate constants  $k$  by subtracting  $k_D$ . As a result, the  $k_I$  was used to calculate the steady-state concentration of carbonate radical in natural waters (equation 2):

$$k_I = 1.8 \times 10^9 \text{ M}^{-1} \text{ s}^{-1} \times [\bullet\text{CO}_3]_{ss} \quad (2)$$

using the second order rate constant of DMA with carbonate radical of  $1.8 \times 10^9 \text{ M}^{-1} \text{ s}^{-1}$ .

This results in a conservative value for  $[\bullet\text{CO}_3]_{ss}$  because the correction for direct photolysis does not reflect the light shielding influence of DOC in each of the tested field waters.

Under the photoreactor with low light intensity, the rate constant of  $k_D$  was  $0.0015 \text{ min}^{-1}$ . The rate constant of indirect photolysis ( $k_I$ ) and the calculated steady state concentration of carbonate radical ( $[\bullet\text{CO}_3]_{ss}$ ) in a variety of field waters are shown in **Table 2.2**. In field water with high nitrate ion, the range of  $[\bullet\text{CO}_3]_{ss}$  was from  $2.0 \times 10^{-14} \text{ M}$  in the Biosphere Reserve Pond to  $5.0 \times 10^{-14} \text{ M}$  in the Thames River. These values were higher than those in the middle nitrate levels,  $4.6 \times 10^{-15} \text{ M}$  in Mazzinaw Lake to  $1.7 \times 10^{-14} \text{ M}$  in Lake Ontario (Toronto), and from  $3.7 \times 10^{-15} \text{ M}$  in Gull Lake to  $1.4 \times 10^{-14} \text{ M}$  in Moira River for low nitrate waters. The lowest  $[\bullet\text{CO}_3]_{ss}$ , ( $<1.0 \times 10^{-14} \text{ M}$ ) were in Mazzinaw Lake and South Branch River with the lowest concentration of bicarbonate ion.

Under high light intensity, the rate constant of  $k_D$  was  $0.0042 \text{ min}^{-1}$ . The calculated steady state concentration of carbonate radical ( $[\bullet\text{CO}_3]_{ss}$ ) in selected field waters under the two light intensities are shown in **Fig. 2.3**. These values of  $k_I$  and the calculated  $[\bullet\text{CO}_3]_{ss}$  were higher than in low light intensity as predicted. The  $[\bullet\text{CO}_3]_{ss}$  were from  $1.4 \times 10^{-14} \text{ M}$  in Gull Lake to  $9.6 \times 10^{-14} \text{ M}$  in the Thames River. These values increased approximately 3 times as compared with low light intensity irradiation. Light intensity has a large influence on the  $[\bullet\text{CO}_3]_{ss}$  in streams, rivers, and lakes.

**Table 2.2.** Rate constants and steady-state concentrations of carbonate radical in field water under the photoreactor with minimum irradiance level at 250 W/m<sup>2</sup>.

Name	k (min <sup>-1</sup> ) <sup>a</sup>	Half-life (min)	k <sub>i</sub> (min <sup>-1</sup> ) <sup>b</sup>	[•CO <sub>3</sub> ] <sub>ss</sub> (M)
<b>High Nitrate Field waters</b> (4.99–20.1 ppm NO <sub>3</sub> <sup>-</sup> )				
Thames River	0.0069	100	0.0054	5.0 x 10 <sup>-14</sup>
Big Otter Creek	0.0047	147	0.0032	3.0 x 10 <sup>-14</sup>
Lynn River	0.0048	144	0.0033	3.1 x 10 <sup>-14</sup>
Grand River	0.0038	182	0.0023	2.1 x 10 <sup>-14</sup>
Big Creek	0.0039	178	0.0024	2.2 x 10 <sup>-14</sup>
Biosphere Reserve Pond	0.0037	187	0.0022	2.0 x 10 <sup>-14</sup>
<b>Middle Nitrate Field Waters</b> (0.94–2.85 ppm NO <sub>3</sub> <sup>-</sup> )				
Credit River	0.0028	248	0.0013	1.2 x 10 <sup>-14</sup>
Lake Ontario (Toronto)	0.0033	210	0.0018	1.7 x 10 <sup>-14</sup>
Lake Huron (Southampton)	0.0026	267	0.0011	1.0 x 10 <sup>-14</sup>
St. Lawrence River	0.0027	257	0.0012	1.1 x 10 <sup>-14</sup>
Lake Erie (Long Point)	0.0030	231	0.0015	1.4 x 10 <sup>-14</sup>
Lake Erie (Port Dover)	0.0032	217	0.0017	1.6 x 10 <sup>-14</sup>
Mazzinaw Lake	0.0020	347	0.0005	4.6 x 10 <sup>-15</sup>
HWY 8 Creek	0.0027	257	0.0012	1.1 x 10 <sup>-14</sup>
<b>Low Nitrate Field Waters</b> (0.20–0.62 ppm NO <sub>3</sub> <sup>-</sup> )				
South Branch River	0.0021	330	0.0006	5.6 x 10 <sup>-15</sup>
Moira River	0.0026	267	0.0011	1.0 x 10 <sup>-14</sup>
Lake Simcoe	0.0030	231	0.0015	1.4 x 10 <sup>-14</sup>
Severn River	0.0030	231	0.0015	1.4 x 10 <sup>-14</sup>
Georgian Bay (Lake Huron)	0.0030	231	0.0015	1.4 x 10 <sup>-14</sup>
Gull Lake	0.0019	365	0.0004	3.7 x 10 <sup>-15</sup>

<sup>a</sup> The data of measured rate constants were reproducible with relative error less than 3 %.

<sup>b</sup> k = k<sub>D</sub> + k<sub>i</sub>; k<sub>D</sub> was rate constant of direct photolysis of DMA in deionized water (k<sub>D</sub> = 0.0015 min<sup>-1</sup>) and k<sub>i</sub> was rate constant of indirect photolysis of DMA in field waters.

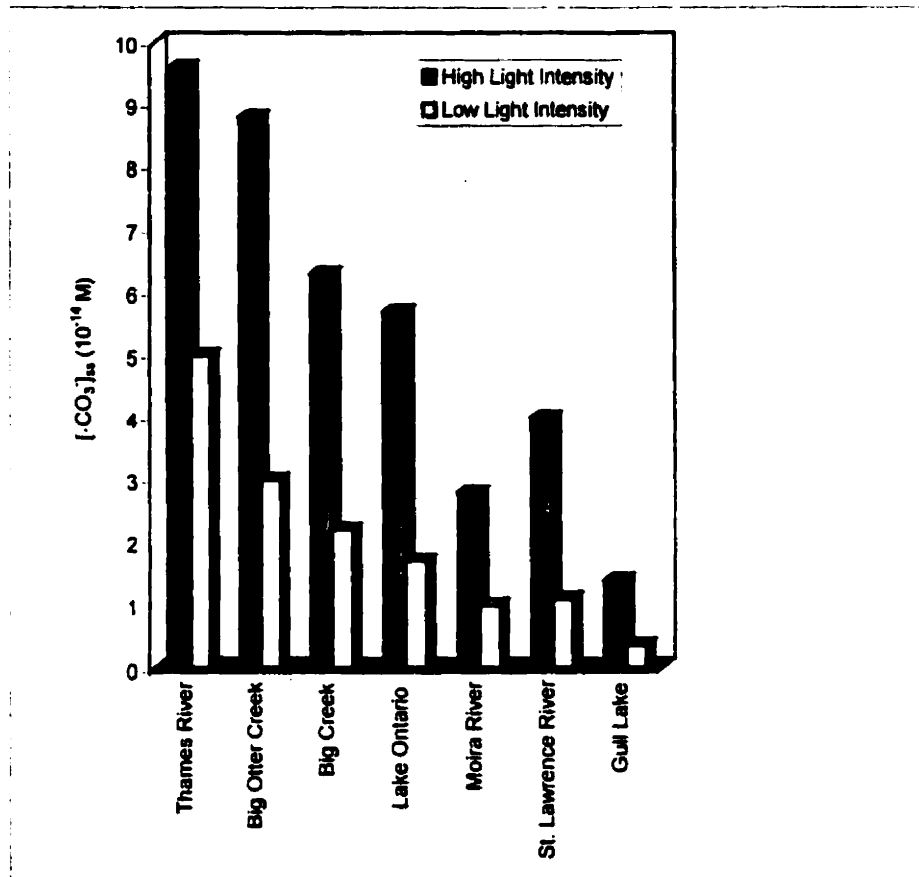


**Figure 2.3.** Steady state concentration of carbonate radical in selected natural waters under a photoreactor with high light intensity ( $765 \text{ W/m}^2$ ) and low light intensity ( $250 \text{ W/m}^2$ ).

### 2.3.6 Photolysis under Sunlight

The selected field waters were also irradiated in noon-day sunlight of July 29 and August 12, to determine the steady state concentration of carbonate radicals; sunlight intensity varied between the two days and within each day due to variable cloudy periods. This led to pseudo-first order rate constants that were not as accurate as those derived from lab experiments in the sunlight simulator. The  $[\bullet\text{CO}_3^-]_{\text{ss}}$  measured on the two days are shown in Fig. 2.4 and ranged from  $7.5 \times 10^{-15} \text{ M}$  in Gull Lake to  $1.0 \times 10^{-13} \text{ M}$  in the Thames River on July 29, and from  $3.7 \times 10^{-15} \text{ M}$  to  $3.5 \times 10^{-14} \text{ M}$  on August 12 respectively. All field waters had higher  $[\bullet\text{CO}_3^-]_{\text{ss}}$  on July 29 than on August 12, which presumably resulted due to the higher UV index of 7.6 on July 29 compared to that on August 12 (6.1) (Environment Canada). The higher UV index indicates that more UV light below 310 nm penetrated to the earth's surface which increased the photoproduction rate of hydroxyl radicals through photolysis of nitrate (below 313 nm), and thus enhanced  $[\bullet\text{CO}_3^-]_{\text{ss}}$  in field waters. The relative magnitude and range of  $[\bullet\text{CO}_3^-]_{\text{ss}}$  in sunlight showed a similar trend to that in the photoreactor. This result indicated that the range of irradiance level of the photoreactor was able to reasonably simulate summer sunlight conditions. Hence, this photoreactor was used to determine the relative importance of each component contributing to the  $[\bullet\text{CO}_3^-]_{\text{ss}}$ .

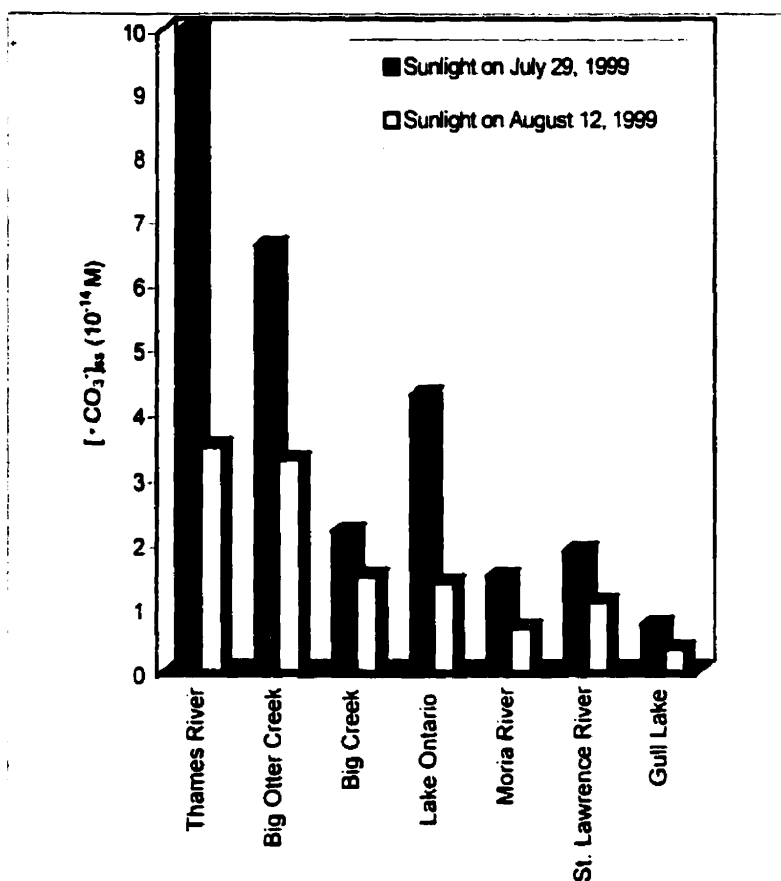


**Figure 2.4.** Steady state concentration of carbonate radical in selected natural waters under different sunlight conditions.

### 2.3.7 Factors that Determine $[\bullet\text{CO}_3]_{\text{ss}}$ .

An important factor that determines  $[\bullet\text{CO}_3]_{\text{ss}}$  in natural waters is the concentration of carbonate/bicarbonate given the role these play in scavenging hydroxyl radical to produce carbonate radical. It was apparent the lowest  $[\bullet\text{CO}_3]_{\text{ss}}$  occurred in natural waters having the lowest concentration of carbonate/bicarbonate ion. This factor can be described by the fraction of  $\bullet\text{OH}$  that reacts with the scavenger (Larson and Zepp, 1988). In natural waters, it was assumed that the primary scavengers of  $\bullet\text{OH}$  were carbonate/bicarbonate ion and DOC.

The  $\bullet\text{OH}$  reacts with excess carbonate or bicarbonate with second-order rate constants of  $4.2 \times 10^8 \text{ M}^1\text{s}^{-1}$  and  $1.5 \times 10^7 \text{ M}^1\text{s}^{-1}$  (Chen and Hoffman, 1974). Hydroxyl reactivity towards DOC has been reported to range from  $1.8$  to  $3.3 \times 10^4 (\text{mg of C/L})^{-1}\text{s}^{-1}$  with an average of  $2.4 \times 10^4 (\text{mg of C/L})^{-1}\text{s}^{-1}$  (Brezonik and Fulkerson-Brekken, 1998) and  $2.5 \times 10^4 (\text{mg of C/L})^{-1}\text{s}^{-1}$  (Zepp *et al.*, 1987; Hoigné and Bader, 1979); the latter 2.5 value was used for this study. The fate of  $\bullet\text{OH}$  in such a system can be assessed through the application of steady-state kinetics (Zepp *et al.*, 1987; Hagg and Hoigné, 1985). The fraction of  $\bullet\text{OH}$  ( $f_{\bullet\text{OH}, i}$ ) that reacts with a system's components,  $S_i$  (e.g., carbonate ion, bicarbonate ion, DOC) with second-order rate constant  $k_i$  is described by equation 3.

$$f_{\bullet\text{OH}, i} = \frac{k_i [S_i]}{\sum_i k_i [S_i]} \quad (3)$$

where  $\sum_i k_i [S_i]$  represents the rate constant for  $\bullet\text{OH}$  scavenging in the system. **Table 2.3** shows three examples of the computed values of  $f_{\bullet\text{OH}, i}$ . Because both carbonate radical and bicarbonate radicals have similar intrinsic reactivities at a low ionic strength (Chen *et al.*, 1975), the carbonate and bicarbonate radicals formed contribute equally to degradation of the probe compound. It is also reported that the carbonate radical was in equilibrium with its conjugate acid (bicarbonate radical) with  $\text{pK}_a$  7.9 (Eriksen *et al.*, 1985). Therefore, the total  $f_{\bullet\text{OH}}(\text{CO}_3^{2-} + \text{HCO}_3^-)$  can be used as an important factor in determining  $[\bullet\text{CO}_3^-]_{\text{ss}}$ . The pH value determines the ratio of carbonate/bicarbonate ion, thereby affecting the  $f_{\bullet\text{OH}, i}$  in the system. Higher pH can enhance the  $f_{\bullet\text{OH}, i}$  of carbonate ion by increasing the ratio of carbonate to bicarbonate ions, and finally enhance the  $f_{\bullet\text{OH}}(\text{CO}_3^{2-} + \text{HCO}_3^-)$ . In water bodies with higher DOCs, the DOC scavenges almost all of the hydroxyl radicals, such that the fraction of total

**Table 2.3.** Kinetic analysis of the reaction pathways for hydroxyl radicals in the selected field samples.

Potential $\bullet\text{OH}$ Scavenger	$[\text{S}_i] \text{ (M)}$	$k_i \text{ (M}^{-1}\text{s}^{-1}\text{)}$	$k_i [\text{S}_i] \text{ (s}^{-1}\text{)}$	$f_{\bullet\text{OH}i}$	Total $f_{\bullet\text{OH}}$ $[\text{CO}_3^{2-} + \text{HCO}_3^-]$
<b>Thames River</b>					
pH = 8.40					
$\text{HCO}_3^{-1}$	$4.3 \times 10^{-3}$	$1.5 \times 10^7$	$6.5 \times 10^4$	0.40	
$\text{CO}_3^{2-}$	$5.2 \times 10^{-5}$	$4.2 \times 10^8$	$2.2 \times 10^4$	0.13	
DOC	3.08 mg DOC/L	$2.5 \times 10^4$	$7.7 \times 10^4$	0.47	
		(mg of C/L) $^{-1}\text{s}^{-1}$	$\sum_i k_i [\text{S}_i] = 1.6 \times 10^5$		0.53
<b>Credit River</b>					
pH = 8.26					
$\text{HCO}_3^{-1}$	$3.3 \times 10^{-3}$	$1.5 \times 10^7$	$4.9 \times 10^4$	0.23	
$\text{CO}_3^{2-}$	$3.0 \times 10^{-5}$	$4.2 \times 10^8$	$1.3 \times 10^4$	0.062	
DOC	5.91 mg DOC/L	$2.5 \times 10^4$	$1.5 \times 10^5$	0.71	
		(mg of C/L) $^{-1}\text{s}^{-1}$	$\sum_i k_i [\text{S}_i] = 1.6 \times 10^5$		0.29
<b>Gull Lake</b>					
pH = 7.48					
$\text{HCO}_3^{-1}$	$4.5 \times 10^{-4}$	$1.5 \times 10^7$	$6.8 \times 10^3$	0.056	
$\text{CO}_3^{2-}$	$7.0 \times 10^{-7}$	$4.2 \times 10^8$	$2.9 \times 10^2$	0.002	
DOC	4.53 mg DOC/L	$2.5 \times 10^4$	$1.13 \times 10^5$	0.94	
		(mg of C/L) $^{-1}\text{s}^{-1}$	$\sum_i k_i [\text{S}_i] = 1.2 \times 10^5$		0.058

$f_{\bullet\text{OH}}(\text{CO}_3^{2-} + \text{HCO}_3^-)$  is very low; for instance Moira River at 0.043 had one of the highest levels of DOC (11.5 mg c/L) measured. The highest  $f_{\bullet\text{OH}}(\text{CO}_3^{2-} + \text{HCO}_3^-)$  of 0.59 occurred in Lynn River with relative high alkalinity and low DOC and overall five of the twenty field waters had  $f_{\bullet\text{OH}}(\text{CO}_3^{2-} + \text{HCO}_3^-)$  above 0.5, hence carbonate/bicarbonate ion in these field waters would be the primary source of scavenging  $\bullet\text{OH}$ . These  $f_{\bullet\text{OH}}(\text{CO}_3^{2-} + \text{HCO}_3^-)$  values compare with recently reported values (Brezonik and Fulkerson-Brekken, 1998) for some Minnesota/Wisconsin field waters which ranged from 0.03 to 0.34; Larson and Zepp (1988) reported a value of 0.19 for Lake Greifensee. The calculated values of  $f_{\bullet\text{OH}}(\text{CO}_3^{2-} + \text{HCO}_3^-)$  for all the field waters are also shown in **Table 2.1** with an overall average value of 0.32.

In order to model the importance of each aqueous constituent to the transformation of DMA in sunlight irradiated waters, and by inference the  $[\bullet\text{CO}_3^-]_{\text{ss}}$ , the individual components have been separated in equation 4:

$$[\bullet\text{CO}_3^-]_{\text{ss}} \propto f_{\bullet\text{OH}}(\text{CO}_3^{2-} + \text{HCO}_3^-) \times [k_1(\text{NO}_3^-) + k_1(\text{DOC})] \quad (4)$$

In the investigated natural waters, hydroxyl radicals are primarily produced through the photolysis of nitrate and DOC. In order to determine the relative contribution of nitrate and DOC towards the indirect photolysis rate, DMA was irradiated in the 1000 ppm bicarbonate solution, with varying nitrate or DOC concentrations in the photoreactor at low light intensity. The nitrate (0.2 ppm to 25 ppm) and DOC concentrations (2.5 mg/L to 15 mg/L) covered the range of these constituents in the natural waters investigated. A good linear relationship of  $k_1$  to nitrate concentration (ppm) was found with  $k_1 = 0.0003 [\text{NO}_3^-] + 0.0036$ , as shown in **Fig. 2.5 (A)**. Because only nitrate was added to the system, the  $f_{\bullet\text{OH}}(\text{CO}_3^{2-} + \text{HCO}_3^-)$  should be 1.0. The  $k_1$  was still 0.0037 ( $\text{min}^{-1}$ ), even at 0.2 ppm nitrate. The rate constant in the 1000 ppm bicarbonate (no nitrate) was similar to that in deionized

water. Therefore, the intercept of 0.0036 ( $\text{min}^{-1}$ ) should be considered in comparison with the relative contribution of DOC towards indirect photolysis rate. The linear relationship of  $k_1$  to DOC concentration ( $\text{mg/L}$ ) was  $k_1 = 0.0004 f_{\bullet\text{OH}}(\text{CO}_3^{2-} + \text{HCO}_3^-) [\text{DOC}]$ , which is shown in **Fig. 2.5 (B)**. This result indicates that nitrate, not DOC, makes the primary contribution towards the indirect photolysis rate of DMA with  $\bullet\text{CO}_3^-$ , even at low nitrate concentrations. From these experimental results, the relationship of  $[\bullet\text{CO}_3^-]_{\text{ss}}$  to  $f_{\bullet\text{OH}}(\text{CO}_3^{2-} + \text{HCO}_3^-)$ , nitrate and DOC was derived as:

$$[\bullet\text{CO}_3^-]_{\text{ss}} \propto f_{\bullet\text{OH}}(\text{CO}_3^{2-} + \text{HCO}_3^-) \times \{0.0003[\text{NO}_3^-] + 0.0036 + 0.0004 [\text{DOC}]\} \quad (5)$$

Dividing by 0.0003 yields the simple linear relationship:

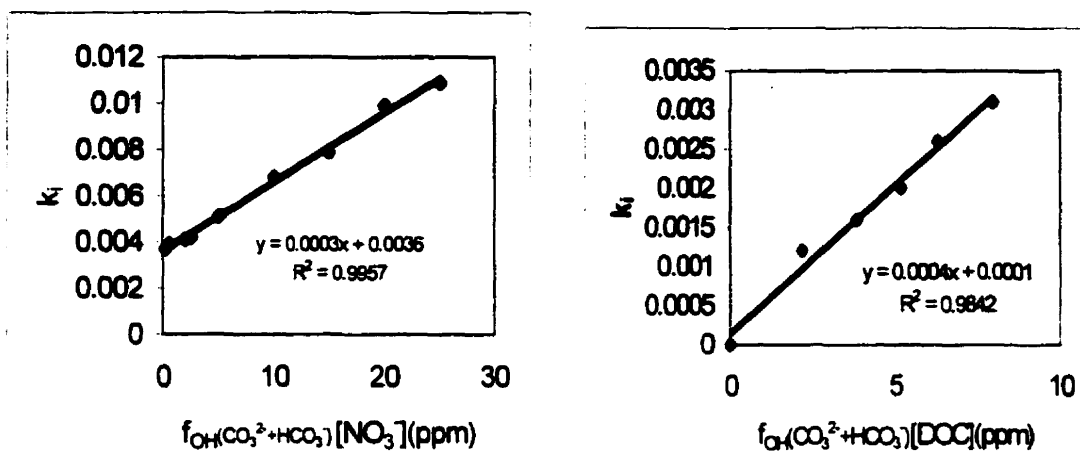
$$[\bullet\text{CO}_3^-]_{\text{ss}} \propto f_{\bullet\text{OH}}(\text{CO}_3^{2-} + \text{HCO}_3^-) \times \{[\text{NO}_3^-] + 12 + 1.3 [\text{DOC}]\} \quad (6)$$

If there is no nitrate in the water, then equation (6) reduces to:

$$[\bullet\text{CO}_3^-]_{\text{ss}} \propto f_{\bullet\text{OH}}(\text{CO}_3^{2-} + \text{HCO}_3^-) \times 1.3 [\text{DOC}] \quad (7)$$

A plot of the measured  $[\bullet\text{CO}_3^-]_{\text{ss}}$  in the twenty natural waters irradiated in the sunlight simulator (low light intensity) versus the respective  $\{f_{\bullet\text{OH}}(\text{CO}_3^{2-} + \text{HCO}_3^-) \times \{[\text{NO}_3^-] + 12 + 1.3 [\text{DOC}]\}\}$  values was strongly correlated ( $r^2$  was 0.92) as indicated in **Fig. 2. 6**. Similarly when applied to sunlight irradiated natural waters (August 12) the linear relationship was also strongly correlated ( $r^2$  was 0.94). These results indicate the simple linear relationship can be used to estimate and compare different  $[\bullet\text{CO}_3^-]_{\text{ss}}$  in natural waters with known pH, nitrate, carbonate/bicarbonate, and DOC values.

Different types of field water DOC will vary with respect to trapping  $\bullet\text{OH}$ , thereby changing the  $f_{\bullet\text{OH}}(\text{CO}_3^{2-} + \text{HCO}_3^-)$  and  $k_1$  (DOC) contributed by DOC (Brezonik and Fulkerson-Brekken, 1998). It is assumed that reaction with DOC is the main fate of carbonate radicals in natural waters, and that the lifetimes of carbonate radical are related to the DOC



(A)

(B)

**Figure 2.5.** The relationship of indirect photolysis rate constants ( $k_i$ ) to the nitrate concentration (A); the relationship of indirect photolysis rate constants ( $k_i$ ) to the DOC concentration (B)

concentration (Larson and Zepp, 1988). Low DOC concentrations in natural waters can increase the lifetime of carbonate radicals, thereby increasing  $[•CO_3^-]_{ss}$ . This might partly explain the relatively high  $[•CO_3^-]_{ss}$  in the Lynn River and Lake Ontario (Table 2.2), where DOC was only 1.89 mg/L and 1.65 mg/L respectively. The contribution of hydrogen peroxide, via photolysis to form hydroxyl, to  $[•CO_3^-]_{ss}$  was ignored because of its relatively small absorption section in the actinic portion of the spectrum (Hagg and Hoigné, 1985). Furthermore, it was reported that hydrogen peroxide generation in water correlated well both with total organic carbon content and the amount of light absorbed by the sample (Cooper and Zika, 1983). Thus, we suggest that the increase in  $[•CO_3^-]_{ss}$  by DOC included

the contribution through  $\text{H}_2\text{O}_2$ . Presumably there still exist some factors not included in Equation 6 that may contribute to the degradation of DMA and therefore  $[\bullet\text{CO}_3]_{\text{ss}}$ .

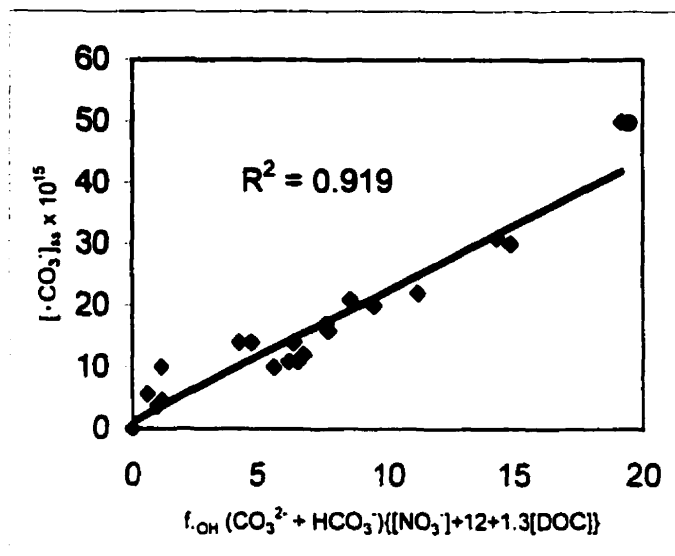


**Figure 2.6.** Using the derived formula in twenty natural waters to obtain the linear regression curve of  $[\bullet\text{CO}_3]_{\text{ss}}$  towards  $f_{\text{OH}} (\text{CO}_3^{2-} + \text{HCO}_3^-) \times \{[\text{NO}_3^-] + 12 + 1.3 [\text{DOC}]\}$ .

On the other hand,  $[\bullet\text{CO}_3]_{\text{ss}}$  strongly depend on the amount of light absorbed by the sample. It can be clearly seen that  $[\bullet\text{CO}_3]_{\text{ss}}$  is higher with increased light intensity; a factor that is not included in our model equation. Future work will focus on including actinometry into the measurement system in order to refine our simple relationship between aqueous parameters and  $[\bullet\text{CO}_3]_{\text{ss}}$  that will allow calculated values to be determined in any field water for  $[\bullet\text{CO}_3]_{\text{ss}}$ ; values for nitrate, DOC, and carbonate alkalinity are available for numerous natural waters (Brezonik and Fulkerson-Brekken, 1998).

Finally, the steady-state concentration of the carbonate radical can be used to predict the relative persistence of certain chemical pollutants. Previously we calculated the theoretical near-surface water half-lives of pesticides based on a calculated  $[\bullet\text{CO}_3]_{\text{ss}}$  of  $5 \times 10^{-14} \text{ M}$ , and found they ranged from 8.0 d for fenthion to 800 d for methyl parathion (Chapter 3). The method described here for the determination of  $[\bullet\text{CO}_3]_{\text{ss}}$  is the first to successfully measure this oxidant in natural waters and will contribute to the development of more accurate models of aquatic persistence.

## 2.4 CONCLUSIONS

DMA was selected as a probe to determine the steady state concentration of carbonate radical in a variety of natural waters. Steady state concentrations of carbonate radicals in natural waters were investigated in a sunlight simulator and in sunlight during summer. The measured  $[\bullet\text{CO}_3]_{\text{ss}}$  strongly depends on light intensity; the range of  $[\bullet\text{CO}_3]_{\text{ss}}$  found in natural waters was from  $5 \times 10^{-15} \text{ M}$  to  $10^{-13} \text{ M}$ . Under the same light intensity, the measured  $[\bullet\text{CO}_3]_{\text{ss}}$  was also related to the major components in natural waters. Nitrate contributes primarily as the source of hydroxyl radicals, and DOC acts as both the source and sink of hydroxyl radicals in natural waters.

## **2.5 REFERENCES**

Brezonik, P.L., Fulkerson-Brekken, J., 1998. Nitrate-induced photolysis in natural waters. Controls on concentrations of hydroxyl radical photo-intermediates by natural scavenging agents. *Environ. Sci. Technol.* 32, 3004-3010.

Chen, S.N., Hoffman, M.Z., 1973. Rate constants for the reaction of the carbonate radical with compounds of biochemical interest in neutral aqueous solution. *Radiation Research* 56, 40-47.

Chen, S.N., Hoffman, M.Z., 1974. Reactivity of the carbonate radical in aqueous solution. Tryptophan and its derivatives. *J. Phys. Chem.* 78, 2099-2102.

Chen, S.N., Hoffman, M.Z., Parsons, G.H., Jr., 1975. Reactivity of the carbonate radical toward aromatic compounds in aqueous solution. *J. Phys. Chem.* 79, 1911-1912.

Cooper, W.J., Zika, R.G., 1983. Photochemical generation of hydrogen peroxide in surface and ground waters exposed to sunlight. *Science* 220, 711-712.

Draper, W.M., Crosby, D.G., 1981. Hydrogen peroxide and hydroxyl radical: intermediates in indirect photolysis in water. *J. Agric. Food Chem.* 29, 699-702.

Eriksen, T.E., Lind, J., Merenyi, G., 1985. On the acid-base equilibrium of the carbonate radical. *Radiat. Phys. Chem.* 26, 197-199.

Faust, B.C., Hoigné, J., 1987. Sensitized photooxidation of phenols by fulvic acid and in natural waters. *Environ. Sci. Technol.* 21, 957-964.

Hagg, W.R., Hoigné, J., 1985. Photo-sensitized oxidation in natural water via OH radicals. *Chemosphere.* 14, 1659-1671.

Hoigné, J., Bader, H., 1977. Beeinflussung der oxidationwirkung von ozon und HO• radikalen durch carbonat. *Vom Wasser*. 48,283-304.

Hoigné, J., Bader, H., 1979. Ozonation of water: "Oxidation-competition values" of different types of waters used in Switzerland. *Ozone Sci. Eng.* 1, 357-372.

Larson, R.A., Weber, E.J., 1994. Reaction mechanisms in environmental organic chemistry. Lewis Publisher. Boca Raton, FL, USA.

Larson, R.A., Zepp, R.G., 1988. Reactivity of the carbonate radical with aniline derivatives. *Environ. Toxicol. Chem.* 7, 265-274.

Mabury, S.A., Crosby, D.G., 1996. Pesticide reactivity toward hydroxyl and its relationship to field persistence. *J. Agric. Food Chem.* 44, 1920-1924.

Mill, T., Hendry, D.G., Richardson, H., 1980. Free-radical oxidants in natural waters. *Science*. 207, 886-887.

Mopper, K., Stahovec, W.L., 1986. Sources and sinks of low molecular weight organic carbonyl compounds in seawater. *Mar. Chem.* 19, 305-321.

Mopper, K., Zhou, X., 1990. Hydroxyl radical photoproduction in the sea and its potential impact on marine process. *Science*. 250, 661-664.

Neta, P., Huie, R.E., 1988. Rate constants for reactions of inorganic radicals in aqueous solution. *J. Phys. Chem. Ref. Data* 17, 1028-1079.

Russi, H., Kotzias, D., Korte, F., 1982. Photoinduzierte hydroxylierungsreaktionen organischer chemikalien in natürlichen gewässern. *Chemosphere*. 11, 1041-1048.

Zafiriou, O.C., 1974. Sources and reactions of OH and daughter radicals in seawater. *J. Geophys. Res.* 79, 4491-4497.

Zafiriou, O.C., Bonneau, R., 1987. Wavelength-dependent quantum yield of OH radical formation from photolysis of nitrite ion in water. *Photochem. Photobiol.* 45, 723-727.

Zepp, R.G., Hoigné, J., Bader, H., 1987a. Nitrate-induced photooxidation of trace organic chemicals in water. *Environ. Sci. Technol.* 21, 443-450.

Zepp, R.G., Braun, A.M., Hoigné, J., Leenheer, J.A., 1987b. Photoproduction of hydrated electrons from natural organic solutes in aquatic environments. *Environ. Sci. Technol.* 21, 485-490.

Zepp, R.G., 1991. Photochemical fate of agrochemicals in natural waters. Pesticide Chemistry: advances in international research, development, and legislation. Proceedings of the Seventh International Congress of Pesticide Chemistry (IUPAC), Hamburg, Germany, August 5-10, 1990, pp. 329-345.

Zepp, R.G., Faust, B.C., Hoigné, J., 1992. Hydroxyl radical formation in aqueous reactions (pH 3-8) of iron (II) with hydrogen peroxide: the photo-Fenton reaction. *Environ. Sci. Technol.* 26, 313-319.

## **Chapter Three**

### **A New Method for Measuring Carbonate Radical Reactivity Towards Pesticides**

### 3.1 INTRODUCTION

The persistence of chemical pollutants in natural waters is determined by the ability of these waters to cleanse themselves of xenobiotics. When sunlight falls on natural waters, it drives a complex series of reactions which produce the oxidants responsible for the self-cleansing capacity of the water. Hydroxyl, hydroperoxyl/superoxide, organoperoxyl, and carbonate radicals as well as singlet oxygen, aqueous electrons, and triple states contribute to systematic cleansing by reaction with aquatic pollutants, which they ultimately degrade (Zepp, 1991). However, little attention has been paid to carbonate radical ( $\bullet\text{CO}_3^-$ ) reactions with organic pesticides, especially the measurement of reaction rate constants.

The carbonate radical has been identified as a transient species with a broad optical absorption in the visible range, with  $\lambda_{\text{max}}$  at 600 nm. It is possible to monitor the formation and disappearance of  $\bullet\text{CO}_3^-$  in the 500-700 nm through flash photolysis, which can be used to determine the rate constants of  $\bullet\text{CO}_3^-$  (Chen and Hoffman, 1973). The carbonate radical is in equilibrium with its conjugate acid (bicarbonate radical) with pKa 9.6 (Chen *et al.*, 1975) or pKa 7.9 (Eriksen *et al.*, 1985), however, no change in optical and ESR spectra have been observed. At low ionic strength, there is little dependence of the rate constant on pH, suggesting that the two forms of the radical have similar intrinsic reactivities (Chen and Hoffman, 1975).

There are several ways to produce the carbonate radical as a secondary radical. The most popular method is through the reaction of hydroxyl radicals with either carbonate or bicarbonate ions. Photolysis of  $\text{H}_2\text{O}_2$  forms hydroxyl radicals, which then react with carbonate anions to produce carbonate radicals (Larson and Zepp, 1988). Carbonate anions

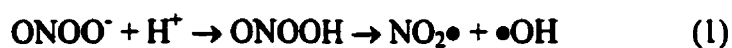
can also react with  $\text{SO}_4^{\bullet-}$  radicals produced by flash photolysis of a sodium persulfate solution to form carbonate radicals (Clifton and Huie, 1993). Additionally, the carbonate radical has been generated through photolytic decomposition of the inorganic complex  $\text{Co}(\text{NH}_3)_4\text{CO}_3^+$  via charge transfer to metal (CTTM) (Chen *et al.*, 1973).

The carbonate radical is a powerful oxidant with a one-electron reduction potential of 1.59 V at pH 12 (Huie *et al.*, 1991), and is capable of the one-electron oxidation of several amino acids and proteins (Adams *et al.*, 1972). In pulse radiolysis and flash photolysis experiments, the carbonate radical has been shown to react rapidly with electron-rich aromatic compounds such as anilines and phenols, primarily as an electron acceptor (Chen *et al.*, 1975). Second-order rate constants are low ( $k < 10^5 \text{ M}^1 \text{ s}^{-1}$ ) for simple aliphatic compounds but higher ( $k = 10^6 - 10^7 \text{ M}^1 \text{ s}^{-1}$ ) for sulfur compounds such as methionine (Chen and Hoffman, 1973). Aromatic compounds show variation in the reactivity depending upon the nature of the substituent on the aromatic ring. The reaction rate constant is high for indole and its derivatives such as tryptophan ( $k > 10^8 \text{ M}^1 \text{ s}^{-1}$ ) (Chen and Hoffman, 1974). The rate constants have been measured for the reaction of carbonate radicals, generated in the flash photolysis of aqueous solution of  $\text{Co}(\text{NH}_3)_4\text{CO}_3^+$ , with a series of substituted benzene derivatives. The rate constants at pH 7, ranged from  $3 \times 10^3 \text{ M}^1 \text{ s}^{-1}$  for benzene to  $1.8 \times 10^9 \text{ M}^1 \text{ s}^{-1}$  for *N, N*-dimethylaniline, correlated well with the Hammett equation using  $\sigma_{\text{para}}^+$  values for electrophilic substitution yielding  $\rho = -3.6$  (Chen *et al.*, 1975). The absolute value of  $\rho$  is higher than that of hydroxyl radical towards benzene and its derivatives with  $\rho = -0.41$  (Anbar *et al.*, 1966), which indicates the lower reactivity and higher selectivity of the carbonate radical. The rate constants towards *p*-substituted anilines have also been determined by the flash photolysis technique, which yield  $\rho = -1.0$  when

using  $\sigma_{\text{para}}^+$  values (Elango *et al.*, 1984); the same  $\rho$  value as observed for the reaction of the carbonate radical with substituted phenols (Moore *et al.*, 1977).

Under environmental conditions, carbonate radicals may react rapidly with aromatic pesticides such as monuron or the carcinogen benzidine, thus influencing their fate in the environment (Larson and Zepp, 1988). Carbonate radicals may oxidize sulfur-containing pesticides, thus limiting their persistence; it may also play an important role in the conversion of organophosphate insecticides to the more toxic oxon derivative in natural waters. Finally, it may contribute to the cycle of naturally occurring sulfur compounds in natural waters.

Methods utilizing UV light may complicate kinetic analysis for those compounds that are also photolabile due to concomitant photo-degradation. King *et al.* (1992) reported a solid-state hydroxyl source, KOONO (potassium peroxonitrite, which was generated by photolysis of  $\text{KNO}_3$  through a 254 nm UV lamp), that upon directly dissolving in water, generated hydroxyl radicals. The addition of KOONO to a solution buffered at pH 7.0 forms pernitrous acid ( $\text{pK}_a = 6.8$ ). The pernitrous acid formed undergoes homolytic fission to form  $\bullet\text{OH}$  and  $\text{NO}_2\bullet$ :



By adding KOONO solution to carbonate or bicarbonate, the  $\bullet\text{OH}$  subsequently reacts with excess carbonate or bicarbonate with second-order rate constants of  $4.2 \times 10^8 \text{ M}^{-1}\text{s}^{-1}$  and  $1.5 \times 10^7 \text{ M}^{-1}\text{s}^{-1}$  to yield  $\bullet\text{CO}_3^-$  (Chen and Hoffman, 1974). The advantages of KOONO as a  $\bullet\text{OH}$  source include the stability of the solid solution, and the lack of light required for initiation of  $\bullet\text{CO}_3^-$  production. The peroxonitrite can be quantified by dissolution in 0.1 M NaOH using  $\epsilon_{302} = 1670 \text{ cm}^{-1}\text{M}^{-1}$  (King *et al.*, 1992); this

quantitation permits reproducible amounts of carbonate radicals to be generated in subsequent experiments.

By utilizing competition kinetics with Fenton's reaction for the production of hydroxyl radicals, the relative reaction rates of 28 constituents of a PCB mixture were measured (Sedlak, 1991). Mabury and Crosby (1996) also used competition kinetics to estimate the reactivity of 10 organic pesticides toward hydroxyl radicals with *p*-nitroso-*N,N*-dimethylaniline (PNDA) as the competitor. A new competition kinetic method for measuring the reactivity of pesticides towards the carbonate radical has been developed in this study by using KOONO as a specific source of hydroxyl radicals to yield the carbonate radicals.

Our objective was to develop a method to generate carbonate radical without light, and measure the reactivity of the carbonate radical towards a number of commonly used sulfur-containing and aromatic pesticides (Fig. 3.1) which have wide use in agriculture. We hypothesized the carbonate radical would contribute to limiting their overall persistence in natural waters.

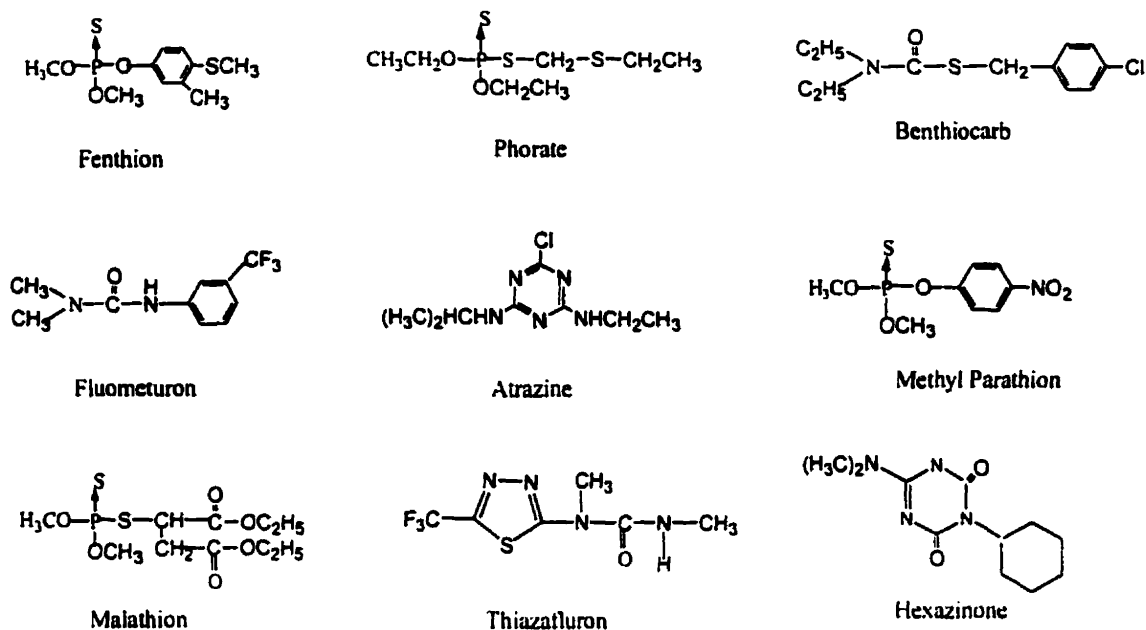


**Figure 3.1.** Chemical structures of pesticides used in this investigation.

## 3.2 MATERIALS AND METHODS

### 3.2.1 Chemicals:

All reagents were of reagent grade or purer. The following compounds were obtained from Aldrich Chemical Company (Oakville, ON): *N,N*-dimethylaniline, *p*-chloroaniline, *p*-nitroaniline, *N*-methylaniline, *p*-nitrophenol, phenol, *p*-toluidine, *p*-amino benzoic acid, thioanisole and methyl phenyl sulfoxide. 4-bromoaniline and *p*-anisidine were purchased from Acros Organics. Aniline was obtained from BDH Chemicals (Toronto, ON). The pesticides, flumeturon, benthicarb, atrazine, hexazinone, fenthion, malathion and methyl parathion were purchased from Chem Service (West Chester, PA); phorate and thiazafluron were obtained from Riedel-deHaen (Supelco, Oakville, ON) and Pestanal (Caledon Labs, Georgetown, ON) respectively.

All the above reagents were dissolved in HPLC grade water; all solvents purchased from Caledon were HPLC grade. KOONO (Potassium peroxonitrite) was generated by photolysis of ground KNO<sub>3</sub> under a 254 nm UV lamp for 10 hours; the final solid material was a mixture of KOONO and KNO<sub>3</sub>.

### 3.2.2 Analytical methodologies:

*N, N*-dimethylaniline, *p*-chloroaniline and *p*-nitroaniline were selected as model competitors, and were monitored by HPLC using an Alltech Econosphere reverse-phase 25 cm C-18 column (5 micron), aqueous acetonitrile as the mobile phase under isocratic conditions, and a detection wavelength appropriate for each competitor; the HPLC system was a Waters 600 pump and 486 tunable absorbance detector. For phenol, the pH of the aqueous phase was modified to pH 2.7 with acetic acid. The HPLC analysis conditions are illustrated in Table 3.1.

**Table 3.1. HPLC Conditions for Competitor Analysis**

Competitor	Detection wavelength (nm)	Mobile phase (H <sub>2</sub> O:CH <sub>3</sub> CN)	Retention time (min)
DMA	254	60:40	7.9
PCA	240	50:50	6.1
PNA	380	45:55	5.5

### 3.2.3 Competition kinetics:

We adapted the competition kinetics system by employing three kinds of competitors, *N,N*-dimethylaniline (DMA), *p*-chloroaniline (PCA) and *p*-nitroaniline (PNA), the loss of which was monitored by HPLC. The rate constants of carbonate radical to competitor are  $1.8 \times 10^9 \text{ M}^{-1}\text{s}^{-1}$ ,  $4.3 \times 10^8 \text{ M}^{-1}\text{s}^{-1}$ , and  $7.3 \times 10^7 \text{ M}^{-1}\text{s}^{-1}$  for DMA, PCA and PNA respectively (Neta and Huie, 1988). These three competitors can be used to measure the rate constants of probes to carbonate radical between  $10^5 \text{ M}^{-1}\text{s}^{-1}$  to  $10^{10} \text{ M}^{-1}\text{s}^{-1}$ . A particular strength of this method is the requirement to only monitor the model competitor while measuring the reactivity of each probe compound. This precludes the necessity of developing a new analytical method for each compound in order to determine its reactivity towards carbonate radical.

If the competition were simply between the probe and standard competitor, it follows that

$$\frac{S_0}{S} = 1 + \frac{k_p[\text{Probe}]}{k_c[\text{Competitor}]} \quad (2)$$

where  $S_0$  represents the rate of loss of the competitor with no probe, and  $S$  represents the rate of loss when the pesticides are present in the system;  $k_c$  and  $k_p$  are the rate constant at which carbonate radicals react with the competitor and pesticide, respectively. If the system is simply a competition between the competitor and probe then a plot of  $S_0/S$  versus  $[\text{Probe}]/[\text{Competitor}]$  produces a straight line with a slope of  $k_p / k_c$ . The validity of the method overall can be tested by the linearity of this relationship. An absolute value can be calculated for  $k_p$  based on the second-order rate constant for the different competitors.

A typical test solution consisted of 1 to 2  $\mu\text{M}$  competitor, and an appropriate concentration of probe in 20 ml 0.01 M  $\text{NaHCO}_3$  solution. The solution was mixed thoroughly with a magnetic stirrer, then injected into HPLC for analysis of the peak area. A second solution was made of 150 mg  $\text{KOONO/KNO}_3$  weighed accurately and quickly dissolved in 0.6 ml 0.1 N NaOH solution; the high pH stabilized the peroxonitrite ion. After adding 100  $\mu\text{l}$  of a  $\text{KOONO/KNO}_3$  /0.1 N NaOH solution to all solutions, the reaction mixture was stirred for three minutes and subsequently analyzed by HPLC. The three minute period was chosen to allow adequate time for the subsequent HPLC injection and resulted in high reproducibility between measurements; early method development indicated the reaction was complete in much less time. The pH value of the mixed solutions was approximately 9.0. At this pH the yield of hydroxyl radical was less than 5% (Crow *et al.*, 1994) and the corresponding quantity of carbonate radical produced from quenching by bicarbonate ion would be quite small. Pseudo-first-order kinetic analysis resulted in a rate constant (S) for each  $[\text{Probe}]/[\text{Competitor}]$  ratio. These data were transformed into plots of  $[\text{Probe}]/[\text{Competitor}]$  vs  $S_0/S$ , which resulted in a slope of  $k_p / k_c$ . Each measurement was replicated at least twice, and the data was highly reproducible (>98%).

The following compounds were selected to measure the rate constant in this system: (1) substituted anilines with PCA or PNA as competitor; (2) *N*-methyl aniline, phenol and thioanisole with DMA, PCA and PNA as competitor respectively; (3) nine pesticides with PNA as competitor.

### **3.2.4. Stopped-flow kinetic experiment:**

In order to confirm the formation of carbonate radicals in our competition kinetic system, a HI-TECH Scientific stopped-flow spectrophotometer was used. Making 0.2 M NaHCO<sub>3</sub> solution and KOONO/NaOH solution in two syringes, the mixing solution with an equal volume was detected at a wavelength of 600 nm. After rapid mixing of the two solutions, the absorption signal of the carbonate radical at 600 nm was observed.

## **3.3 RESULTS AND DISCUSSION**

### **3.3.1 Formation of the carbonate radical**

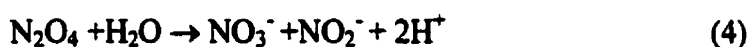
Previous studies have shown that the carbonate radical is formed through the reaction with the hydroxyl radical in high carbonate water. Carbonate radicals decay with a second-order rate constant of  $2.0 \times 10^7 \text{ M}^{-1} \text{ s}^{-1}$  at pH 12.8 in the absence of a scavenger (Elango *et al.*, 1985); their fate in natural waters depends on their steady-state concentration relative to the concentration of organic, and possibly inorganic scavengers.

In this study, carbonate radicals were produced in 0.01M NaHCO<sub>3</sub> by adding a solution of KOONO/KNO<sub>3</sub>/0.1 N NaOH. At pH 9.0, peroxonitrite ions can still acidify to pernitrous acid HOONO. As a result, the hydroxyl radical produced from HOONO homolysis, would quickly be scavenged by bicarbonate solution to form bicarbonate and carbonate radicals. At the fixed pH of our system the quantity of hydroxyl radicals produced should be reproducible based on an equivalent amount of KOONO/KNO<sub>3</sub> added to the system. The excess of bicarbonate, relative to probe/competitor, in the system assured the hydroxyl radicals produced were scavenged to form carbonate radical rather than react directly with the probe or competitor. Evidence for this condition being met is available from the high linearity observed for each probe tested (Fig. 3.3) and excellent agreement between second-order rate

constants measured for substituted aromatic amines and literature values (Table 3.2). Further evidence was obtained by directly observing the formation of carbonate radical. The pH-dependent yield of hydroxyl radical products from peroxonitrite was reported (Crow *et al.*, 1994). It was proposed that the pKa of 6.8 corresponded to the protonation of cis-peroxonitrite anion, whereas the loss of hydroxyl radical-like reactivity with a pKa of 8.0 corresponded to that of the trans-peroxonitrite anion. Therefore, the pKa of 8.0 of trans peroxonitrous acid was favorable for the production of hydroxyl radical in comparison with pKa of 6.8 of peroxonitrous acid (king *et al.*, 1992) in our pH 9.0 system. The formation of bicarbonate and carbonate radicals can be identified by the stopped-flow spectrophotometer with the detecting wavelength set at 600 nm. By putting the 0.02 M NaHCO<sub>3</sub> and KOONO solution in dilute NaOH in two syringes, the absorption signal of the carbonate radical at 600 nm appeared immediately. The concentration of NaHCO<sub>3</sub> was about 0.02 M and the NaOH is about 0.005 N, which makes the final pH of the mixing solution pH 9.0. It was consistent with the pH value in our competition kinetic system. If the NaOH were 0.1 N, no absorption signal appeared after mixing with 0.02M NaHCO<sub>3</sub> solution. Since the rate of formation of pernitrous acid is proportional to the concentration of H<sup>+</sup>, there is very limited pernitrous acid at pH 13. If KOONO were in neutral water, there still was no absorption signal from mixing with 0.02 M NaHCO<sub>3</sub> because the KOONO likely decomposed before reacting with the NaHCO<sub>3</sub>. The formation of carbonate radical in our system depends strongly on the pH value of the solution. The KOONO solution should be kept highly basic to maintain its stability and reproducibility. The ideal pH value of the final solution for making carbonate radicals was approximately 9.0.

### 3.3.2 Nitrogen dioxide radicals in our system.

The carbonate radical as a secondary free radical is formed through reaction with the hydroxyl radical. In our system, the hydroxyl radical was formed through the homolytic decomposition of HOONO through Equation (1). At the same time, nitrogen dioxide radicals were also formed, which have been found to be stable in the gas phase but unstable in aqueous solution (Huie and Neta, 1986). The one electron reduction potential of nitrogen dioxide is 1.03 V (Huie and Neta, 1986), and this value is lower than the value of the carbonate radical of 1.59 V. So, it is impossible for nitrogen dioxide to react with carbonate ion to form carbonate radical. Nitrogen dioxide undergoes a rapid disproportionation and proceeds in the following two steps with rate constants of  $9.0 \times 10^8 M^{-1}s^{-1}$  and  $1.0 \times 10^3 M^{-1}s^{-1}$  in aqueous solution (Forni *et al.*, 1986):



The rate is faster than carbonate radical decay at  $2.0 \times 10^7 M^{-1}s^{-1}$ . Additionally, nitrogen dioxide can also react with the carbonate radical with a rate constant of  $1.0 \times 10^9 M^{-1}s^{-1}$ , which can decrease the amount of nitrogen dioxide radicals as well as carbonate radicals. The amount of the nitrogen dioxide would thereby be lower in comparison with that of the carbonate radical. Aniline and phenoxide were selected as electron rich compounds to determine whether nitrogen dioxide was formed in our system. By using 2  $\mu\text{m}$  aniline and phenol in the competition system at pH 9.0, *p*-nitroaniline and *p*-nitrophenol, respectively, were detected through HPLC as products. About 80% of the aniline and the phenol reacted while 12% of the aniline form *p*-nitroaniline, and 10% of the phenol form *p*-nitrophenol, which is presumably through reaction with the nitrogen dioxide

radical. These results indicate the carbonate radical was the most important reactant with the selected electron-rich compounds such as aniline and phenoxide. For sulfur-containing compounds, especially the aliphatic compounds such as phorate, the rate constant towards nitrogen dioxide should be slower than that for the carbonate radical due to the lower one-electron reduction potential of nitrogen dioxide and the lack of the aromatic ring for electrophilic substitution. As a result, the relative error of this method for such compounds would presumably be small.

### 3.3.3 Competition kinetic method

In order to validate this method, aromatic compounds with known rate constants determined using other methods, were selected as probes to measure the rate constant in our competition kinetic system. The measured rate constant of *N*-methyl aniline was about  $2.5 \times 10^9 \text{ M}^1\text{s}^{-1}$  with DMA as competitor, which is close to the reference value of  $1.8 \times 10^9 \text{ M}^1\text{s}^{-1}$  (Neta and Huie, 1988). The rate constant of phenol was found to be  $1.2 \times 10^8 \text{ M}^1\text{s}^{-1}$ , with PNA as competitor at pH 9.0. Phenol is an electron-rich aromatic compound, especially at high pH. The rate constants of carbonate radicals with phenol vary with the pH, which is due to the ionization of the phenolic OH group. Because the pKa of phenol is 10.2, there was a rapid increase in the rate-constant between pH 9 and pH 11. Our measured rate constant ( $1.2 \times 10^8 \text{ M}^1\text{s}^{-1}$ ) was between the reference values  $2.2 \times 10^7 \text{ M}^1\text{s}^{-1}$ , at pH 7.0, and  $1.2 \times 10^9 \text{ M}^1\text{s}^{-1}$ , at pH 11.2 (Moore *et al.*, 1977).

Thioanisole was selected as a model sulfur-containing aromatic compound with the measured rate constant of  $2.3 \times 10^7 \text{ M}^1\text{s}^{-1}$  towards carbonate radical in our competition kinetic system. One of the oxidized products of thioanisole is methyl phenyl

sulfoxide, which was identified through HPLC and comparison of a standard, indicating that the reaction site is presumably on the sulfur atom. However, the rate constant of methyl phenyl sulfoxide could not be determined with PNA as competitor even though probe concentration was 400 times higher than that of PNA. This indicated that the rate constant of methyl phenyl sulfoxide was lower than  $10^4 \text{ M}^{-1} \text{ s}^{-1}$ .

The rate constants of the substituted anilines *p*-bromoaniline, *p*-chloroaniline, *p*-methylaniline, *p*-methoxyaniline, aniline and *p*-amino-benzoic acid were measured with PCA and PNA as probes. The measured and reference values as well as the substituent constants are shown in **Table 3.2**; an excellent correlation ( $r^2 = 0.992$ ) between measured and reference values was obtained with slope of 0.999.

Many types of organic reactions are sensitive to electron density at the site on the nitrogen atom and can be explored using the Hammett equation relating reaction rates and structure for para- or meta-substituted benzene derivatives. The carbonate radical reactivity towards substituted aniline was described previously by the Hammett equation with good linear relationship yielding  $\rho = -1.0$  (Elango *et al.*, 1984). Based on our measured rate constants, the Hammett plot of the logarithm of the ratio of the rate constants for the substituted anilines versus their substituent constant  $\sigma_{\text{para}}^+$  is shown in **Figure 3.2**. The Hammett plot shows that the reaction constant is  $\rho = -0.89$  with a good correlation coefficient of 0.98. The negative value of  $\rho$  indicates the carbonate radical is strongly electrophilic and the reaction rate depends on electron density in the ring. For

**Table 3.2.** Rate constants<sup>a</sup> and Hammett constants<sup>b</sup> for substituted anilines.

Substituent	Rate Constant (M <sup>-1</sup> s <sup>-1</sup> )	σ <sub>para</sub> <sup>+</sup>	Reference k <sup>c</sup> (M <sup>-1</sup> s <sup>-1</sup> )
-OCH <sub>3</sub>	1.9 x 10 <sup>9</sup>	-0.78	
-CH <sub>3</sub>	9.1 x 10 <sup>8</sup>	-0.31	9.1 x 10 <sup>8</sup> <sup>d</sup>
-H	4.6 x 10 <sup>8</sup>	0.0	5.0 x 10 <sup>8</sup> <sup>c</sup>
-Cl	4.3 x 10 <sup>8</sup>	0.11	4.3 x 10 <sup>8</sup> <sup>c</sup>
-Br	4.1 x 10 <sup>8</sup>	0.15	3.8 x 10 <sup>8</sup> <sup>c</sup>
-COOH	1.9 x 10 <sup>8</sup>	0.42	2.0 x 10 <sup>8</sup> <sup>d</sup>
-NO <sub>2</sub>	7.3 x 10 <sup>7</sup>	0.79	7.3 x 10 <sup>7</sup> <sup>c</sup>

<sup>a</sup> Data from our competition kinetic method at pH 9.0.

<sup>b</sup> Hammett constants from reference (Elango *et al.*, 1984)

<sup>c</sup> Data from reference (Elango *et al.*, 1984)

<sup>d</sup> Data from reference (Nata and Huie, 1988)

*p*-substituted anilines, the best correlation was obtained with  $\sigma_{\text{para}}^+$  while other values proved unsatisfactory. It was also found that the ionization potentials of *p*-substituted anilines correlate well with  $\sigma_{\text{para}}^+$  (Crable and Kearns, 1962). Thus it is likely the rate constants are influenced by the ionization potential of the amine suggesting possible electron transfer from aniline to the carbonate radical (Elango *et al.*, 1984). It is probable that the rate-determining step for the reaction is the removal of an electron, most likely from the basic nitrogen atom by carbonate radical to form an anilino radical (Larson and Zepp, 1988). The formed anilino radical can be stabilized through conjugation. The  $\rho$  value of  $-0.89$  is similar to that of the reference value, which provides good evidence that this method is an accurate way to measure the rate constant of carbonate radical without any light interference.

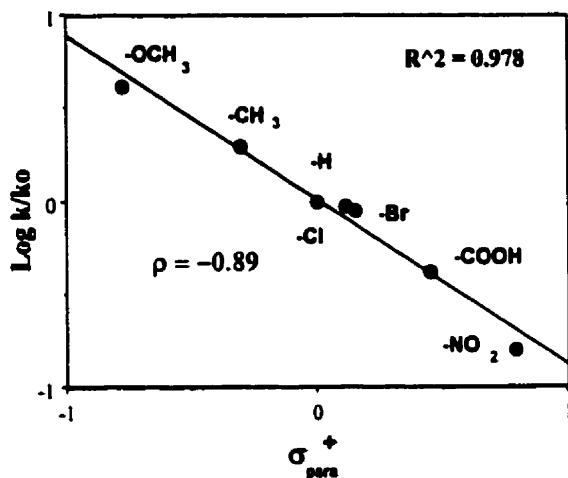


**Figure 3.2.** Hammett plot of substituted aniline reactivity towards carbonate radicals.

### 3.3.4 Pesticide reactivity toward carbonate radicals.

Many of the pesticides were sulfur-containing compounds, and PNA was the model competitor in our competition kinetics system because the rate constant of most sulfur-containing compounds was around  $10^7 M^1 s^{-1}$  (Chen and Hoffman, 1973). A requirement of the competition kinetic system was that competition for carbonate radicals be simply between PNA and the probe pesticide. PNA was stable in aqueous solution and was detected at 380 nm without interference from the selected pesticide, which typically had absorption below 300 nm.

Based on the reactivity of pesticides toward carbonate radical, as well as their solubility, they were divided into the following two groups to be measured more accurately. The concentration ratio of pesticide to PNA was from 0 to 20 in the more reactive group, and the concentration ratio was from 0 to 200 in the less reactive group. Following equation (2), typical results for five probe pesticides are shown in **Figure 3.3**. The steeper the slope ( $k_p/k_c$ ), the more reactive the pesticide towards carbonate radicals; second-order rate constants are shown in **Table 3.3**.

Fenthion was the most reactive toward carbonate radicals, followed by the sulfur-containing pesticide, phorate. The measured rate constant of fenthion ( $2.0 \times 10^7 M^1 s^{-1}$ ) was close to the rate constant of thioanisole ( $2.3 \times 10^7 M^1 s^{-1}$ ). The electron density on the sulfur atom of fenthion would be the most likely site of the oxidation reaction with carbonate radicals. Phorate has two electron-rich sulfur atoms on the aliphatic chain, which makes it highly reactive with carbonate radicals. This result is consistent with the reference rate constants of aliphatic sulfur-containing compounds ranging from  $10^6 M^1 s^{-1}$  to  $10^7 M^1 s^{-1}$  (Chen and Hoffman, 1973).

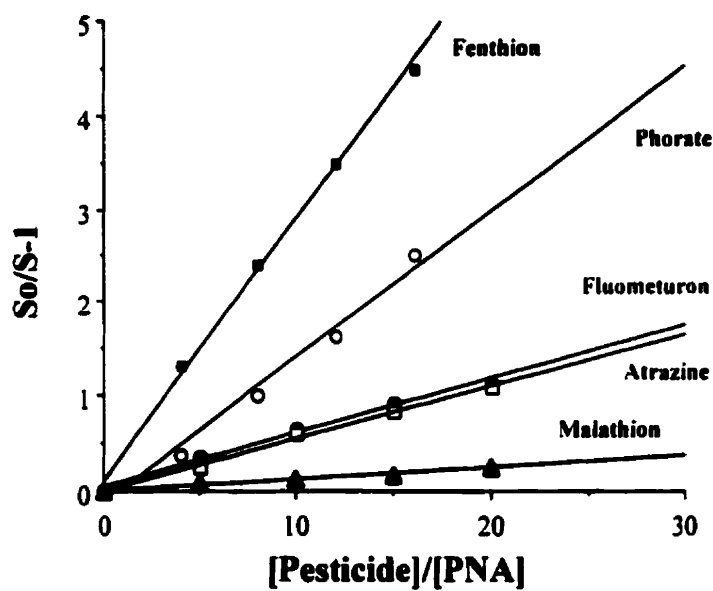


**Figure 3.3.** Typical results indicating pesticide reactivity towards carbonate radicals.

**Table 3.3. Measured Rate Constants for Pesticides towards Carbonate Radical.**

Pesticides	Rate constant	Rate constant	Theoretical half-life <sup>b</sup>
	( $M^1 s^{-1}$ ) measured, $k_M$	( $M^1 s^{-1}$ ) reference	$t_{1/2}$ (d)
Fenthion	$2.0 \times 10^7$		8.0
Phorate	$1.2 \times 10^7$		13
Fluometuron	$4.2 \times 10^6$		38
Atrazine	$4.0 \times 10^6$	$6.1 \times 10^6$ <sup>a</sup>	40
Malathion	$8.9 \times 10^5$		180
Thiazafluron	$3.6 \times 10^5$		446
Benthiocarb	$2.8 \times 10^5$		573
Hexazinone	$2.4 \times 10^5$		685
Methyl-parathion	$2.0 \times 10^5$		802

<sup>a</sup> From data of Larson and Zepp (1988); reaction rate presumably included direct photolysis.

<sup>b</sup> Based on a steady-state concentration of carbonate radical  $[\bullet CO_3^-]_{ss} = 5 \times 10^{-14} M$ .

Fluometuron and atrazine had intermediate rate constants of  $4.2 \times 10^6 \text{ M}^{-1} \text{ s}^{-1}$  and  $4.0 \times 10^6 \text{ M}^{-1} \text{ s}^{-1}$ , and these values are relatively lower than aniline derivatives. The attack of the carbonate radical is presumably on the site of nitrogen atom of those compounds. The electron density on the nitrogen atom of fluometuron is decreased by the adjacent carbonyl group, and the electronegative nitrogen atoms on the heteroatom aromatic ring decrease electron density on the nitrogen atom of the *N*-isopropyl group of atrazine. From the pseudo-first order rate constant of atrazine toward carbonate radicals measured by Larson and Zepp (1988), the second-order rate constant of atrazine toward carbonate radicals was obtained as  $6.1 \times 10^6 \text{ M}^{-1} \text{ s}^{-1}$ . This value is calculated from the pseudo-first order rate constant with carbonate radicals, and it may include the contribution of direct photolysis; our value is lower, however, it does not include any direct photodegradation. Malathion has only one sulfur atom on the aliphatic carbon chain, and the diester group would decrease the electron density on that sulfur atom; the rate constant was lower than that for phorate with two sulfur atoms and an electron-donating ethyl group. This indicates that the number of sulfur atoms on the carbon chain can influence the rate constant toward carbonate radicals.

The other pesticides, thiazafluron, benthocarb, hexazinone and methyl-parathion, showed low reactivity toward carbonate radicals. The lone pair electron of the sulfur atom in thiazafluron maintains the aromatic characteristic of 6 e on the heterocycle, so the reactivity was decreased compared with the aliphatic sulfur-containing compounds. The lower reactivity of hexazinone could be due to the reduced presence of olefinic character. The electron-withdrawing effect of chlorine and carbonyl groups connecting with sulfur contributes to the low reactivity observed for benthocarb. Compared with

fenthion, the strong electron-withdrawing effect of the nitro group gives methyl parathion the lowest reactivity, with a second-order rate constant of only  $2.0 \times 10^5 M^{-1}s^{-1}$ . It is likely the reaction occurred at the sulfur atom and converted the pesticide into the oxon derivative.

Compared with the reactivity of the hydroxyl radical toward pesticides (Mabury and Crosby, 1996), the second-order rate constants of the hydroxyl radical was greater than that of the carbonate radical and varied over one order of magnitude. The most reactive pesticide was carbaryl with a rate constant of  $3.4 \times 10^9 M^{-1}s^{-1}$ , and the least reactive pesticide was quinclorac, with a rate constant of  $3.6 \times 10^8 M^{-1}s^{-1}$ . The rate constants of pesticides toward carbonate radicals vary over two orders of magnitude from the most reactive fenthion ( $2.0 \times 10^7 M^{-1}s^{-1}$ ) to the least reactive methyl parathion ( $2.0 \times 10^5 M^{-1}s^{-1}$ ). These results indicate that the hydroxyl radical is more reactive and less selective than the carbonate radical.

In the near surface natural waters, the steady-state concentration of the carbonate radical is about  $5 \times 10^{-15} M$  to  $10^{-13} M$  (Chapter 2), which is much higher than that for the hydroxyl radical with  $1.5 \times 10^{-18} M$  to  $5 \times 10^{-16} M$  (Mabury and Crosby, 1994), especially in carbonate rich waters (Larson and Zepp, 1988). Even though the rate constant of the carbonate radical was lower, it may still play an important role by limiting the persistence of reactive pesticides given the higher steady-state concentration. Suppose that the steady-state concentrations of the carbonate radical  $[CO_3^{\bullet-}]_{ss}$  is equal to  $5.0 \times 10^{-14} M$  in sunlight near surface natural waters. The pseudo first-order rate constant for the reaction of the pesticide is  $k_{\text{pesticide}} = [CO_3^{\bullet-}]_{ss} \times k_m$ , where  $k_m$  is the measured second-order rate constant of the pesticide. The resulting theoretical half-life of each pesticide is shown in **Table 3.3**

without considering direct photolysis, hydrolysis, or other oxidants such as the hydroxyl radical, singlet oxygen or other radicals. The theoretical surface half-life of fenthion is about 8.0 d while that of methyl-parathion is about 802 d in natural waters. In comparison the steady-state concentration of the hydroxyl radical  $[\bullet\text{OH}]_{\text{ss}}$  varies considerably, but a typical value would be around  $1.0 \times 10^{-17} \text{ M}$  in sunlit near surface natural waters (Mabury and Crosby, 1994). Taking the measured second-order rate constant for atrazine and hexazinone ( $8.2 \times 10^8 \text{ M}^{-1}\text{s}^{-1}$  and  $6.2 \times 10^8 \text{ M}^{-1}\text{s}^{-1}$  respectively (Mabury and Crosby, 1996)) the near surface half-life for reaction with hydroxyl would be 978 and 1294 d respectively. These are longer than the values of 40 and 685 d for reaction with carbonate radical. These calculations indicate the carbonate radical likely will contribute to the degradation of highly reactive pesticides that are not efficiently removed via other pathways.

### 3.4 CONCLUSIONS

This study demonstrated that carbonate radicals could be generated through a solid hydroxyl radical source without UV light interference. The formation of carbonate radical was detected by stopped-flow spectroscopy at 600 nm. The new competition kinetic method was used to measure the rate constant of carbonate radical towards a suite of chemical probes using a model competitor; competition kinetics requires only the monitoring of the model competitor for each unknown probe being measured thus greatly simplifying the analysis. The measured rate constants of selected compounds were close to reference values; for substituted anilines, the reaction constant  $\rho$  was -0.89. Of nine pesticides tested, fenthion was most reactive and followed by phorate, with both rate constants above  $10^7 \text{ M}^{-1}\text{s}^{-1}$ , while fluometuron and atrazine were intermediate and

methyl parathion was the slowest ( $2.0 \times 10^5 M^{-1}s^{-1}$ ); the relative error of this method is approximately 10%. This method will assist in our efforts to fully characterize the role of carbonate radical in sunlight driven natural cleansing of field waters.

### 3.5 REFERENCES

Adams, G.E., Bisby, R.H., Cundall, R.B., Redpath, J.L., Willson, R.L., 1972. Selective free radical reactions with proteins and enzymes: the inactivation of ribonuclease. *Radiation Research* 49, 290-299.

Anbar, M., Meyerstein, D., Neta, P., 1966. The reactivity of aromatic compounds toward hydroxyl radicals. *J. Phys. Chem.* 70, 2660-2662.

Chen, S.N., Cope, V.W., Hoffman, M.Z., 1973. Behavior of  $CO_3^-$  radicals generated in the flash photolysis of carbonatoamine complexes of cobalt (III) in aqueous solution. *J. Phys. Chem.* 77, 1111-1116.

Chen, S.N., Hoffman, M.Z., 1973. Rate constants for the reaction of the carbonate radical with compounds of biochemical interest in neutral aqueous solution. *Radiation Research* 56, 40-47.

Chen, S.N., Hoffman, M.Z., 1974. Reactivity of the carbonate radical in aqueous solution. Tryptophan and its derivatives. *J. Phys. Chem.* 78, 2099-2102.

Chen, S.N., Hoffman, M.Z., 1975. Effect of pH on the reactivity of the carbonate radical in aqueous solution. *Radiation Research* 62, 18-27.

Chen, S.N., Hoffman, M.Z., Parsons, G.H., Jr., 1975. Reactivity of the carbonate radical toward aromatic compounds in aqueous solution. *J. Phys. Chem.* 79, 1911-1912.

- Clifton, C.L., Huie, R.E., 1993. Rate constants for some hydrogen abstraction reactions of carbonate radical. *Int. J. Chem. Kinet.* 25, 199-203.
- Crable, G.F., Kearns, G.L., 1962. Effect of substituent groups on the ionization potentials of benzenes. *J. Phys. Chem.* 66, 436-439.
- Crow, J.P., Spruell, C., Chen, J., Gunn, C., Ischiropoulos, H., Tsai, M., Smith, C.D., Radi, R., Koppenol, W.H., Beckman, J.S., 1994. On the pH-dependent yield of hydroxyl radical products from peroxyxynitrite. *Free Radical Biology & Medicine* 16, 331-338.
- Elango, T.P., Ramkrishnan, V., Vancheesan, S., Kuriacose, J.C., 1984. Reaction of the carbonate radical with substituted anilines. *Proc. Indian. Acad. Sci.* 93, 47-52.
- Elango, T.P., Ramkrishnan, V., Kuriacose, J.C., 1985. Generation and reaction of inorganic radicals with special reference to carbonate radicals. *J. Indian. Chem. Soc.* LXII, 1033-1037.
- Eriksen, T.E., Lind, J., Merenyi, G., 1985. On the acid-base equilibrium of the carbonate radical. *Radiat. Phys. Chem.* 26, 197-199.
- Forni, L.G., Mora-Arellano, V.O., Packer, J.E., Willson, R.L., 1986. Nitrogen dioxide and related free radical: Electron-transfer reactions with organic compounds in solutions containing nitrite or nitrate. *J. Chem. Soc.* 2, 1-6.
- Huie, R.E., Neta, P., 1986. Kinetics of one-electron reactions involving  $\text{ClO}_2$  and  $\text{NO}_2$ . *J. Phys. Chem.* 90, 1191-1198.
- Huie, R.E., Shoute, L.C.T., Neta, P., 1991. Temperature dependence of the rate constants for reactions of the carbonate radical with organic and inorganic reductants. *Int. J. Chem. Kinet.* 23, 541-552.

- King, P.A., Anderson, V.E., Edwards, J.O., Gustafson, G., Plumb, R.C., Suggs, J.W., 1992. A stable solid that generates hydroxyl radical upon dissolution in aqueous solutions: reaction with proteins and nucleic acid. *J. Am. Chem. Soc.* 114, 5430-5432.
- Larson, R.A., Zepp, R.G., 1988. Reactivity of the carbonate radical with aniline derivatives. *Environ. Toxicol. Chem.* 7, 265-274.
- Mabury, S.A., Crosby, D.G., 1994. The relationship of hydroxyl reactivity to pesticide persistence. Aquatic and surface photochemistry. CRC Press, Boca Raton, FL, USA, pp 149-161.
- Mabury, S.A., Crosby, D.G., 1996. Pesticide reactivity toward hydroxyl and its relationship to field persistence. *J. Agric. Food Chem.* 44, 1920-1924.
- Moore, J.S., Phillips, G.O., Sosnowski, A., 1977. Reaction of the carbonate radical anion with substituted phenols. *Int. J. Radiat. Biol.* 31, 603-605.
- Neta, P., Huie, R.E., 1988. Rate constants for reactions of inorganic radicals in aqueous solution. *J. Phys. Chem. Ref. Data* 17, 1028-1079.
- Sedlak, D.L., Andren, A.W., 1991. Aqueous-phase oxidation of polychlorinated biphenyls by hydroxyl radicals. *Environ. Sci. Technol.* 25, 1419-1427.
- Willson, R.L., Greenstock, C.L., Adams, G.E., Wageman, R., Dorfman, L.M., 1971. The standardization of hydroxyl radical rate data from radiation chemistry. *Int. J. Radiat. Phys. Chem.* 3, 211-220.
- Zepp, R.G., 1991. Photochemical fate of agrochemicals in natural waters. Pesticide Chemistry: advances in international research, development, and legislation. Proceeding of the Seventh International Congress of Pesticide Chemistry (IUPAC), Hamburg, Germany, August 5-10, 1990, PP. 329-345.

## **Chapter Four**

### **The Role of Carbonate Radical in Limiting the Persistence of Sulfur Containing Chemicals in Sunlit Natural Waters**

## 4.1 INTRODUCTION

The persistence of chemical pollutants in natural waters is determined by the ability of such waters to cleanse themselves of xenobiotics. Sunlight-induced direct and indirect photoreactions provide an important sink for chemical pollutants in such environments; direct photolysis contributes only partially to these sunlight-induced reactions. The rate constants for direct photolysis in sunlight of a specific chemical requires information regarding the absorption spectrum of the chemical, the quantum yield of the process ( $\Phi$ , the efficiency), and the light intensity as a function of wavelength, latitude, season, and time of day (Zepp and Cline, 1977). Indirect photolysis involving photochemically produced reactive chemical transients is also an important fate for these pollutants (Zepp, 1991). Such transients include alkylperoxy, hydroxyl, and carbonate radicals, singlet oxygen, aqueous electrons, and triplet states. The nature and steady state concentration of these transients strongly depend upon the composition of the water, particularly on the concentrations of dissolved organic matter, nitrate, nitrite, and trace metals. The rate of indirect photolysis can be predicted from the second-order rate constant for its reaction with the transient and the steady state concentration of the transient (Zepp, 1991).

Carbonate radical ( $\bullet\text{CO}_3^-$ ) is a sunlight generated secondary radical produced from the reaction of hydroxyl radical ( $\bullet\text{OH}$ ) with either carbonate or bicarbonate ions. In sunlit natural waters, the hydroxyl radical is formed primarily through the photolysis of nitrate (Zepp *et al.*, 1987; Hagg and Hoigné, 1985); hydroxyl can also be formed through the photolysis of  $\text{H}_2\text{O}_2$  (Larson and Zepp, 1988), nitrite (Zafiriou, 1974), and dissolved organic carbon (DOC) (Mill *et al.*, 1980) although these are generally considered minor pathways.

Carbonate radical is a more selective oxidant than hydroxyl radical which leads to relatively higher steady-state concentrations (Zepp, 1991); the concentration of  $\bullet\text{CO}_3^-$  will be a function of hydroxyl production rates, and the relative proportion of scavenging by DOC or carbonate/bicarbonate.

Larson and Zepp (1988) investigated the reaction pathway of the carbonate radical with a number of aromatic amine compounds and concluded that, particularly for electron rich systems, the carbonate radical reacts rapidly by electron transfer. The second-order rate constant of  $\bullet\text{CO}_3^-$  was high for indole and its derivatives such as tryptophan ( $k > 10^8 \text{ M}^{-1} \text{ s}^{-1}$ ) (Chen and Hoffman, 1974). As a selective oxidant,  $\bullet\text{CO}_3^-$  may play an important role in oxidizing sulfur containing compounds with a rate constant at  $10^6$  to  $10^7 \text{ M}^{-1} \text{ s}^{-1}$  (Chen and Hoffman, 1973), thus contributing to their transformation. Ultimately, carbonate radical may also affect the cycling of naturally occurring sulfur compounds in aqueous systems. Therefore, it is important both to measure the reactivity and to understand the pathways of a carbonate radical reaction with sulfur-containing compounds.

The compounds selected for this investigation were thioanisole, fenthion, and dibenzothiophene (Fig. 4.1). Thioanisole was selected to identify the reaction pathways of

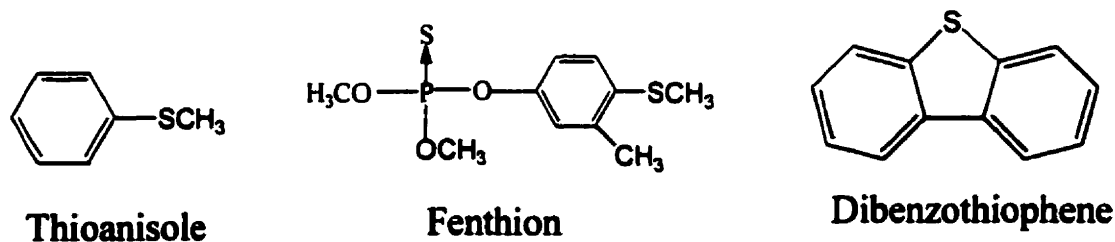


**Figure 4.1.** Chemical structures of selected sulfur-containing compounds.

•CO<sub>3</sub><sup>-</sup> towards an aromatic sulfur compound with structural similarities to an organophosphorous insecticide, fenthion (Cabras *et al.*, 1991). Once used extensively as an effective insecticide, fenthion was classified by the U. S. EPA as a Restricted Use Pesticide (RUP) on the basis of its toxicity (Kamrin, 1997). Five metabolites of fenthion have been isolated in animals and plants (Cabras *et al.*, 1993). The fenthion sulfoxide and fenthion sulfone were observed as fenthion photolysis products on fruit surfaces (Minelli *et al.*, 1996). Degradation kinetics of fenthion in different waters under various environmental conditions have previously been investigated (Lartigues and Garrigues, 1995). Fenthion degraded much faster under sunlight conditions than in the dark, with the following half-lives at 22 °C: 42 d in darkness and 2 d under sunlight for river water at pH 7.3; 26 d in darkness and 5 d under sunlight for sea water at pH 8.1. In estuarine waters, the half-lives of fenthion and its major transformation product, fenthion sulfoxide were reported to be 4.6 d and 6.9 d, respectively (Lacorte *et al.*, 1995). Dibenzothiophene (DBT) is found in fossil fuels, the fuel value of which is partly lowered due to the high organic sulfur content which, upon combustion, can release sulfur dioxide into the atmosphere, causing acid rain. A desulfurization process for DBT through a combination of photochemical reaction and liquid-liquid extraction have been investigated (Hirai *et al.*, 1997). During the desulfurization of DBT by *Rhodococcus* sp. strain IGTS8, the formation of key metabolites, including dibenz [c,e][1,2] oxathiin 6-oxide (sultine) and dibenz [c,e][1,2] oxathiin 6,6-dioxide (sultone) were investigated through extensive GC/FTIR/MS analysis (Olson *et al.*, 1993). The metabolites from the biodesulfurization of DBT in bitumen was also reported by using SPME/GC-MS (Macpherson *et al.*, 1998).

Our hypothesis was that carbonate radical would contribute to the natural cleansing of these model pollutants from sunlit natural waters. Our objectives were to identify the major photodegradation products of these selected aromatic sulfur-containing compounds and measure their reactivities under varying natural and synthetic field water (SFW) conditions to reveal the relative importance of  $\bullet\text{CO}_3^-$  to limiting their persistence.

## **4.2 MATERIALS AND METHODS**

### **4.2.1 Chemicals**

Thioanisole, methyl phenyl sulfoxide, dibenzothiophene and dibenzothiophene sulfone were obtained from Aldrich (Oakville, ON), as well as sodium nitrate, sodium carbonate and sodium bicarbonate. Fenthion was obtained from Chem Service (West Chester, PA). The intermediate photo-degradation products, such as fenthion sulfone, were synthesized from slightly modified published methods (Cabras *et al.*, 1991). An aqueous 0.15 M solution of  $\text{KMnO}_4$  was added to a solution of fenthion in acetic acid. The reaction mixture was then agitated for 12 h, diluted with water and extracted with chloroform. Using silica gel column chromatography with 60 % ethyl acetate and 40 % hexane as the mix solvent, the crude fenthion sulfone residue was purified to yield a white crystalline solid; methyl phenyl sulfone was synthesized through similar procedures. Fenthion sulfoxide and dibenzothiophene sulfoxide were synthesized respectively from fenthion and dibenzothiophene in methanol by reaction with equimolar  $\text{H}_2\text{O}_2/\text{SeO}_2$ . The reaction mixture was cleaned up using silica gel column chromatography. DOC was obtained by photobleaching Aldrich humic acid in direct sunlight for 2 weeks. The

mixture was diluted with HPLC grade water to a final concentration of 50 mg carbon/L as determined by a DOC analyzer (OI Corporation Model 1010 TOC analyzer); final absorbance of the solutions was 0.43 in a 1 cm path length at 370 nm. The stock solution was kept in the refrigerator with no headspace in the container.

#### ***4.2.2 Photolysis***

Irradiation of the sample solutions in quartz test tubes was carried out in a sunlight simulator (Atlas Suntest CPS ). Carbonate radical was generated from the photolysis of 0.1 M Na<sub>2</sub>CO<sub>3</sub> and 3 mM H<sub>2</sub>O<sub>2</sub> (Larson and Zepp, 1988) in order to determine reaction pathways. Synthetic field waters (SFWs) with varying concentrations of nitrate, DOC, and bicarbonate were then run at fixed positions in the photoreactor (Table 1); the sunlight simulator was set at a maximum irradiance level of 765 W/m<sup>2</sup>. Dark controls were run excluding light, while direct photolysis was run in distilled/deionized HPLC grade water; all experiments were run in duplicate.

#### ***4.2.3 Field water analysis***

A Lake Huron water sample served as our reference field water. DOC was determined as previously described while nitrate and bicarbonate ions were analyzed via ion-exchange chromatography with a Perkin Elmer series 200 IC pump and an Alltech 550 conductivity detector, equipped with an ERIS 1000 HP Autosuppressor. The column was an IonPac AS 14 4-mm and IonPac AG 14 4-mm (Dionex). The gradient was initiated and held for six minutes at 4% 50 mM borate and 96% deionized water followed by a linear

increase to 30:70 (borate: deionized water) over 18 minutes; the instrument was allowed to reequilibrate for 5 minutes at initial conditions.

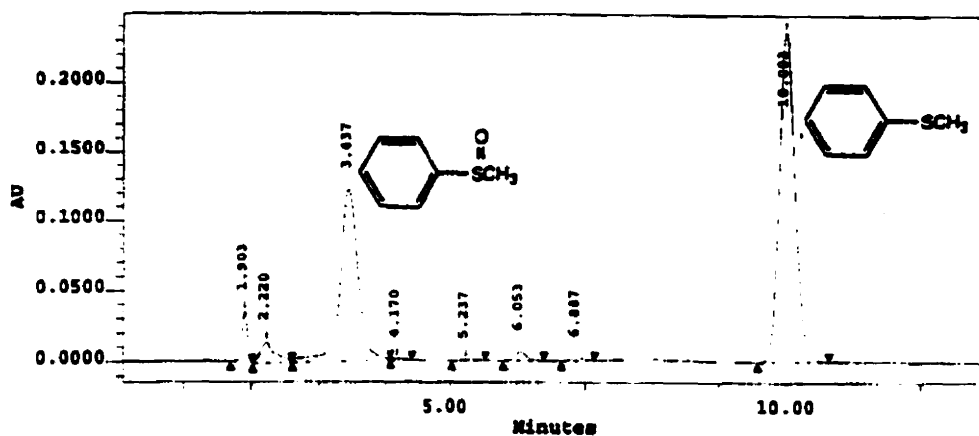
#### **4.2.4 Analysis**

Photo-degradation products were extracted and concentrated by solid-phase extraction (500 mg C18 SPE, Supelco), with subsequent reverse phase HPLC analysis (Waters 600S) with a 996 PDA detector (C18 column; 250 mm X I.D. 4.6 mm) and GC analysis using a Perkin Elmer Autosystem XL GC with an FPD detector analysis. The GC column was equipped with Supelco MDN-5 column (0.25 mm x 30 m; 0.25  $\mu$ m film thickness) (Split ratio: 5:1) and injector temperature of 250 °C; initial temperature was 50 °C for 1 min, followed by a 10 °C/min ramp to 200 °C, with a final 1 min at 200 °C. Hydrogen was used as carrier gas with a flow rate of 5 ml/min. The flow rate of air and hydrogen was 90 ml/min and 75 ml/min respectively. Structural confirmation was obtained by GC-MS (TurboMass) or LC-MS (PE Sciex API 3) in comparison with authentic standards. Kinetic analysis of each probe during photolysis was obtained through direct injection onto the HPLC-PDA under isocratic conditions with acetonitrile-water (varying ratios) at a flow rate of 1.0 ml/min; all injections were conducted in triplicate.

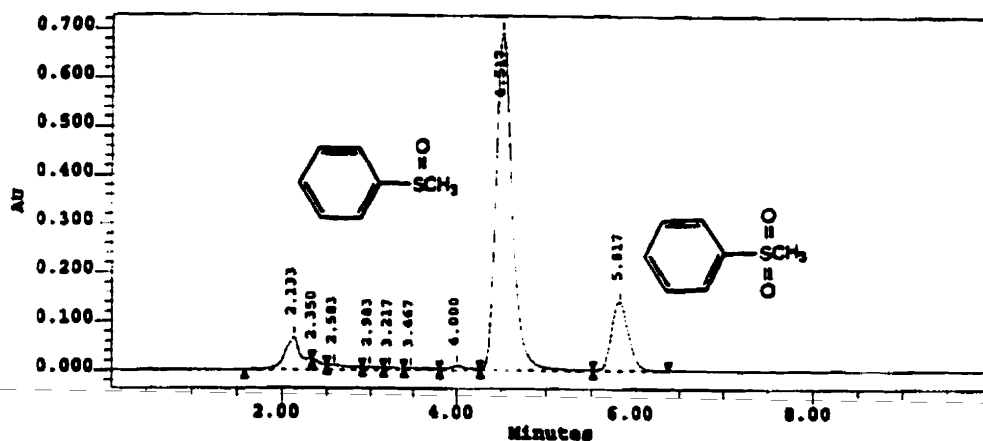
## 4.3 RESULTS AND DISCUSSION

### 4.3.1 Reaction Pathways

Fenthion and thioanisole both react rapidly with  $\bullet\text{CO}_3^-$  with a second order rate constant of  $2.0 \times 10^7 \text{ M}^{-1} \text{ s}^{-1}$  and  $2.3 \times 10^7 \text{ M}^{-1} \text{ s}^{-1}$  respectively, which we previously measured using a new competition kinetic system (Chapter 2). Methyl phenyl sulfoxide was identified by reverse-phase HPLC-PDA as the major product after the irradiation of thioanisole with carbonate radicals (Fig. 4.2); the UV spectrum and retention time of the unknown peak matched those for an authentic standard of methyl phenyl sulfoxide. The reacted sample was extracted and concentrated through C-18 solid phase extraction (SPE) cartridge and was subsequently run on a GC-FPD detector to show clearly the presence of the sulfoxide product; final structural confirmation was provided by GC-MS with  $m/z$  140 ( $\text{M}^+$ , 100), 125 (95), 97 (40) and 77 (53). Methyl phenyl sulfoxide was run under the same conditions and yielded slow conversion to the sulfone (Fig. 4.2), which was confirmed by HPLC-PDA, GC-FPD and GC-MS. Direct injection of thioanisole photolysate into an LC-MS (negative ion mode) tentatively identified benzenesulfonic acid as a minor product. A molecular ion peak at  $m/z$  157 and fragment at  $m/z$  79.6 of  $\text{SO}_3^-$  were observed which were the same as observed for a standard injection.



(A)



(B)

**Figure 4.2.** Thioanisole photoreaction with carbonate radical for 1 h; the sample was concentrated through SPE and separated by HPLC (60% acetonitrile and 40% water as mobile phase; flow rate = 1.0 ml/min) (A); Methyl phenyl sulfoxide photoreaction with carbonate radical for 1.2 h; the sample was concentrated through SPE and separated through HPLC (40% acetonitrile and 60% water as mobile phase; flow rate = 1.0 ml/min) (B).

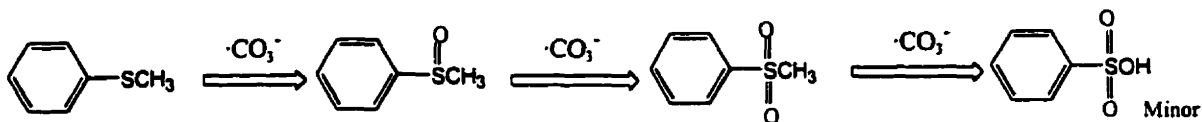
Fenthion irradiated with  $\bullet\text{CO}_3^-$  for 15 minutes resulted in many observed peaks in the HPLC chromatogram. Fenthion sulfoxide was the major product, which was similar to previous reports of photolysis in environmental matrices (Cabras *et al.*, 1991; Lacorte *et al.*, 1995). Further reaction with  $\bullet\text{CO}_3^-$  yielded fenthion sulfone; the presence of both compounds were confirmed using UV and GC-MS spectra. Elucidation of the reaction pathways of fenthion with  $\bullet\text{CO}_3^-$  were complicated, due to the likely hydrolysis of the photo-oxidized products. In previous work we showed each of the metabolites of fenthion to hydrolytically degrade faster than the parent compound (Chapter 5).

Similarly, dibenzothiophene irradiated with  $\bullet\text{CO}_3^-$  for 15 min yielded DBT-sulfoxide, identified through HPLC-PDA and structurally confirmed through GC-MS, as the major product; DBT-sulfone was confirmed as the product of  $\bullet\text{CO}_3^-$  reaction with DBT-sulfoxide. Similar metabolites were also reported in the biodesulfurization of DBT in bituman (Macpherson, 1998). All primary reaction pathways of the selected compounds with the carbonate radical are shown in **Fig. 4.3**.

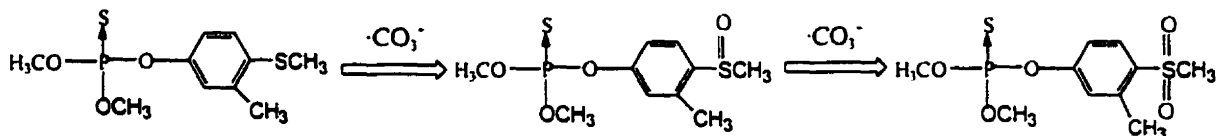
#### **4.3.2 Reaction Mechanism**

The most reactive site of the selected aromatic compounds when reacting with  $\bullet\text{CO}_3^-$  occurred at the sulfur atom. The primary reaction pathway of the compounds selected indicated primary conversion to the corresponding sulfoxide followed by slow production of the sulfone. A study of aquatic photodegradation of albendazole under sunlight showed similar metabolites of

### Thioanisole



### Fenthion



### Dibenzothiophene

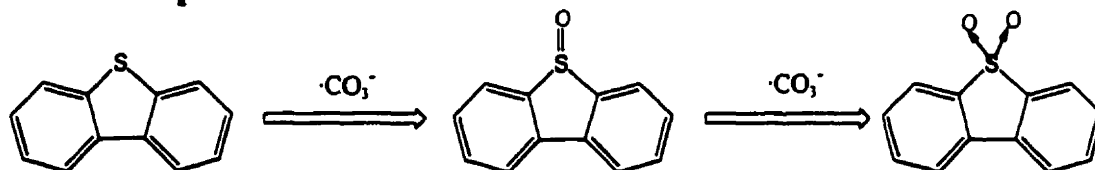


**Figure 4.3.** Primary reaction pathways towards carbonate radical.

albendazole sulfoxide and sulfone (Weerasinghe, 1992). Huie *et al.* (1991) reported that methionine reacted with carbonate radical to form the sulfur-containing radical cation through electron transfer. Draper and Crosby (1984) investigated solar photooxidation of sulfur-containing pesticides in dilute hydrogen peroxide. Electron transfer reactions were proposed to initiate sulfur oxidation observed in the thiocarbamates molinate and thiobencarb with sulfoxide formation resulting from radical coupling of dissolved oxygen in water. This mechanism may partially explain results in this investigation with carbonate radicals as the initiator of the electron transfer that ultimately yields the corresponding

sulfoxide and sulfone. Under direct photolysis conditions in DI water, relatively small amounts of sulfoxide and sulfone were produced, which presumably occurred through a similar mechanism.

Alternatively under high  $\bullet\text{CO}_3^-$  conditions, sulfoxide formation could also proceed through  $\text{O}^-$  transfer from a second  $\bullet\text{CO}_3^-$ . Initial electron transfer from the sulfur atom to carbonate radical, as described above, occurs to form the cation radical. The second step involves  $\text{O}^-$  transfer from a second carbonate radical to the sulfur cation radical. It was shown that  $\bullet\text{CO}_3^-$  could react with other radicals via the transfer of an  $\text{O}^-$  ion, and  $\text{O}^-$  transfer to molecules with closed electron shells has not previously been observed (Lilie *et al.*, 1978). The reaction of carbonate radical probably occurred through both mechanisms. However, under realistic natural water conditions, the steady-state concentration of carbonate radical would be too low for  $\text{O}^-$  transfer to be significant in comparison to dissolved oxygen.

#### **4.3.3 Persistence in different matrices**

During a cloudless summer noon hour, surface waters receive approximately 1 kW/m<sup>2</sup> of sunlight. The photoreactor simulated sunlight wavelengths with a fixed irradiance level at 765 W/m<sup>2</sup>. A suite of synthetic field waters (Table 4.1) were used to delineate more clearly the putative role of carbonate radical contributing to the natural cleansing of sulfur containing chemical pollutants in field waters. The amount of DOC was about 5 mg/mL, which is a reasonable range for most field waters. DOC can not only contribute to the production of transients in natural waters including hydroxyl radical, but can also

scavenge the hydroxyl radical with a second-order rate constant of  $2.5 \times 10^4$  (mg of C/L)<sup>-1</sup>s<sup>-1</sup> (Larson and Zepp, 1988). The rate constants and half-lives of selected compounds in different matrices are shown in **Table 4.2**; the rate constants for duplicate runs had relative errors less than 5%.

**Table 4.1.** Synthetic field waters and photolysis solutions.

Matrix	pH	Components
DI water	6.5	Pure DI water
High carbonate radical	11.05	0.04 M Na <sub>2</sub> CO <sub>3</sub> + 1.5 mM H <sub>2</sub> O <sub>2</sub>
Biocarbonate radical	8.30	500 ppm HCO <sub>3</sub> <sup>-</sup> + 50 ppm NO <sub>3</sub> <sup>-</sup>
Synthetic field water	8.30	5 mg/L DOC + 500 ppm HCO <sub>3</sub> <sup>-</sup> + 50 ppm NO <sub>3</sub> <sup>-</sup>
DOC/Bicarbonate	8.28	5 mg/L DOC + 500 ppm HCO <sub>3</sub> <sup>-</sup>
DOC/Nitrate	6.75	5 mg/L DOC + 50 ppm NO <sub>3</sub> <sup>-</sup>
Lake Huron waters	8.10	2.6mg/L DOC + 105 ppm HCO <sub>3</sub> <sup>-</sup> +6.2 ppm NO <sub>3</sub> <sup>-</sup>
Dark control matrix	8.30	500 ppm HCO <sub>3</sub> <sup>-</sup> + 50 ppm NO <sub>3</sub> <sup>-</sup>

**Table 4.2.** Photoreaction rate constants and half-lives of selected compounds at different matrices.

Reaction Matrix	Thioanisole		Fenthion		DBT	
	k (min <sup>-1</sup> )	t <sub>1/2</sub> (min)	k (min <sup>-1</sup> )	t <sub>1/2</sub> (min)	k (min <sup>-1</sup> )	t <sub>1/2</sub> (min)
High Carbonate Radical	2.02 x 10 <sup>-2</sup>	34.4	3.84x 10 <sup>-2</sup>	18.0	2.80 x 10 <sup>-2</sup>	24.8
Bicarbonate Radical	9.46 x 10 <sup>-3</sup>	73.2	2.76 x 10 <sup>-2</sup>	25.1	2.76 x 10 <sup>-3</sup>	251
Synthetic Field Water	9.18 x 10 <sup>-3</sup>	75.5	2.26 x 10 <sup>-2</sup>	30.7	2.60 x 10 <sup>-3</sup>	267
DOC + Bicarbonate	6.84 x 10 <sup>-3</sup>	101	1.95 x 10 <sup>-2</sup>	35.5	1.92 x 10 <sup>-3</sup>	361
DOC + Nitrate	9.23 x 10 <sup>-3</sup>	75.1	2.22 x 10 <sup>-2</sup>	31.2	2.71 x 10 <sup>-3</sup>	256
Filtered Field Water	8.08 x 10 <sup>-3</sup>	85.8	2.63 x 10 <sup>-2</sup>	26.3	2.47 x 10 <sup>-3</sup>	281
DI Water	7.15 x 10 <sup>-3</sup>	96.9	2.48 x 10 <sup>-2</sup>	27.9	1.98 x 10 <sup>-3</sup>	350

The pseudo-first order photoreaction of thioanisole in the different waters is shown in Fig. 4.4. In the dark control solution at pH 11.0, there was no apparent change of concentration over the time of the experiment. In contrast with direct photolysis in DI water, the most rapid photoreaction occurred in the matrix with a relatively high concentration of Na<sub>2</sub>CO<sub>3</sub> (0.04 M) and H<sub>2</sub>O<sub>2</sub> (1.5 mM) owing to the higher production of hydroxyl and thus higher carbonate radical produced via the scavenging by carbonate (Chen and Hoffman, 1974). The rate constants ranged from 7.15 x 10<sup>-3</sup> min<sup>-1</sup> in DI water to 2.02 x 10<sup>-2</sup> min<sup>-1</sup> in a high carbonate radical matrix, which correspond to half-lives of 96.9 min and 34.4 min respectively. More importantly the degradation rates under realistic carbonate radical concentrations were faster than direct photolysis (Fig. 4.4). In the filtered Lake Huron water at pH 8.1, the concentration of nitrate and bicarbonate was 6.2

ppm and 105 ppm respectively, while the amount of DOC was about 2.5 mg/l. These values were lower than in SFW, especially the amount of nitrate ion. The SFW and Lake Huron water yielded half-lives of 75.5 and 85.8 min respectively. Enhanced degradation in these solutions suggests that the carbonate radical could contribute to the cleansing of this compound from sunlit natural waters. Photolysis in the solution containing only DOC/bicarbonate was similar (half-life = 101 min) to direct photolysis in DI water. The rate in DOC/nitrate was the same as in SFW, indicating an increased hydroxyl radical availability for reaction with thioanisole and reduced bicarbonate scavenging.

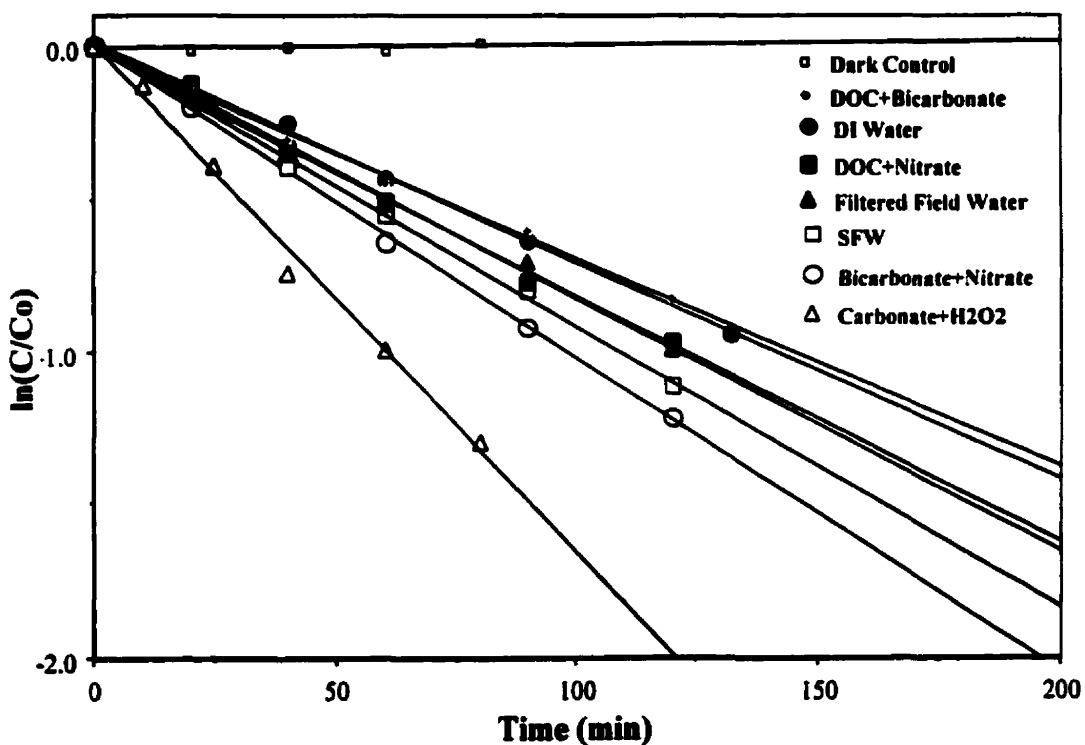


**Figure 4.4.** Photoreaction kinetics of thioanisole in different reaction matrices under a sunlight simulator (765 W/m<sup>2</sup>).

Fenthion and DBT show similar reactivities in different matrices (**Table 4.2**). The most rapid photoreaction was in the sodium carbonate with hydrogen peroxide matrix, followed by the sodium bicarbonate with nitrate ion matrix. The slowest photoreaction occurred in the matrix of DOC with sodium bicarbonate. The photolysis rate constants for fenthion were higher than thioanisole and ranged from  $2.48 \times 10^{-2} \text{ min}^{-1}$  in DI water to  $3.84 \times 10^{-2} \text{ min}^{-1}$  in a high carbonate radical matrix; corresponding to half-lives of 27.9 min to 18.0 min respectively. Due to the relatively high direct photolysis rate in DI water for fenthion, the differences in rate constants between various matrices were small. The direct photolysis rate (half-life = 27.9 min) of fenthion was even slightly higher than the rate in SFW (half-life = 30.7 min) and in the DOC plus nitrate matrix (half-life = 31.2 min), while the slowest rate (half-life = 35.5 min) was in the DOC/bicarbonate ion matrix.

Photodegradation of fenthion in three matrices containing DOC all showed slower photolysis rate than the direct photolysis. These results suggest DOCs primary role in fenthion photolysis was to reduce the overall light intensity available for production of aqueous reagents and also to reduce the inherent direct photolysis pathway (Torrents *et al.*, 1997). The filtered Lake Huron water and the bicarbonate radical solution yielded rate constants marginally faster than direct photolysis (26.3 and 25.1 min half-lives, respectively). In comparison to direct photolysis, the hydrolysis rate constant of fenthion at 25 °C was  $8.7 \times 10^{-6} \text{ min}^{-1}$  at pH 9 (Chapter 5), which is much slower than that for the photolysis rate observed here; similar conclusions for fenthion sulfoxide hold since the hydrolysis rate is  $1.4 \times 10^{-5} \text{ min}^{-1}$  at pH 9. Therefore, photolysis of fenthion should

contribute significantly to its primary degradation in sunlit field waters. The role of indirect photolysis via carbonate radical reaction would be small.

Dibenzothiophene had a high photolysis rate constant of  $2.80 \times 10^{-2} \text{ min}^{-1}$  in the high carbonate radical matrix (half-life of 24.8 min), which was much higher than the direct photolysis rate constant of  $1.98 \times 10^{-3} \text{ min}^{-1}$  in DI water (half-life of 350 min) (Table 4.2). The rate constant in the high carbonate matrix was also much higher than the rate constant in the bicarbonate matrix ( $2.76 \times 10^{-3} \text{ min}^{-1}$ ), which indicated that the higher steady-state concentration of carbonate radical formed in the system could enhance the photolysis rate dramatically. The lowest rate constant for DBT of  $1.92 \times 10^{-3} \text{ min}^{-1}$  was found in the DOC and bicarbonate ion matrix as well. However, the measured half-life value of DBT in DI photolysis was much faster than the reference value (94 hr) reported by Mill *et al.* (1981), presumably due to different wavelength and light intensities.

In general, the absorption of DOC gradually decreases with increasing wavelength, with essentially no absorption occurring above 550 nm. Most of the solar energy absorbed by DOC is between 300 to 500 nm. As the concentration of DOC increases, the integrated absorption also increases. As a result, DOC could shield the light intensity to lower the photolysis rate for the tested compounds and provides some indication that secondary DOC radicals (alkyl peroxy radicals) are not contributing much if any to the indirect photolysis pathway.

#### **4.3.4 Photodegradation products**

The primary photodegradation product for thioanisole in the different matrices was methyl phenyl sulfoxide. Approximately 30% of the thioanisole was converted to methyl phenyl sulfoxide in the high carbonate radical matrix, while only 6 % thioanisole was in DI water. Methyl phenyl sulfoxide was relatively stable in DI for the duration of these experiments (>2 hrs). No methyl phenyl sulfone was detected as a degradation product of thioanisole in different matrices due to the lower reactivity of methyl phenyl sulfoxide toward the carbonate radical (Chapter 3).

The primary photodegradation product for fenthion was fenthion sulfoxide and 3-methyl 4-methylthiophenol. In addition to direct oxidation on the sulfur atom, as observed with thioanisole, direct photolysis breaking the P-O bond to form the 3-methyl 4-methylthiophenol also occurred; as indicated above, hydrolysis would be too slow to yield the amount of phenol observed. Both mechanisms could have contributed to a more rapid photolysis of fenthion in comparison with thioanisole. Moreover, no fenthion sulfone was detected as a degradation product, presumably for similar reasons as for thioanisole.

Contrary to our expectations, DBT sulfoxide was not observed as a degradation product in the photolysis of DBT in the SFW and related solutions. Under direct photolysis in DI water, DBT sulfoxide degraded faster, with a rate constant of  $5.0 \times 10^{-2} \text{ min}^{-1}$  in comparison with DBT with a rate constant of  $2.0 \times 10^{-3} \text{ min}^{-1}$ . Approximately 5 % of the DBT sulfoxide was converted into DBT. It was also reported that photolysis of DBT sulfoxide in organic solvents resulted in the formation of dibenzothiophene and oxidized solvent (Gregory *et al.*, 1997). These two observations may explain why a

sufficient amount of DBT sulfoxide was not found in the DBT photolysis. Furthermore, no DBT sulfone was detected which may indicate its rapid photolysis or an alternate pathway of DBT sulfoxide degradation. In contrast the “high carbonate radical” solution did yield small amounts of DBT sulfoxide but these were observed only after concentrating the sample.

#### **4.4 CONCLUSIONS**

The primary reaction pathways of the selected sulfur containing compounds with carbonate radicals were through the sulfoxide, followed by the corresponding sulphone products. Three selected compounds were investigated in different reaction matrices under a photoreactor. Among all matrices, the most rapid photodegradation occurred in a carbonate radical matrix and bicarbonate radical matrix in comparison with direct photolysis. Because of the relatively high photodegradation rate in deionized water, the contribution of indirect photolysis through carbonate radicals was of intermediate importance.

#### **4.5 REFERENCES**

- Cabras, P., Plumitallo, A., Spanedda, L., 1991. High-performance liquid chromatographic separation of fenthion and its metabolites. *J. Chromatogr.* 540, 406-410.
- Cabras, P., Garau, V.L., Melis, M., Pirisi, F.M., Spanedda, L., 1993. Persistence and fate of fenthion in olives and olive products. *J. Agric. Food Chem.* 41, 2431-2433.

- Chen, S.N., Hoffman, M.Z., 1973. Rate constants for the reaction of the carbonate radical with compounds of biochemical interest in neutral aqueous solution. *Radiation Research* 56, 40-47.
- Chen, S.N., Hoffman, M.Z., 1974. Reactivity of the carbonate radical in aqueous solution. Tryptophan and its derivatives. *J. Phys. Chem.* 78, 2099-2102.
- Draper, W.M., Crosby, D.G., 1984. Solar photooxidation of pesticides in dilute hydrogen peroxide. *J. Agric. Food Chem.* 32, 231-237.
- Gregory, D.D., Wan, Z, Jenks, W.S., 1997. Photodeoxygenation of dibenzothiophene sulfoxide: Evidence for a unimolecular S-O cleavage mechanism. *J. Am. Chem. Soc.* 119, 94-102.
- Hagg, W.R., Hoigné, J., 1985. Photo-sensitized oxidation in natural water via OH radicals. *Chemosphere* 14, 1659-1671.
- Hirai, T., Shiraushi, Y., Ogawa, K., Komasaawa, I., 1997. Effect of photosensitizer and hydrogen peroxide on desulfurization of light oil by photochemical reaction and liquid-liquid extraction. *Ind. Eng. Chem. Res.* 36, 530-533.
- Huie, R.E., Shoute, L.C.T., Neta, P., 1991. Temperature dependence of the rate constants for reactions of the carbonate radical with organic and inorganic reductants. *Int. J. Chem. Kinet.* 23, 541-552.
- Kamrin, M.A., 1997. *Pesticide Profiles: Toxicity, Environmental Impact, and Fate.* CRC Lewis Publisher, New York.

- Lacorte, S., Lartigue, S.B., Garrigues, P., Barcelo, D., 1995. Degradation of organophosphorous pesticides and their transformation products in estuarine waters. *Environ. Sci. Technol.* 29, 431-438.
- Larson, R.A., Zepp, R.G., 1988. Reactivity of the carbonate radical with aniline derivatives. *Environ. Toxicol. Chem.* 7, 265-274.
- Lartigue, B.S., Garrigues, P.P., 1995. Degradation kinetics of organophosphorous and organonitrogen pesticides in different waters under various environmental conditions. *Environ. Sci. Technol.* 29, 1246-1254.
- Lilie, J., Hanrahan, R.J., Hengkein, A., 1978. O- transfer reactions of the carbonate radical anion. *Radia. Phys. Chem.* 11, 225-227.
- Macpherson, T., Greer, C.W., Zhou, E., Jones, A.M., Wisse, G., Lau, P.C.K., Sankey, B., Grossman, M.J., Hawari, J., 1998. Application of SPME/GC-MS to characterize metabolites in the biodesulfurization of organosulfur model compounds in bitumen. *Environ. Sci. Technol.* 32, 421-426.
- Mill, T., Hendry, D.G., Richardson, H., 1980. Free-radical oxidants in natural waters. *Science* 207, 886-887.
- Mill, T., Mabey, W.R., Lan, B.Y., Baraze, A., 1981. Photolysis of polycyclic aromatic hydrocarbons in water. *Chemosphere.* 10, 1281-1290.
- Minelli, E.V., Cabras, P., Angioni, A., Garau, V.L., Melis, M., Pirisi, F.M., Cabitza, F., Cubeddu, M., 1996. Persistence and metabolism of fenthion in orange fruit. *J. Agric. Food Chem.* 44, 936-939.

Olson, E.S., Stanley, D.C., Gallagher, J.R., 1993. Characterization of intermediates in the microbial desulfurization of dibenzothiophene. *Energy & Fuels*. 7, 159-164.

Torrents, A., Anderson, B.G., Bilbouljian, S., Johnson, W.E., Hapeman, C.J., 1997. Atrazine photolysis: Mechanistic investigations of direct and nitrate-mediated hydroxyl radical processes and the influence of dissolved organic carbon from Chesapeake Bay. *Environ. Sci. Technol.* 31, 1476-1482.

Weerasinghe, C.A., Lewis, D.O., Mathews, J.W., Jeffcoat, A.R., Troxler, P.M., Wang, R.Y., 1992. Aquatic photodegradation of albendazole and its major metabolites I. Photolysis rate and half-life for reaction in a tube. *J. Agric. Food. Chem.* 40, 1413-1418.

Zafiriou, O.C., 1974. Sources and reactions of OH and daughter radicals in seawater. *J. Geophys. Res.* 79, 4491-4497.

Zepp, R.G., Cline, D.M., 1977. Rates of direct photolysis in aquatic environment. *Environ. Sci. Technol.* 11, 359-366.

Zepp, R.G., Hoigné, J., Bader, H., 1987. Nitrate-induced photooxidation of trace organic chemicals in water. *Environ. Sci. Technol.* 21, 443-450.

Zepp, R.G. 1991. Photochemical fate of agrochemicals in natural waters, Pesticide Chemistry: Advances in international research, development, and legislation. Proceeding of the Seventh International Congress of Pesticide Chemistry (IUPAC) Hamburg 1990. VCH publishers, Weinheim, New York, NY, PP. 329-345.

## **Chapter Five**

### **Hydrolysis Kinetics of Fenthion and its Metabolites in Buffered Aqueous Media**

## 5.1 INTRODUCTION

Organophosphorous insecticides are widely used in agriculture and animal production for the control of various insects. These compounds generally have higher acute toxicity than other chlorinated insecticides, which is due to the inhibition of the enzyme cholinesterase, an essential component of the animal nervous system (Aly and Badaway, 1982). The persistence of organophosphorous insecticides in aquatic environments is affected by several factors, such as oxidation, photolysis (Ohkawa *et al.*, 1974), and biological degradation (Ruzicka *et al.*, 1967). Chemical hydrolysis of organophosphorous insecticides was reported to play an important role in the persistence of these compounds in the environment (Cowart *et al.*, 1971). In addition to the aquatic environment, rainfall, atmospheric water vapor, and soil moisture all provide ample opportunity for hydrolysis.

Fenthion (*O, O*-dimethyl *O*-4- (methylthio)-*m*-tolyl phosphorothioate (I) (Fig. 5.1) is used as a contact and stomach insecticide in the control of fruit flies in many crops (Cabras *et al.*, 1991). Once used extensively as an effective insecticide, fenthion was classified by the U. S. EPA as a Restricted Use Pesticide (RUP) due to its toxicity (Kamrin, 1997). Residual levels of fenthion have been reported in various environmental matrices (Wang *et al.*, 1987). Five metabolites of fenthion have been isolated in animals and plants and include fenthion sulfoxide (II), fenthion sulfone (III), fenoxon (IV), fenoxon sulfoxide (V), and fenoxon sulfone (VI) (Fig. 1) (Cabras *et al.*, 1993). The metabolites showed higher toxicity than the parent compounds: the lethal dose (LD<sub>50</sub>) was 220 mg/kg for I; 125 mg/kg for II-IV; 50 mg/kg for V and 30 mg/kg for VI. The sulfoxide (II) and sulfone (III) were

observed as fenthion photolysis products on orange fruit surfaces (Minelli *et al.*, 1996). Photo-induced oxidation of sulfur to the sulfoxide and sulfone has been commonly observed in water or simulated natural waters; examples include molinate and thiobencarb (Draper and Crosby, 1984) and albendazole (Weerasinghe *et al.*, 1992). Oxidation of the sulfur in phosphorothioates has also been observed in field water (e.g. fenitrothion to fenitrooxon) although the oxon derivative is generally unstable (Lacorte and Barcelo, 1994). Since hydrolysis is the principal detoxification mechanism for organophosphorous insecticides, hydrolysis of I-VI leads to compounds of low toxicity (FAO/WAO, 1971). The chemical structures of the three primary base-catalyzed hydrolysis products (H-I, H-II, and H-III) of fenthion are shown in Fig. 5.1.

Several studies concerning the persistence of fenthion in the aquatic environment have been carried out. It is relatively stable under acidic conditions, and moderately stable in alkaline conditions, with the following half-lives at 22 °C: 223 d at pH 4, 200 d at pH 7, and 151 d at pH 9 (Tomlin, 1994). Fenthion degrades faster in river water (Eichelberger and Lichtenberg, 1971) than in the presence of sediment (difference in half-life was from 7 to 23 d), biodegradation being a relevant process (Walker *et al.*, 1988). Fenthion degrades much faster under sunlight conditions than in darkness (Lartigues and Garrigues, 1995), with the following half-lives at 22 °C: 42 d in darkness and 2 d under sunlight for river water at pH 7.3; 26 d in darkness and 5 d under sunlight for sea water at pH 8.1. The half-lives of fenthion and its photo-oxidation product, fenthion sulfoxide, in estuarine waters were reported to be 4.6 d and 6.9 d, respectively (Lacorte *et al.*, 1995).

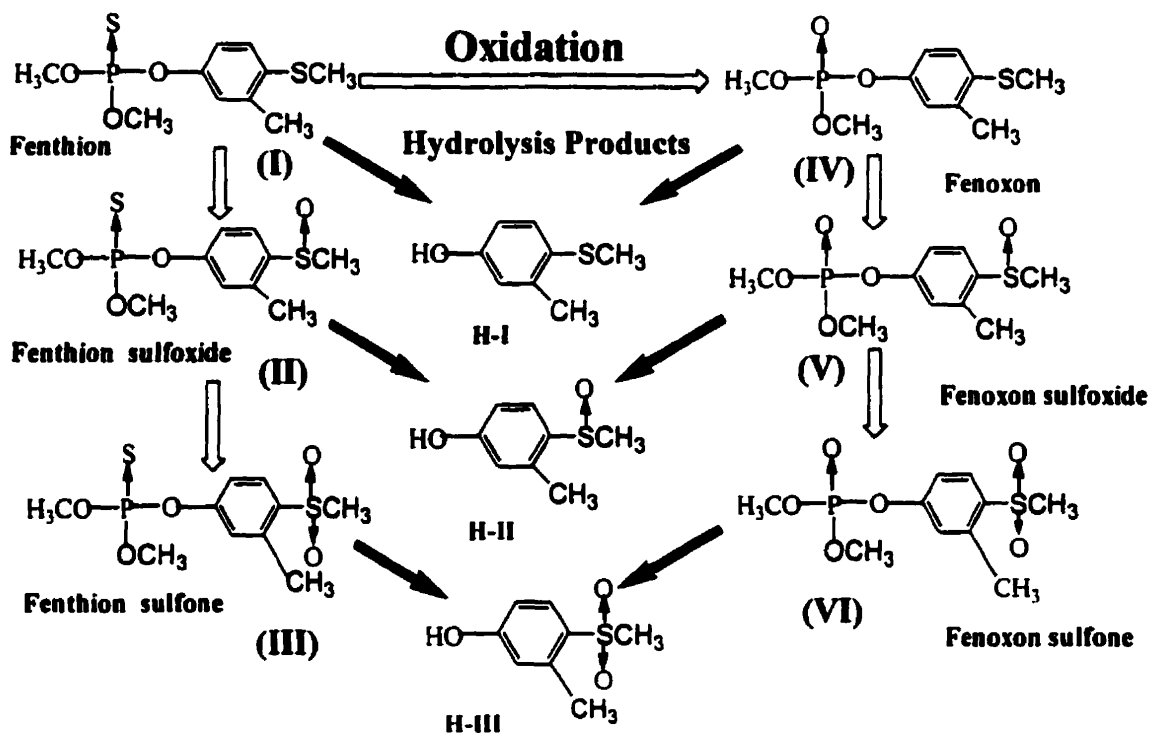


**Figure 5.1.** Fenthion (I), its five metabolites (II-VI) and three hydrolysis products H-I to H-III.

We hypothesized photo-degradation of fenthion in natural waters would lead to similar degradation products (II to VI; results to be published elsewhere) which are more toxic than the initial insecticide. Fenthion provides an excellent structural template in order to observe the influence of oxidation on hydrolysis rates. We further hypothesized the structural changes produced through photo-oxidation would render the products more susceptible to hydrolysis, thus ultimately yielding a detoxification pathway. In this study, we investigated the kinetics of hydrolysis of fenthion and its five metabolites at different pH values and temperatures; we also identified and measured the primary hydrolysis products to more accurately determine the reaction mechanism. The aim of this

investigation was to enhance the knowledge of the fate of fenthion and its metabolites in aqueous solutions and the hydrolysis mechanisms at different pH values.

## **5.2 MATERIALS AND METHODS**

### **5.2.1 Chemicals.**

Fenthion (98%) was obtained from Chem Service (West Chester, PA). Sodium phosphate dibasic (ACS grade) and potassium phosphate (ACS grade) were obtained from ACP Chemicals, Inc. (Montreal, Quebec). Disodium tetraborate (Borax, ACS grade) was purchased from BDH Inc. (Toronto, ON). Potassium permanganate, *m*-cresol (99%), hydrogen peroxide (30%), sodium sulfate anhydrous (ACS grade) and silica gel (70~230 mesh, 60 Å) were obtained from Aldrich Chemical Company (Oakville, ON). Selenium dioxide (99%) was obtained from BPH Chemicals Ltd. (Poole, England). Sulfuric acid (ACS grade) was purchased from J.T. Baker Inc. (Phillipsburg, NJ). Methyl disulfide (98%) was obtained from MC/B (Norwood, OH). Acetonitrile (HPLC grade), water (HPLC grade), methanol (HPLC grade), hexanes (ACS grade), ethyl acetate (ACS grade) and acetic acid (99.7%) were purchased from Caledon (Georgetown, ON). Other metabolites and hydrolysis products were synthesized from the following procedures.

### **5.2.2 Synthesis of Compounds.**

**II, III and VI** were prepared from fenthion following the general procedure reported by Cabras *et al.* (1991) with some modifications.

**Fenthion sulfoxide (II).** 15 ml 0.15 M  $\text{H}_2\text{O}_2/\text{SeO}_2$  in methanol solution was added, dropwise to a solution of 0.85g fenthion in 10-ml methanol at room temperature using a magnetic stirrer. The reaction mixture was then agitated for 15 min, diluted with a 20 ml saturated sodium chloride solution and extracted with chloroform. The chloroform layer was cleaned up and dehydrated with anhydrous sodium sulfate, and subsequently removed by rotary evaporation to give the crude fenthion sulfoxide as yellow oil. Using silica gel column chromatography with 60 % ethylacetate and 40 % hexane as the mixing solvent, the fenthion sulfoxide residue was purified to yield a yellow oil. The chemical structure was confirmed by GC-MS with  $m/z$  294 ( $\text{M}^+$ , 32), 279 (100), 247 (14), 169 (42), 153 (40), 138 (31), 125 (87) and 109 (47); a Perkin Elmer Autosystem XL GC with a MDN-5 column (30 m x 0.25 mm, 0.25  $\mu\text{m}$  film thickness) coupled to a PE TurboMass mass spectrometer in electron impact (EI, 70 eV) mode was used for obtaining mass spectra of synthesized compounds. The UV spectra had a maxima at 245 nm and was obtained on a Waters HPLC system containing a diode array detector (Model 996) and C-18 column (Alltech Econosphere).

**Fenthion sulfone (III).** 10 ml 0.15 M  $\text{KMnO}_4$  in methanol were added, to a solution of 0.50g fenthion in 10-ml acetic acid at room temperature with a magnetic stirrer. The reaction mixture was then agitated for 12 h, diluted with 35 ml HPLC grade water and extracted with chloroform. The chloroform layer was neutralized with  $\text{NaHCO}_3$ , cleaned up and dehydrated with anhydrous sodium sulfate. After evaporation of solvent, crude **III** appeared as a white solid. Using silica gel column chromatography with 60 % ethylacetate and 40 % hexane as the mixing solvent, **III** residue was purified to yield a white crystalline

solid. The chemical structure was confirmed by GC-MS with  $m/z$  310 ( $M^+$ , 65), 136 (28), 125 (100), 109 (71) and 105 (33), and UV spectra with a maxima at 225 nm.

Fenoxon sulfone (VI) was obtained by procedures similar to those used for fenthion sulfoxide: 60 ml 0.20 M  $KMnO_4$  in methanol were added to a solution of 0.50g fenthion in 10 ml acetic acid. The reaction mixture was then agitated for 16 h. Using silica gel column chromatography with 60 % ethylacetate and 40 % hexane as the mixing solvent, VI residue was purified to yield a white crystalline solid. The chemical structure was confirmed by GC-MS with  $m/z$  294 ( $M^+$ , 88), 269 (25), 215 (67), 207 (33) and 109 (100), and UV spectra with a specific peak at 225 nm.

Intermediate to the synthesis of fenoxon (II), 3-methyl 4-methylthiophenol (H-I), was prepared by reaction of *m*-cresol with methyl disulfide (Ho *et al.*, 1987). Next, 3.82 g concentrated sulfuric acid was added to a mixture of 5.4 g *m*-cresol and 4.7 g methyl disulfide, and the reaction mixture was agitated for 6 h in an ice bath. The solution was diluted with 20 ml HPLC grade water and extracted with chloroform. The organic layers were neutralized with  $NaHCO_3$ , washed with water and dehydrated with anhydrous sodium sulfate. Under reduced pressure of 10 torrs, the organic solvent and the remaining *m*-cresol were removed to give crude 3-methyl 4-methylthiophenol. Using silica gel column chromatography with 5% ethylacetate and 95 % hexane as the mixing solvent, H-I residue was purified to obtain a white crystalline solid. The chemical structure was confirmed by GC-MS with  $m/z$  154 ( $M^+$ , 100), 139 (65), 107 (100), 95 (32) and 77 (23),  $^1H$  NMR  $\delta_H$  2.33 (s, 3H), 2.40 (s, 3H), 5.56 (s, 1H), 6.69 (d, 2H) and 7.15 (d, 1H), and UV spectra with a specific peak at 250 nm.

Fenoxon (IV) was prepared by reaction of 3-methyl 4-methylthiophenol with dimethyl phosphorochloride in acetone in the presence of sodium carbonate following the general procedure reported by Green *et al.* (Green *et al.*, 1987). First, 120 mg MMTP were put in 10-ml acetone and 1 g Na<sub>2</sub>CO<sub>3</sub> and 1.0 ml dimethyl phosphorochloride were added. The reaction mixture was refluxed at 60~70 °C water bath for 5 h. After acetone was removed, the solution was diluted and extracted with chloroform. The organic layer was washed with water and dehydrated with anhydrous sodium sulfate. A rotary evaporator was used to obtain crude IV liquid. Using silica gel column chromatography with 33 % ethylacetate and 67 % hexane as the mixing solvent, fenoxon residue was purified via TLC to yield a liquid. The chemical structure was confirmed by GC-MS with *m/z* 262 (M<sup>+</sup>, 100), 247 (22), 153 (10) and 109 (40), and UV spectra with a maxima at 252 nm.

Fenoxon sulfoxide (V) was obtained by the same procedures as those used for fenthion sulfoxide. Using silica gel column chromatography with 95 % ethylacetate and 5 % hexane as the mixing solvent, fenoxon sulfoxide residue was purified to produce a yellow oil. The chemical structure was confirmed by GC-MS with *m/z* 278 (M<sup>+</sup>, 17), 263 (85), 262(100), 247 (20), 217 (11), 203 (13) and 109 (45), and UV spectra with a specific peak at 245 nm.

The other two hydrolysis products of its metabolites, 3-methyl 4-methylsulphonylphenol (H-II) and 3-methyl 4-methylsulphonylphenol (H-III), were prepared by hydrolysis of fenthion sulfoxide and fenoxon sulfone under strong basic conditions. Fenthion sulfoxide (0.4 g) or fenoxon sulfone (0.4g) was added in 25 ml 1N NaOH ethanol solution (ethanol: water =1:1). The reaction mixture was agitated under magnetic stirring for 8 h in 50~ 60 °C water bath, and

then 10 ml 2.5 N HCl were added to neutralize the mixture. The mixture was diluted with saturated sodium chloride and extracted with ethyl acetate. The organic layer was washed with water and dehydrated with anhydrous sodium sulfate. The rotary evaporator was used to convert crude **H-II** and **H-III** into crystals. Using silica gel column chromatography with 80 % ethylacetate and 20 % hexane or 70 % ethylacetate and 30 % hexane as the mixing solvent, **H-II** and **H-III** residue were purified to yield separate white crystalline solids. The chemical structure of **H-II** was identified by GC-MS with  $m/z$  186 ( $M^+$ , 100), 171 (95), 123 (39), 107 (56) and 77 (40) and UV spectra with a specific peak at 240 nm. The chemical structure of **H-III** was identified by GC-MS with  $m/z$  170 ( $M^+$ , 35), 155 (87), 154 (100), 139 (42), 107 (23) and 109 (24), and UV spectra with a specific peak at 240 nm.

### **5.2.3 Experimental procedures.**

Buffer solutions were utilized for determination of hydrolysis kinetics in order to assure consistent pH over the course of the experiment given the production of weak acids following cleavage of the ester bond; our primary aim was elucidation of reaction kinetics and mechanism which required strict control of solution conditions. Individual solutions were prepared to pH 7 (0.025 M  $\text{KH}_2\text{PO}_4$  and 0.025 M  $\text{Na}_2\text{HPO}_4$ ) or pH 9 (0.01 M Borax), which were adjusted with 0.1 M HCl and 0.1 M NaOH at different temperatures of 25 °C, 50 °C or 65 °C; the water used was filter sterilized (0.45 micron) to preclude microbial degradation. Individual solutions of **I** to **VI** 50 to 100  $\mu\text{M}$  in duplicate, at pH 7 and pH 9 buffers were prepared in filled 15-ml screw-top test tubes which were wrapped with foil to preclude photolysis. The test tubes were placed into a water bath at varying temperatures. Samples at appropriate time intervals were taken for analysis

of the organophosphate and corresponding hydrolysis product; each time point was determined in triplicate.

#### **5.2.4 Analysis by HPLC.**

**I to VI** and the primary hydrolysis products (**H-I to H-III**) concentration were determined by direct injection in an HPLC. A complete Waters HPLC system was employed with a Waters 600 pump and controller and a Waters 486 tunable absorbance detector. Separations were performed using a reverse-phase Econosil C18 column (Alltech) 25 cm long with an inner diameter of 4.6 mm and 5 micron particle size. Concentrations (50 to 100  $\mu\text{M}$ ) were chosen so that aqueous samples were analyzed directly, without preconcentration or sample purification. The isocratic conditions were carried out with acetonitrile-water in various ratios at a flow rate of 1.0 ml/min; HPLC analysis conditions including mobile phase, detection wavelength, and retention time are shown in **Table 5.1**. Calibration was performed daily using external standards.

**Table 5.1. HPLC Analysis Conditions**

Analysis Compounds	Mobile phase (ACN: H <sub>2</sub> O)	$\lambda$ (nm)	Retention time (min)
Fenthion (I) H-I	75:25	250	I, 7.5; H I, 3.9
Fenoxon (IV) H-I	65:35	250	IV, 5.7; H I, 4.8
Fenthion sulfoxide (II) H-II	35:65	245	II, 18; H II, 3.6
Fenoxon sulfoxide (V) H-II	30:70	245	V, 6.2; H II, 4.2
Fenthion sulfone (III) H-III	55:45	225	III, 8.3; H III, 3.7
Fenoxon sulfone (VI) H-III	40:60	225	VI, 5.6; H III, 4.5
H-I	65:35	250	H I, 4.8
H-II H-III	30:70	240	H II, 4.2 H III, 5.7

## 5.3 RESULTS AND DISCUSSION

### 5.3.1 Effect of pH on hydrolysis.

Chemical hydrolysis of fenthion and its metabolites was investigated using buffered solutions at pH 7 and pH 9; a typical range of natural waters. All plots of  $\ln(C/C_0)$  ( $C_0$  is the reactant concentration at  $T = 0$ ,  $C$  is the reactant concentration at various time) versus time were linear at pH 7 and pH 9, indicating that the reaction tends to be a

pseudo-first-order as indicated in **Fig. 5.2**. The hydrolysis rate constant and half-life (**Table 5.2**) indicate the relative stability of fenthion and its metabolites in a neutral medium. The stability of these compounds decreased as the pH increased from pH 7 to pH 9, and the hydrolysis rate constants were higher at pH 9 than that at pH 7 for fenthion and each of the metabolites investigated. At 50 °C, the hydrolysis half-life varied from 4.86 d for fenthion to 1.55 d for fenoxon sulfone at pH 7, and from 4.80 d for fenthion to 0.55 d for fenoxon sulfone at pH 9. Chemical hydrolysis of fenthion and its metabolites at 25 °C and 65 °C was also investigated using the same buffered solutions. As a result, the hydrolysis rate constant and half-life indicate the same relative stability in a neutral medium, which is shown in **Table 5.2**. Hydrolysis proceeded at higher rates under alkaline conditions, suggesting that the reaction was more effectively catalyzed by hydroxide ions than by neutral water molecules or hydronium ions. The relatively rapid hydrolysis of the fenthion oxidation derivatives perhaps explains the lack of literature citations for these compounds in field waters.

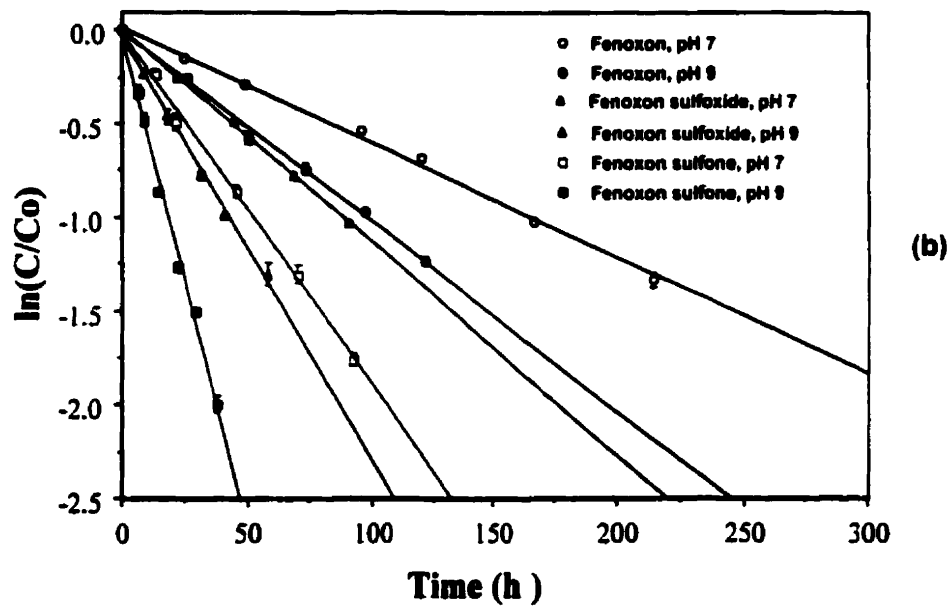
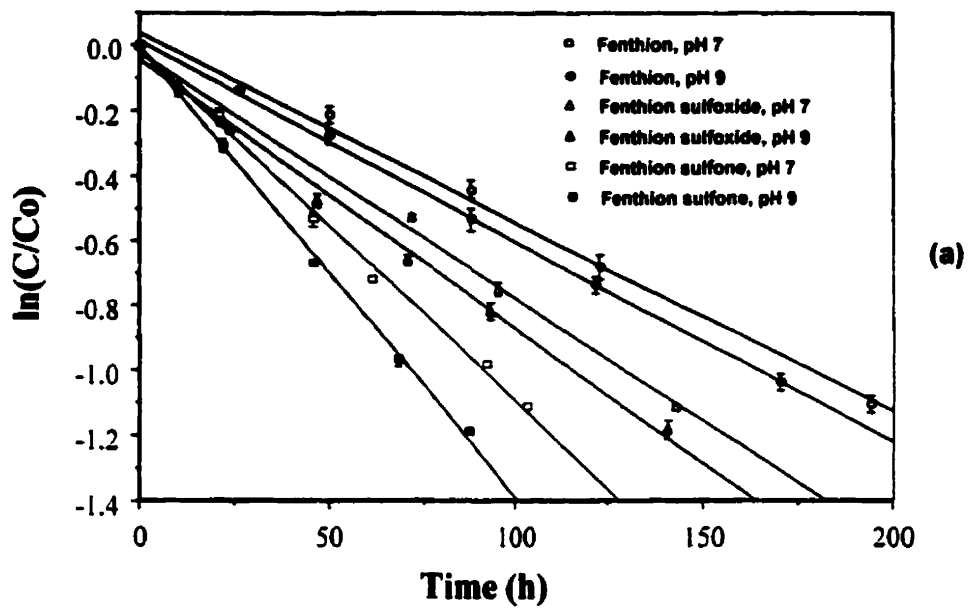


**Figure 5.2.** Hydrolysis rate of I-III at 50 °C (a) and IV-VI at 50 °C (b); N=2.

**Table 5.2.** Hydrolysis rate constant  $k$  and half-life  $t_{1/2}$  at different temperatures

Temperature	Compounds	$k$ ( $\text{h}^{-1}$ ) at pH 7	$t_{1/2}$ (h) at pH 7	$k$ ( $\text{h}^{-1}$ ) at pH 9	$t_{1/2}$ (h) at pH 9
25 °C	Fenthion	0.000489	1417	0.000520	1333
	Fenthion Sulfoxide	0.000705	983	0.000833	832
	Fenthion Sulfone	0.00116	597	0.00192	361
	Fenoxon	0.000621	1116	0.000889	780
	Fenoxon Sulfoxide	0.00136	510	0.00177	392
	Fenoxon Sulfone	0.00175	396	0.00304	228
50 °C	Fenthion	0.00594	116.7	0.00601	115.3
	Fenthion Sulfoxide	0.00754	91.9	0.00805	86.2
	Fenthion Sulfone	0.0107	64.6	0.0138	50.6
	Fenoxon	0.00609	113.8	0.0103	67.1
	Fenoxon Sulfoxide	0.0131	61.3	0.0232	29.9
	Fenoxon Sulfone	0.0186	37.3	0.0522	13.3
65 °C	Fenthion	0.0227	30.5	0.0243	28.5
	Fenthion Sulfoxide	0.0229	30.3	0.0302	22.9
	Fenthion Sulfone	0.0450	15.4	0.0596	11.6
	Fenoxon	0.0251	27.6	0.0319	21.7
	Fenoxon Sulfoxide	0.0427	16.2	0.111	6.20
	Fenoxon Sulfone	0.0765	9.10	0.111	6.20

### 5.3.2 Effect of temperature on hydrolysis.

At 25 °C, the half-life of fenthion is 59 d at pH 7 and 55.5 d at pH 9, which is relatively shorter in comparison with half-lives of fenthion reported at 22 °C: 223 d at pH 4, 200 d at pH 7, and 151 d at pH 9 (Tomlin, 1994) and half-lives of fenthion at 23.5 °C: 101.8 d at pH 7 and 101.7 d at pH 9 (Wang *et al.*, 1989). The slight difference of reported half-lives of fenthion at pH 7 and pH 9 are consistent with our results. The half-lives of fenthion as 189 d at 6 °C and 71 d at 22 °C in darkness for Mill-Q water at pH 6.1 was reported by Lartiges & Garrigues (Lartiges and Garrigues, 1995). The half-life of fenthion in buffered aqueous media is much longer than in environmental water systems, such as half-lives of 26 d at 22°C in darkness, 5d under sunlight condition for seawater at pH 8.1 (Lartiges and Garrigues, 1995); persistence of up to 4 weeks in river water (Eichelberger and Lichtenberg, 1971); half-life of 4.6 d in estuarine waters (Lacorte *et al.*, 1995). Other reaction pathways to degrade organophosphate pesticides in natural waters such as oxidation, photolysis, and microbial degradation in addition to hydrolysis, would contribute to increase the overall transformation rate of fenthion.

Using the data shown in **Table 5.2**, the activation energy can be derived from the Arrhenius equation:

$$K = Ae^{-E_a/RT} \quad (1)$$

Where  $k$  ( $\text{time}^{-1}$ ) is the rate constant at temperature  $T$ ,  $A$  is the frequency factor ( $\text{time}^{-1}$ ),  $E_a$  is the activation energy, and  $R$  is the gas constant. The effect of temperature on the rate constants is presented in **Fig. 5.3**. The activation energy ( $E_a$ ) and frequency factor ( $A$ ) were calculated using the Arrhenius equation. The range of  $E_a$  was from 17.3 kcal/mol for fenoxon

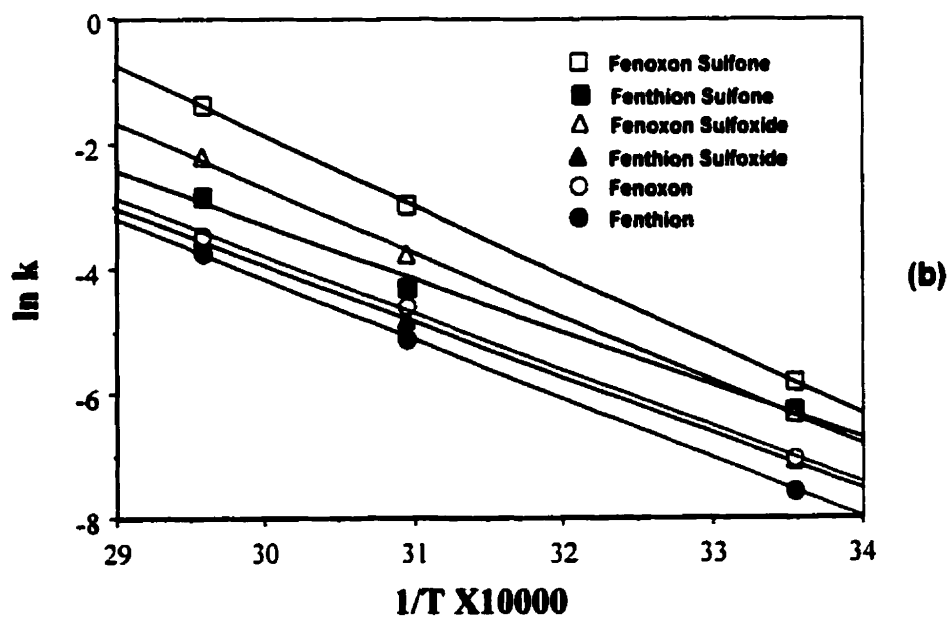
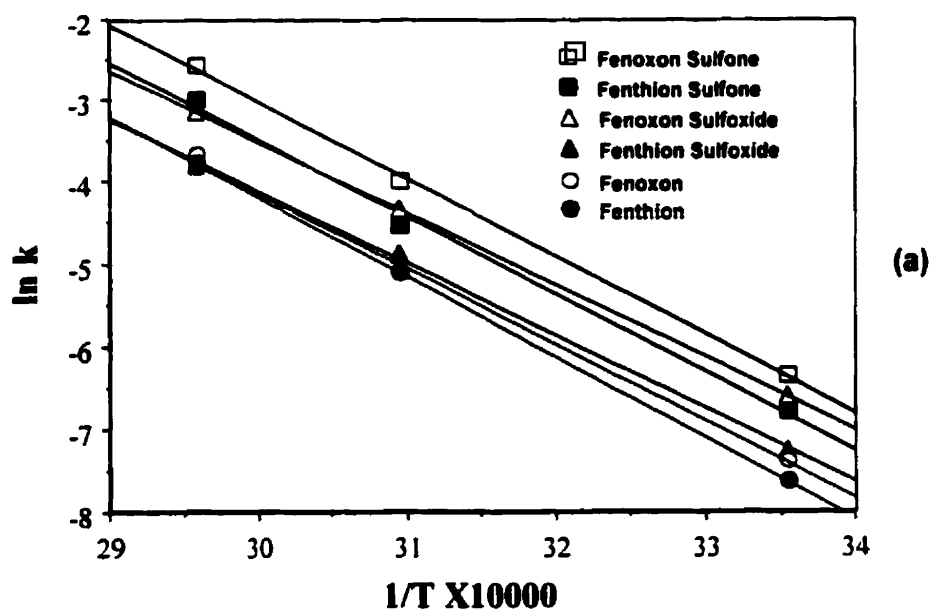


**Figure 5.3.** Effect of temperature on the rate constants at pH 7 (a) and pH 9 (b).

sulfoxide to 19.2 kcal/mol for fenthion at pH 7 and from 16.7 kcal/mol for fenthion sulfone to 22.1 kcal/mol for fenoxon sulfone at pH 9. These  $E_a$  values were consistent with the activation energies for a range of organophosphate pesticide hydrolysis, ranging from 14 to 22 kcal/mol (Freed *et al.*, 1979). Although pH determines the hydrolytic mechanism, its effect on  $E_a$  is less clear since  $E_a$  depends both on the structure of the molecule and on the mechanism. The magnitude of the activation energy provides an indication of the sensitivity of the reaction to temperature change. Thus, the persistence of compounds with larger  $E_a$  values would show a greater dependence on temperature than those with a lower  $E_a$ .

Fenoxon sulfone and fenoxon sulfoxide at pH 9 have the highest rate constants in comparison with other metabolites at different temperatures. However, their activation energies were also highest among the compounds investigated with 22.1 (kcal/mol) and 20.6 (kcal/mol) respectively. So, the highest rate constants were due to the frequency factors A. The frequency factor (A) of V and VI at pH 9 were  $5.52 \times 10^8$  and  $1.40 \times 10^{10}$  ( $S^{-1}$ ) respectively; these values were larger than the frequency factors for the other compounds. The relatively higher frequency factor is due to the entropy effect based on the activated complex theory (Ruff and Csizmadia, 1994). In order to prove this point, the activation entropies ( $\Delta S^\ddagger$ ) were calculated using the equation of Ruff and Csizmadia (1994); all values are shown in **Table 5.3**. The entropy of activation for fenthion were  $-27.7$  cal/mol.K and  $-27.9$  cal/mol.K at pH 7 and 9, which is higher than that of **II** and **III** and due to the hydrogen bonding on the O atom of the sulphinyl and sulphonyl group with water at the activated complex. As a result, the entropy of activation of **II** and **III** is decreased in comparison with **I**.

**Table 5.3.** Activation Energy  $E_a$ , Frequency Factor  $A$  and Activation Entropy  $\Delta S^\ddagger$ 

Compounds	$E_a$ (kcal/mol)	$A$ ( $S^{-1}$ )	$\Delta S^\ddagger$ (Cal/mol.K)
At pH 7			
Fenthion	19.2	$1.65 \times 10^7$	-27.7
Fenthion Sulfoxide	17.4	$1.31 \times 10^6$	-32.7
Fenthion Sulfone	18.6	$1.28 \times 10^7$	-28.3
Fenoxon	18.4	$5.05 \times 10^6$	-29.9
Fenoxon Sulfoxide	17.3	$1.74 \times 10^6$	-32.1
Fenoxon Sulfone	18.8	$2.97 \times 10^7$	-26.4
At pH 9			
Fenthion	19.2	$1.61 \times 10^7$	-27.9
Fenthion Sulfoxide	17.9	$3.00 \times 10^6$	-31.2
Fenthion Sulfone	16.7	$1.33 \times 10^6$	-32.6
Fenoxon	18.1	$4.11 \times 10^6$	-30.4
Fenoxon Sulfoxide	20.6	$5.52 \times 10^8$	-20.6
Fenoxon Sulfone	22.1	$1.40 \times 10^{10}$	-11.7

On the other hand, the entropy of activation for fenoxon and **V** and **VI** at pH 9 was apparently decreased from  $-30.4$  cal/mol.K for fenoxon to  $-20.6$  cal/mol.K and  $-11.7$  cal/mol.K for **V** and **VI** respectively. This large difference presumably comes from the electrostatic force between the P atom and hydroxide ion. The strong electronegative O atom connecting to the P atom would make the phosphorous of **IV**, **V** and **VI** more positive than that of **I**, **II** and **III** when the S atom replace the O atom. In addition, the strong electron-withdrawing group of sulphonyl and sulphinyl on **V** and **VI** result in the P atom being even more positive than that of **IV**. Therefore, the P atom on **V** and **VI**, with a partial positive charge, can form an ion pair with hydroxide ion through electrostatic force, which greatly decrease the entropy of reactants. Then, the entropy of activation  $\Delta S^\ddagger$  between the entropy of the activated complex and reactants would increase; ( $\Delta S^\ddagger$ ) results were consistent with the frequency factor (A). This entropy effect may explain why **VI** and **V** at pH 9 with the highest activation energy ( $E_a$ ) also have the highest reaction constants. At pH 7, the same entropy effect was not apparent for **IV**, **V** and **VI** which we believe is due to the lack of an ion pair formed with the neutral water molecule.

### **5.3.3 Stability of the hydrolysis products.**

From their chemical structures in **Fig.5.1**, **H-I**, **H-II**, and **H-III** are the hydrolysis product of **(I)** and **(IV)**, **(II)** and **(V)**, and **(III)** and **(VI)** respectively. These products result from base-catalyzed hydrolysis of the parent compound and can be determined simultaneously after direct injection into the HPLC. The percentage of the reactant converted into the relative product at different temperature is shown in **Table 5.4**; % conversion was calculated at the

first time point. The percentage is much higher at pH 9 than at pH 7, which indicates that there exist different mechanisms at different pHs. At 50 °C, there are 88% and 62% of the hydrolysis products for **II** and **III** at pH 9, and only 34% and 2% at pH 7. There are 88% and 96% of the hydrolysis products for **V** and **VI** at pH 9, and only 34 % and 61 % of the hydrolysis products at pH 7. Even in neutral medium, **H-III** is still the primary product through water molecules-catalyzed hydrolysis of fenoxon sulfone. The percentage shows the similar amount for **H-II** and **H-III** at three temperatures. However, the percentage of **H-I** is higher at high temperature than that at low temperature. At pH 9, there are 33% **H-I** and 49 % **H-I** for fenthion and fenoxon at 50 °C, and only 8.3 % and 14 % **H-I** at 25 °C respectively. At 50 °C, the percentage of fenthion and its metabolites converted into hydrolysis products at the first time point is shown in **Fig. 5.4**.

It was necessary to determine the stability of three hydrolysis products at different pHs. **Fig. 5.5** shows the stability of three hydrolysis products at 50 °C. It can be seen that **H-III** is stable at pH 7 as well as at pH 9, and **H-II** is stable only at pH 7. Also, **H-II** is relatively stable at pH 9 with a first-order rate constant of  $0.0634 \text{ d}^{-1}$ . **H-I** is not stable at pH 7 or at pH 9, with a first-order rate constant of  $0.232 \text{ d}^{-1}$  and  $2.59 \text{ d}^{-1}$  respectively, which are higher than the hydrolysis rate constant of fenthion and fenoxon at similar pH. This may explain in part, why the percentage of **H-I** is lower than that of the other two products.

**Table 5.4.** Percentage of reactant converted into the relative products.

Compounds	% at 25 °C	% at 50 °C	% at 65 °C
Fenthion at pH 7	4.3	8.0	7
Fenthion at pH 9	8.3	33	33
Fenthion sulfoxide at pH 7	34	34	28
Fenthion sulfoxide at pH 9	87	88	82
Fenthion sulfone at pH 7	3.3	2	4.2
Fenthion sulfone at pH 9	66	62	68
Fenoxon at pH 7	2	2	4.6
Fenoxon at pH 9	14	49	48
Fenoxon sulfoxide at pH 7	68	34	59
Fenoxon sulfoxide at pH 9	92	88	95
Fenoxon sulfone at pH 7	48	61	54
Fenoxon sulfone at pH 9	98	96	99

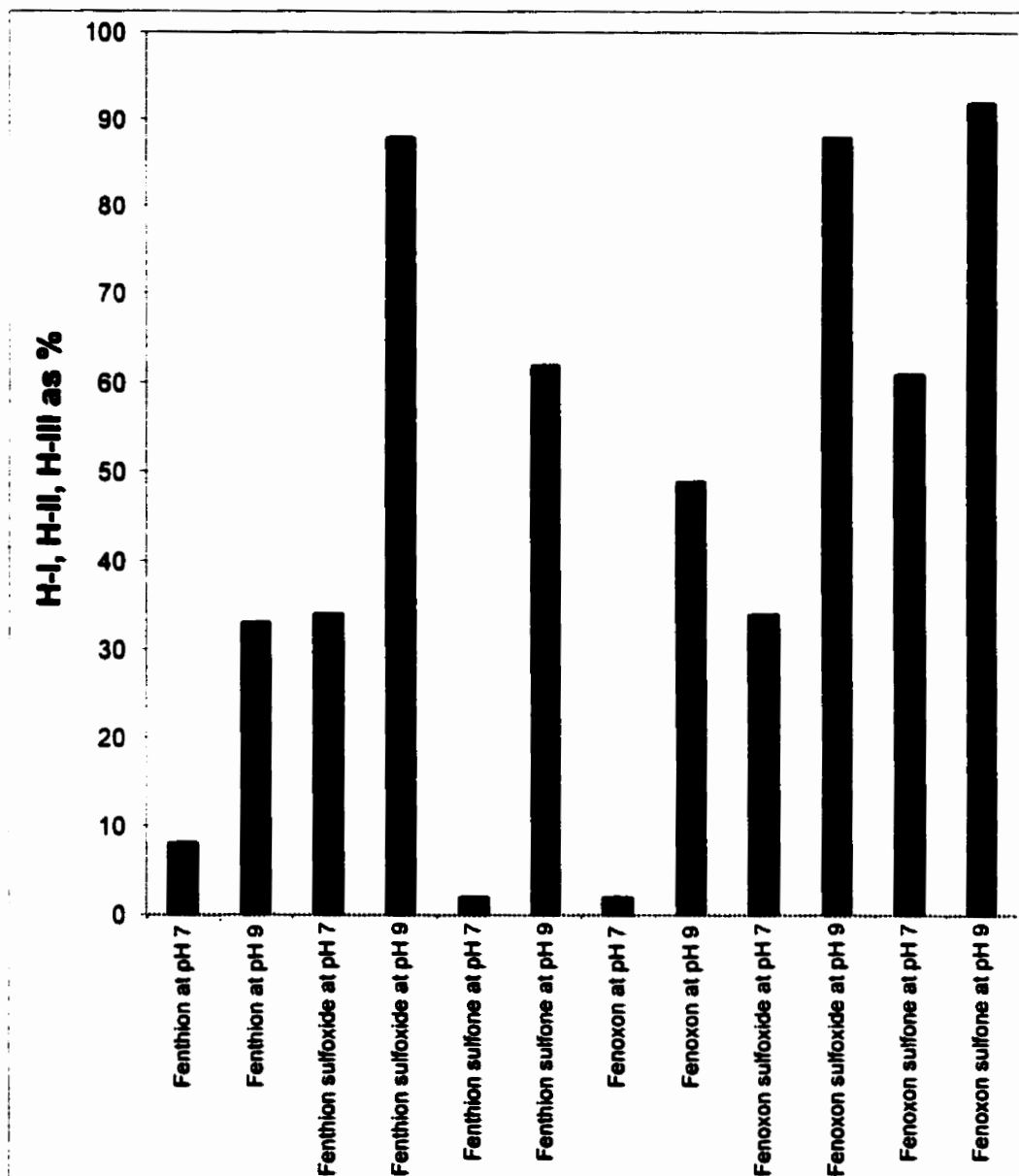


**Figure 5.4.** At 50 °C, the percentage of fenthion and its metabolites converted into H-I to H-III at the first time point.

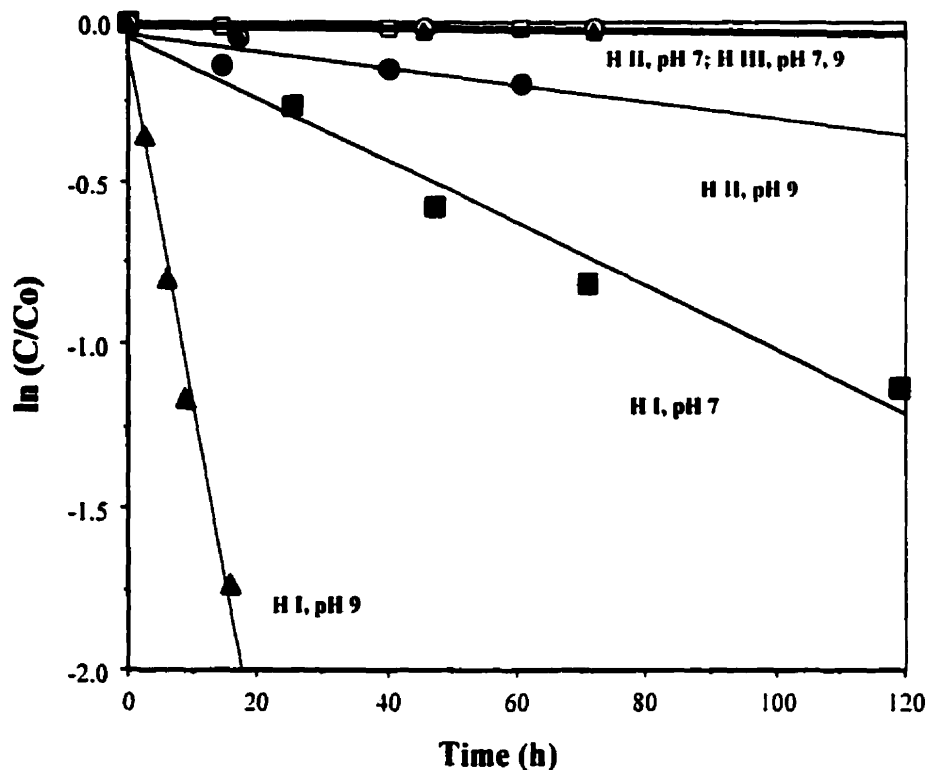


**Figure 5.5.** Stability of three hydrolysis products at 50 °C.

#### **5.3.4 Hydrolysis mechanism.**

Fenthion and its metabolites are thiophosphate or phosphate esters. The hydrolysis of such compounds occurs through reaction with a nucleophile by nucleophilic substitution ( $S_N2$ ), both at the phosphorous atom with an alcohol moiety as the leaving group and at the carbon bound to the oxygen of an alcohol moiety with the diester as the leaving group (Schwarzenbach *et al.*, 1993). The reaction rate of the  $S_N2$  reaction depends on the electrophilic ability of the central atom and on the presence of a good leaving group. The hydrolysis mechanisms of fenthion and its metabolites are fundamentally different at pH 7 and

pH 9. At pH 9, hydrolysis of these compounds results in the formation of phenol derivatives and dialkylphosphoric acid because  $\text{OH}^-$  is about  $10^8$  times stronger than  $\text{H}_2\text{O}$  as a nucleophile towards P atom (Barnard *et al.*, 1961). The formation of two compounds is presumably due to the attack of the  $\text{OH}^-$  ion at the phosphorous atom, which results in cleavage of the P-O aryl bond. Because **H-I** is not stable at pH 9, the  $\text{S}_{\text{N}}2$  reaction occurring at the P atom is still likely the primary mechanism for fenoxon and fenthion even if the percentage of product is lower than that of other metabolites. The proposed reaction mechanism is shown in **Fig. 5.6**. This mechanism is similar to that reported for parathion which showed both dearylation and dealkylation important at different pH values (Weber, 1976).

The percentages of phenol derivative products of fenoxon (**IV**) and its oxidized compounds (**V**, **VI**) are higher than those of fenthion and its oxidized compounds (**II**, **III**) because of the increased electrophilicity of the P atom when an O atom replaces an S atom. On the other hand, **H-III** is a better leaving group than **H-II** or **H-I** because the negative charge on the oxygen atom after the P-O bond breakup can delocalize on the two oxygen atoms on the sulfur atom. Similarly, **H-II** is a better leaving group than **H-I**. Therefore, the percentages of hydrolysis products increase from fenthion and fenoxon to their sulfoxides, and then to their sulfones. Even at pH 7, there is 62% of **H-III** for **VI** due to the good leaving group (50 °C), which indicates that the  $\text{S}_{\text{N}}2$  reaction occurring at the phosphorous atom is still the primary mechanism of hydrolysis (**Fig.5.6**). There are still 68% and 59% of hydrolysis products for **V** at 25 °C and 65 °C at pH 7, therefore, we still suggest that **H-II** is a primary product of hydrolysis of fenoxon sulfoxide through water molecule catalysis at neutral condition.

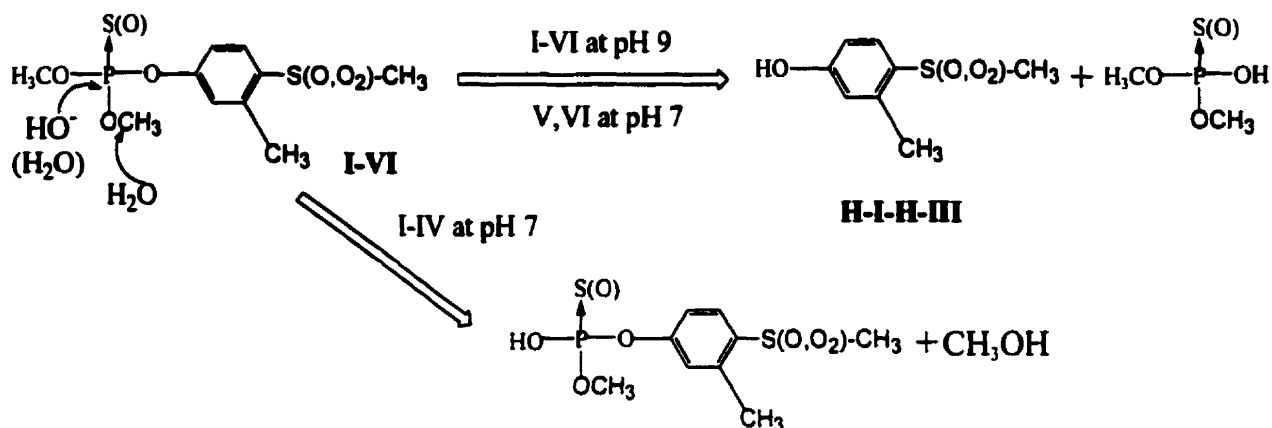


**Figure 5.6.** Proposed primary hydrolysis pathway for I to VI at pH 7 and pH 9.

Under neutral conditions, the amount of phenol derivative products is lower than that under alkaline conditions because water molecules are weaker nucleophiles than hydroxide ions. The primary reaction mechanism is presumably through dealkylation of organophosphate pesticides, which is associated with the reaction of nucleophiles at the alkyl carbon atom, followed by cleavage of the C-OP bond to form the corresponding alcohol (Trucklik and Kovacicova, 1977); we were unable to determine the products due to lack of standards for the resulting phosphate. The dealkylation of organophosphate insecticides has previously been observed in buffered distilled water (Greenhalgh *et al.*, 1980) and in natural water systems (Maguire and Hole, 1980). We propose the primary reaction mechanism of fenthion, fenoxon, and fenthion sulfone at pH 7 is an S<sub>N</sub>2 reaction occurring at the carbon bound to the oxygen to form methanol (Fig. 5.6). If a good leaving group is present, the

neutral reaction may proceed by both reaction mechanisms, that is, C-O as well as P-O cleavage (Schwarzenbach *et al.*, 1993). At 50 °C, there are still 34% of the H-II in II and V at pH 7. Both reaction mechanisms therefore exist under neutral conditions.

## 5.4 CONCLUSIONS

The rate constants, half-lives, activation energies (Ea), and proposed hydrolysis mechanisms presented clearly indicate pH and structure have a large influence on the rate and mechanism of hydrolysis. Furthermore, these results support the hypothesis that photo-oxidation of fenthion results in intermediates that are rapidly degraded through hydrolytic cleavage. These hydrolysis products are generally nontoxic and indicate the importance of the role sunlight plays in the natural cleansing of field waters. This investigation can be used to enhance the predictive capabilities of determining persistence of related insecticides by including a more accurate model of hydrolysis to the large knowledge base available for predicting volatilization and sorption.

## 5.5 REFERENCES

- Aly, O.A., Badawy, M.I., 1982. Hydrolysis of organophosphate insecticides in aqueous media. *Environment International*. 7, 373-377.
- Barnard, P.W, Burton. C.A., L'lewellyn, D.R., Vernon, C.A., Welch, V.A., 1961. The reactions of organic phosphates. Part V. The hydrolysis of triphenyl and trimethyl phosphates. *J. Chem. Soc.* 3, 2670-2676.

Cabras, P., Plumitallo, A., Spanedda, L., 1991. High-performance liquid chromatographic separation of fenthion and its metabolites. *J. Chromatogr.* 540, 406-410.

Cabras, P., Garau, V.L., Melis M., Pirisi, F.M., Spanedda, L., 1993. Persistence and fate of fenthion in olives and olive products. *J. Agric. Food Chem.* 41, 2431-2433.

Cowart, P.R., Bonner, F.L., Epps, E.A., 1971. Rate of hydrolysis of seven organophosphate pesticides. *Bull. Environ. Contam. Toxicol.* 6, 231-234.

Draper, W.M., Crosby, D.G., 1984. Solar Photooxidation of Pesticides in Dilute Hydrogen Peroxide. *J. Agric. Food Chem.* 32, 231-237.

Eichelberger, J.W., Lichtenberg, J. J.D., 1971. Persistence of pesticides in river water. *Environ. Sci. Technol.* 5, 541-544.

FAO/WHO, 1973. *Pesticides residues in Food*, 1971 Evaluations; FAO/WHO: Roma, pp 110-149.

Freed, V.H, Chlou, C.T., Schmeding, D.W., 1979. Degradation of selected organophosphate pesticides in water and soil. *J. Agric. Food Chem.* 27, 706-708.

Green, M. B., Hartley, G. S., West, T.F., 1987. *Chemicals for crop improvement and pest management*, Pergamon Press, New york, 3rd ed. pp 93-95.

Greenhalgh, R., Dhawan, K.L., Weinberger, P., 1980. Hydrolysis of fenitrothion in model and natural aquatic systems. *J. Agric. Food Chem.* 28, 102-105.

Ho, H.W., Liu, Z.J., Zou, D.P., Yan, G., 1987. Methylthiolation of phenols (I). Synthesis of 3-methyl-4-(methylthio)phenol. *Huazhong Shifan Daxue Xuebao, Ziranhexueban*. 21, 367-375.

Kamrin, M.A., 1997. *Pesticides Profiles: Toxicity, Environmental impact, and Fate*. CRC Lewis Publishers. pp 180-184.

Lacorte, S., Lartigue, S.B., Garrigues, P., Barcelo, D., 1995. Degradation of organophosphorous pesticides and their transformation products in estuarine waters. *Environ. Sci. Technol.* 29, 431-438.

Lacorte, S., Barcelo, D., 1994. Rapid Degradation of Fenitrothion in Estuarine Waters. *Environ. Sci. Technol.* 28, 1159-1163.

Lartigues, B.S., Garrigues, P.P., 1995. Degradation kinetics of organophosphorous and organonitrogen pesticides in different waters under various environmental conditions. *Environ. Sci. Technol.* 29, 1246-1254.

Maguire, R.J., Hole, E.J., 1980. Fenitrothion sprayed on a pond: kinetics of its distribution and transformation in water and sediment. *J. Agric. Food Chem.* 28, 372-378.

Minelli, E.V., Cabras, P., Angioni, A., Garau, V.L., Melis, M., Pirisi, F.M., Cabitza, F., Cubeddu, M., 1996. Persistence and Metabolism of Fenthion in Orange Fruit. *J. Agric. Food Chem.* 44, 936-939.

Ohkawa, H., Mikami, N., Miyamoto, J., 1974. Photodecomposition of sumithion [*O,O*-dimethyl-*O*-(3-methyl-4-nitrophenyl)-phosphorothioate]. *Agr. Biol. Chem.* 38, 2247-2255.

Ruff, F., Csizmadia, I.G., 1994. *Organic reaction*, Elsevier, pp 132-134.

Ruzicka, J.H., Thomson, J.H., Wheals, B.B., 1967. The gas-chromatographic examination of organophosphorous pesticides and their oxidation products. *J. Chromatogr.* 30, 92-97.

Schwarzenbach, R.P., Gschwend, P.M., Imboden, D.M., 1993. *Environmental organic chemistry*, John Wiley & Sons, Inc. 372- 399.

Tomlin, C., 1994. *The pesticide Manual*, Crop Production Publications, pp 451-452.

Trucklik, S.; Kovacicova, J., 1977. *Fenitrothion symposium*, Ottawa, Canada, NRC publication No. NRCC 16-73.

Wang, T.C., Lenahan, R.A., Tucker, J.W., Jr., 1987. Deposition and persistence of aerially-applied fenthion in a florida estuary. *Bull. Environ. Contam. Toxicol.* 38, 226-231.

Wang, T.C., Kadiac, T., Lenahan, R., 1989. Persistence of fenthion in aquatic environment. *Bull. Environ. Contam. Toxicol.* 42, 389-394.

Walker, W.W., Cripe, C.R., Pritchard, P.H., Bourquin, A.W., 1988. Biological and abiotic degradation of xenobiotic compounds in in Vitro estaurine water and sediment/water systems. *Chemosphere* 17, 2255-2270.

Weber, K., 1976. Degradation of parathion in seawater. *Water Research.* 10, 237-241.

Weerasinghe, C.A., Lewis, D.O., Mathews, J.M., Jeffcoat, A.R., Troxler, P.M., Wang, R.Y., 1992. Aquatic Photodegradation of Albendazole and Its Major Metabolites. 1. Photolysis Rate and Half-Life for Reactions in a Tube. *J. Agric. Food Chem.* 40, 1413-1418.

## **Chapter Six**

### **Conclusions and Future Work**

## 6.1 CONCLUSIONS

Carbonate radical can be generated through flash photolysis and pulse radiolysis in the laboratory. This radical is a powerful oxidant with a one-electron reduction potential of 1.59 V vs the NHE at pH 12 and acts predominantly as an electron acceptor and oxidizes many organic and inorganic compounds. The carbonate radical shows a wide range of reactivity with organic compounds. It can react rapidly with electron-rich chemicals, especially aromatic and sulfur-containing compounds. The carbonate radical can also oxidize some inorganic anions and the metal center of transition metal complexes to its higher oxidation state through electron transfer. In biological systems, carbonate radicals also act as an intermediate in free radical-mediated damage and in biological oxidation. In natural waters, the carbonate radical ( $\bullet\text{CO}_3^-$ ) is a secondary radical that results from the scavenging of hydroxyl radical ( $\bullet\text{OH}$ ) by carbonate/bicarbonate. Numerous sources and pathways exist for generation of hydroxyl radicals in natural waters and vary for each depending on the varying dissolved components. As a photo-induced transient, the carbonate radical can contribute to degrading chemical pollutants, thus limiting their persistence in natural waters and contributing to the self-cleaning of these waters.

*N,N*-dimethylaniline (DMA) was found to be a selective probe for measuring the steady state concentration of this radical in a variety of natural waters. The pH, nitrate, total carbonate/bicarbonate, and DOC in selected field waters were quantitatively analyzed. Hydroxyl radicals were hypothesized to be produced primarily from the slow photolysis of nitrate and DOC, and then scavenged by carbonate/bicarbonate that were competing with DOC. Steady state carbonate radical concentrations ( $[\bullet\text{CO}_3^-]_{ss}$ ) in natural waters were

investigated under a photoreactor with varying light intensity. The measured  $[\bullet\text{CO}_3^-]_{ss}$  strongly depended on light intensity; the range of  $[\bullet\text{CO}_3^-]_{ss}$  found in natural waters was  $5 \times 10^{-15}$  to  $10^{-13}$  M. Through kinetic analysis,  $[\bullet\text{CO}_3^-]_{ss}$  was related to the major components in natural waters and a simple linear relationship was derived:  $[\bullet\text{CO}_3^-]_{ss} \propto f_{\bullet\text{OH}}(\text{CO}_3^{2-} + \text{HCO}_3^-) \times \{[\text{NO}_3^-] + 12 + 1.3 [\text{DOC}]\}$ ,  $f_{\bullet\text{OH}}(\text{CO}_3^{2-} + \text{HCO}_3^-)$  is the fraction of  $\bullet\text{OH}$  scavenged by carbonate/bicarbonate. Using this formula in the twenty natural waters investigated, a 0.92 linear regression coefficient was obtained.

Carbonate radical reactivity ( $\bullet\text{CO}_3^-$ ) was measured by competition reactions between a chemical of known reactivity and a compound with unknown reactivity towards  $\bullet\text{CO}_3^-$ . Carbonate radical was produced using a novel method whereby KOONO (potassium peroxonitrite) was dissolved into 0.01 NaHCO<sub>3</sub> solution initially producing hydroxyl radical which was rapidly scavenged by HCO<sub>3</sub><sup>-</sup> yielding  $\bullet\text{CO}_3^-$ . Carbonate radical production was monitored using a stopped-flow spectrometer at the absorption band for  $\bullet\text{CO}_3^-$  of 600 nm. Results using this competition kinetic method indicated the second-order rate constants for substituted anilines corresponded to reference values with a relative error less than 10%. Using  $\sigma_{\text{para}}^+$  values, the rate constants of substituted anilines at pH 9.0 correlated well ( $r^2 = 0.98$ ) with the Hammett equation yielding  $\rho = -0.89$ . The *p*-nitroaniline (PNA) was selected as the standard competitor in measuring the reactivity of pesticides to the carbonate radical. Of the nine pesticides tested, fenthion was the most reactive, followed by phorate, with rate constants above  $10^7 \text{ M}^{-1}\text{s}^{-1}$ . Fluometuron and atrazine were of intermediate reactivity, and methyl parathion was one of the least reactive of the pesticides investigated.

Thioanisole, dibenzothiophene, and fenthion were selected as sulfur-containing compounds to investigate the degradation pathways involving carbonate radicals. The major photodegradation products of thioanisole and dibenzothiophene were the corresponding sulfoxides. The sulfoxide products were further oxidized through reaction with  $\bullet\text{CO}_3^-$  to the corresponding sulfone derivatives. Fenthion showed a similar pathway with appearance of fenthion sulfoxide as the major product. The proposed mechanism involves abstraction of an electron on sulfur to form a radical cation, which is then oxidized by dissolved oxygen. Each of the sulfur probes was further investigated in a sunlight simulator under varying matrix conditions. The highest rate constants were in the carbonate radical matrix, and the lowest were in a matrix of DOC and bicarbonate. In synthetic and natural field waters, thioanisole photodegraded faster than under direct photolysis. Fenthion photodegraded more rapidly than thioanisole. Dibenzothiophene photodegraded rapidly in a carbonate radical matrix in comparison with direct photolysis. Ultimately, carbonate radical was found to contribute toward the photo-degradation of sulfur-containing compounds in natural waters.

Since fenthion provided an excellent structural template in observing the influence of photo-oxidation on hydrolysis rates, the hydrolysis kinetics of fenthion and its five metabolites were investigated in pH 7 and pH 9 buffered aqueous media at varying temperatures. Rate constant and half-life studies revealed that fenthion and its metabolites were relatively stable in neutral media, and their stability decreased as pH increased. The half-lives at 25 °C ranged from 59.0 d for fenthion to 16.5 d for fenoxon sulfone at pH 7, and from 55.5 d for fenthion to 9.50 d for fenoxon sulfone at pH 9. The activation energy

(Ea) was found to range from 16.7 to 22.1 kcal/mol for the compounds investigated. The phenol derivative product of fenthion and fenoxon, 3-methyl 4-methylthiophenol was not stable in pH 7 and pH 9 buffered solutions at 50 °C, whereas 3-methyl 4-methylsulphonylphenol and 3-methyl 4-methylsulphinyphenol were relatively stable under the same conditions. In an alkaline medium, the compounds investigated underwent hydrolysis, resulting in the formation of phenol derivatives; in neutral media, decomposition was primarily via dealkylation.

In natural waters, carbonate radicals primarily act as selective oxidants. The steady-state concentrations of carbonate radicals in surface waters are relatively higher in comparison with those of hydroxyl radicals, particularly in high carbonate-containing field waters. So, carbonate radicals could contribute to limiting the persistence of some aquatic pollutants including electron-rich aromatic compounds and sulfur-containing compounds. Based on this research, we have gained an improved understanding of the role of sensitized photolysis in the environmental fate of aquatic pollutants and therefore furthering our predictive ability as to the persistence of these compounds in natural waters. Ultimately, this knowledge will allow regulators to preclude the use of chemicals that will cause adverse environmental impacts.

## **6.2 FUTURE WORK**

*N, N*-dimethylaniline (DMA) was selected as a specific probe to determine the steady-state concentrations of carbonate radical (Chapter 2). A simple linear relationship between  $[\bullet\text{CO}_3]_{ss}$  and concentration of nitrate and DOC in natural waters was obtained. If

the amount of light at different wavelengths in the sunlight simulator can be obtained and the quantum yield at each wavelength calculated, the  $[\bullet\text{CO}_3]_{\text{ss}}$  in the sunlight simulator can be quantified as a function of wavelength. If sunlight at different wavelengths absorbed by the sample can be quantified through actinometry, the  $[\bullet\text{CO}_3]_{\text{ss}}$  in sunlight can also be quantified under different conditions. Because the sunlight intensity and UV index would vary during the different periods of daytime, the average light intensity at different wavelengths can be used to predict the  $[\bullet\text{CO}_3]_{\text{ss}}$  in field waters. In addition, this method can be used to calculate the average  $[\bullet\text{CO}_3]_{\text{ss}}$  in selected field water during different seasons or years based on the weather database from Environment Canada. Finally, the calculated average  $[\bullet\text{CO}_3]_{\text{ss}}$  can be used to predict the persistence of organic pollutants in natural waters.

Phorate, an aliphatic sulfur-containing pesticide, has the measured rate constant of  $1.2 \times 10^7 \text{ M}^{-1} \text{ s}^{-1}$  to carbonate radical (Chapter 3). The reaction pathway of phorate toward carbonate radical and its persistence in sunlit field waters should be addressed in future work. Using the GC-FPD and GC-MS, the reaction pathways and reactivities in sunlit field water can be investigated. Other aliphatic sulfur chemicals of environmental importance such as dimethyl sulfide and 2-(methylthio)benzothiazole can also be selected to investigate the reaction pathways and reactivities with carbonate radical.

Advanced oxidation processes (AOPs) have promise because they effect on-site destruction of the contaminants. AOPs are by definition oxidation processes that use the hydroxyl radical as a primary contaminant oxidation mechanism. Hong *et al.* (1996) developed a kinetic model and associated rate expressions for AOPs to facilitate evaluation

and optimization of treatment performance. Using this kinetic modeling system, Umschlag and Herrmann (1999) recently reported that the degradation of some aromatic compounds in water treatment processes may proceed via the carbonate radical in polluted, carbonate-containing waters. Therefore, the kinetic data of other chemical pollutants in natural waters can also be used in the same kinetic modeling system to test the contribution of carbonate radical toward degradation of selected compounds. The selected chemical pollutants are treated with AOPs at the high carbonate-containing waters in future work. The steady-state concentration of carbonate radical can be measured through the method reported by Huang and Mabury (Chapter 2). It is suggested that the steady-state concentration of carbonate radical is much higher than hydroxyl radical. The contribution of carbonate radical to the degradation of this compound can be investigated. Considering the other reactions for selected chemical pollutants such as hydrolysis and microbial degradation, the persistence of the corresponding compound can be predicted. Since the steady-state concentrations of carbonate radical can be enhanced by artificially increasing the carbonate/bicarbonate ion and nitrate within the advanced oxidation water treatment, it would contribute to limiting the persistence of such compounds with relatively higher rate constant with respect to carbonate radical. In addition, a new kinetic modeling for AOPs should be formulated and used to derive a rate expression that predicts the carbonate radical concentration according to various operation conditions. Once experimentally verified, the model can be used to optimize AOPs for hazardous-waste treatment and thereby reduce remediation costs.

Finally, carbonate radical was reported to be an intermediate in free radical-mediated damage in biological systems (Bisby *et al.*, 1998, Meli *et al.*, 1999) and involved in

biological oxidation (Wolcott *et al.*, 1994). The steady-state concentrations of carbonate radicals in biological systems should be measured in the near future. Moreover, decreasing the carbonate radical level in biological systems and preventing the carbonate radical from damaging the biological system may have particularly significance to human beings.

### **6.3 REFERENCES**

Bisby, R.H., Johnson, S.A., Parker, A.W., Tavender, S.M., 1998. Time-resolved resonance Raman spectroscopy of the carbonate radical. *J. Chem. Soc., Faraday Trans.* 94, 2069-2072.

Hong, A., Zappi, M.E., Kuo, C.H., Hill, D., 1996. Modeling kinetics of illuminated and dark advanced oxidation processes. *J. Environ. Eng.* 122, 58-62.

Meli, R., Nauser, T., Koppenol, W.H., 1999. Direct observation of intermediates in the reaction of peroxyxynitrite with carbon dioxide. *Helv. Chim. Acta* 82, 722-725.

Umschlag, T., Herrmann, H., 1999. The carbonate radical ( $\text{HCO}_3/\text{CO}_3^-$ ) as a reactive intermediate in water chemistry: kinetics and modeling. *Acta Hydrochim. Hydrobiol.* 27, 214-222.

Wolcott, R. G., Franks, B.S., Hannum, D.M., Hurst, J.K., 1994. Bactericidal potency of hydroxyl radical in physiological environments. *J. Biol. Chem.* 269, 9721-9728.